2019

OLEIC ACID VESICLES: FORMATION, MECHANISMS OF REACTIVITY, AND USES IN DETERMINATION OF TERPENE ACTIVITY

Laura A. Walther
University of Kentucky, lwalther@asbury.edu
Digital Object Identifier: https://doi.org/10.13023/etd.2019.166

Right click to open a feedback form in a new tab to let us know how this document benefits you.

STUDENT AGREEMENT:

I represent that my thesis or dissertation and abstract are my original work. Proper attribution has been given to all outside sources. I understand that I am solely responsible for obtaining any needed copyright permissions. I have obtained needed written permission statement(s) from the owner(s) of each third-party copyrighted matter to be included in my work, allowing electronic distribution (if such use is not permitted by the fair use doctrine) which will be submitted to UKnowledge as Additional File.

I hereby grant to The University of Kentucky and its agents the irrevocable, non-exclusive, and royalty-free license to archive and make accessible my work in whole or in part in all forms of media, now or hereafter known. I agree that the document mentioned above may be made available immediately for worldwide access unless an embargo applies.

I retain all other ownership rights to the copyright of my work. I also retain the right to use in future works (such as articles or books) all or part of my work. I understand that I am free to register the copyright to my work.

REVIEW, APPROVAL AND ACCEPTANCE

The document mentioned above has been reviewed and accepted by the student's advisor, on behalf of the advisory committee, and by the Director of Graduate Studies (DGS), on behalf of the program; we verify that this is the final, approved version of the student's thesis including all changes required by the advisory committee. The undersigned agree to abide by the statements above.

<div align="right">

Laura A. Walther, Student

Dr. Bert C. Lynn, Major Professor

Dr. Mark A. Lovell, Director of Graduate Studies

</div>

OLEIC ACID VESICLES:
FORMATION, MECHANISMS OF REACTIVITY,
AND USES IN DETERMINATION OF TERPENE ACTIVITY

_____

DISSERTATION

_____

A dissertation submitted in partial fulfillment of the
requirements for the degree of Doctor of Philosophy in the
College of Arts and Sciences
at the University of Kentucky

By
Laura A. Walther
Wilmore, Kentucky

Director: Dr. Bert C. Lynn, Professor of Chemistry
Lexington, Kentucky

2019

ABSTRACT OF DISSERTATION

OLEIC ACID VESICLES:
FORMATION, MECHANISMS OF REACTIVITY,
AND USES IN DETERMINATION OF TERPENE ACTIVITY

This dissertation will focus on the volatile compounds released upon the burning of incense which are numerous and varied. The first part of this dissertation is the gas chromatography-mass spectral (GC-MS) analysis of burning incense collected via solid phase microextraction (SPME) with the aim of developing a library of compounds found in incense as used in the Orthodox church.

The second part of this dissertation has the aim of developing a method for forming oleic acid bilayer vesicle membranes and a fluorescence spectroscopy method by which the reactivities of these vesicles can be analyzed. These reactivities include permeability, fluidity, aggregation, and fusion of the membranes.

One family of the volatile compounds found in incense are the terpenes and terpenoids. The reactivity of the terpenes and terpenoids found in incense will be analyzed using the oleic acid vesicles with the hypothesis that terpenes of the same structural groups will act similarly on oleic acid vesicle membranes and these reactivities can be related to mechanistic interactions.

KEYWORDS: Incense, Oleic acid vesicles, Terpenes, Fluorescence, Anisotropy, FRET

Laura A. Walther
_____

4/30/19

OLEIC ACID VESICLES:
FORMATION, MECHANISMS OF REACTIVITY,
AND USES IN DETERMINATION OF TERPENE ACTIVITY

By

Laura A. Walther

<div align="right">

Bert C. Lynn
(Director of Dissertation)

Mark A. Lovell
(Director of Graduate Studies)

4/30/19

</div>

Acknowledgements

I would like to thank my family for their support. My husband, Bert, for his unfailing belief in my achieving this PhD degree. My daughters, Beth and Becca, for giving up mom-time so I could go back to school, for their many hugs and for making me laugh in times of high stress. My dad for reminding me that I am not getting any younger and that now is the time to pursue my dreams. And my mom for always being my foundation.

My advisor, Dr. Bert Lynn, agreed to take me on as a very non-traditional student. Without his willingness to listen to my many stochastic ravings about research, I would not have made it through the last eight years. I so appreciate his guidance in my studies, his depth of knowledge, and his vast breadth of experience in so many areas.

Asbury University has supported me unfailingly through this endeavor of going back to school. My colleagues in the Natural Science department have put up with my absences so I could attend graduate classes; understood when I was distracted; encouraged me when I was tired; and prayed for me through all the exams and deadlines. A special thanks to Dr. Bonnie Banker for emboldening me to pursue the goal of obtaining my PhD; to Dr. Dan Strait for inspiring me to teach enthusiastically; to my bosses, Dr. Steve Clements, Dr. Bobby Baldridge, and Dr. Vins Sutlive for following my progress, and encouraging me along the way.

Table of Contents

List of Tables

List of Figures

Chapter 1 - Introduction

1.1 Background

Incense has been used in religious practices for several millennial [1].

Countless studies have been done on both the contents [2-6] and negative health

effects [7-9] of the VOCs (Volatile Organic Compounds) present in various types of

incense [10-15] and various types of incense delivery methods. The aim of the

present study is to determine if the family of VOCs known as terpenes, which are

found in incense as used in the Orthodox church, have any effect on an *in vitro*

system of oleic acid vesicles. These vesicles are used as biomimicry material to

study permeability, fluidity, aggregation and fusion of the vesicle membranes upon

the addition of terpene compounds.

1.2 Incense

Incense has been used in religious practices for numerous millennia and in

Christianity since the 4th century [1]. In the Catholic and Orthodox churches incense

is burned on smoldering charcoal in a small vessel called a censer hung at the end of

long chains. The censer is swung toward the icons (the religious art) and the people

standing in the temple space. The smoke comes out of the censer in puffs (and

sometimes billows) at the apex of the swing. This billowing smoke fills up the

church, permeating everything as is shown in the picture below. (Figure 1)

Figure 1 - Orthodox deacon censing [16]

Incense used in ecclesiastical settings today is most commonly Athonite style, meaning that it is made the way the monks of the monasteries on Mt. Athos have made incense since the 10th century. A base of frankincense (or olibanum) is ground into powder. After adding the desired fragrances as essential oils of various herbs and flowers, it is kneaded, rolled out, cut, and coated in an inactive fine china powder to prevent the incense from being sticky. Incense is usually aged for a minimum of 30 days [17].

Certain scents are traditionally used for different times of the year. For example, Gethsemene or Coptic incense is commonly used during the Lenten season before Easter; Cassia (cinnamon) for the fall; and Evergreen and Embers or Shepherd's Field incense is used for the Christmas season. Occasionally scents are used in combinations of two or more at one time.

While 'frankincense' is used as the base for all Athonite-style incense, there are several species of the *Boswellia* genus of plants that produce what is called 'frankincense' – *B. sacra* (or *B. carterii*) from Somalia, *B. frereana* from Northern

Somalia, *B. papyrifera* from Ethiopia, and *B. serrata* from India. Frankincense is the resin secreted by the *Boswellia* tree either naturally or after cutting the bark. The resin 'tears' are left to dry on the tree for several days and then harvested. They vary widely in commercial quality, primarily based on color and the smell of the smoke on burning. Numerous studies have been done to determine the differences between the species of the *Boswellia* genus with most focusing on the chemical compounds present in these resins.

Hamm *et al.* [5] used headspace SPME GC-MS (see Section 1.5 for details on instrumentation) on different species of *Boswellia* to determine the unique identifiable compounds for each. They compiled a database of 131 compounds and determined the characteristic compounds, or ratios of similar compounds for each species. They then applied these fingerprint findings to several samples of unknown origin. Of particular interest to our study are the findings of a Mt. Athos "traditional incense". The paper does not have a specific scent listed for the incense but the results, while identifying *B. papyrifera* as the frankincense base, do show a substantial amount of "other substances, probably Damask rose and jasmine."

1.3 Terpenes

One family of organic compounds that are particularly prevalent in frankincense are the terpenes. Terpene chemistry [18] is integral to the study of
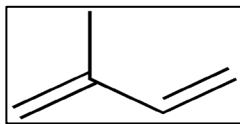
Figure 2 - Isoprene Unit

incense because of the plant origin of frankincense. All terpene chemistry is based on the isoprene unit, C_5H_8. (Figure 2) The volatile and semi-volatile combinations of this unit are the smaller compounds – monoterpenes (two isoprene units, $C_{10}H_{16}$), sesquiterpenes (three isoprene units, $C_{15}H_{24}$) and some diterpenes (four isoprene units, $C_{20}H_{32}$). Basar *et al.* [2] worked on identifying the larger diterpene compounds for the first time, but the smaller terpene compounds have been recognized as components of frankincense for quite some time.

An interesting sample tested in the Hamm study [5] was a 2000-year-old archaeological sample from Yemen, I-IV century AD. Of particular note is the presence of the volatile monoterpenes found in frankincense even after 2000 years which indicates that terpene compounds can be present for very long periods of time even given their volatility.

The terpene compounds commonly found in frankincense can be divided into classes using several structural aspects: (1) the number of rings - acyclic, mono-cyclic, di-cyclic; (2) the number of isoprene units - monoterpene, sesquiterpenes, and di-terpenes; and (3) the presence of other organic functional groups – alcohols, aldehydes, ketones, phenols. This third group is usually referred to as terpenoid compounds. The classification and structures of the terpene and terpenoid compounds of particular interest to this study are shown in Table 1.

Table 1 - Classes of Terpenes
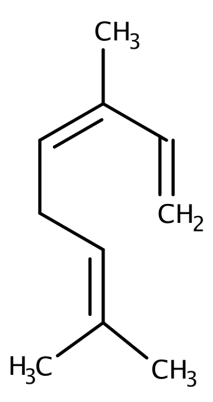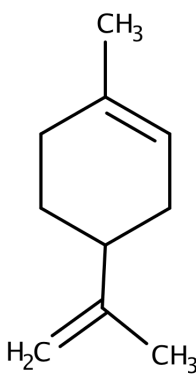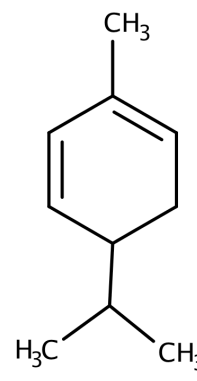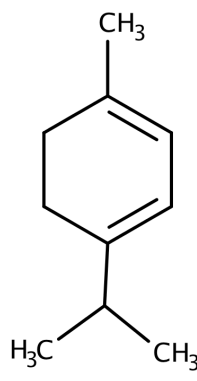
Terpenes	
Acyclic Monoterpene	

Ocimene

Monocyclic Monoterpenes		

| Limonene | α-Phellandrene | α-Terpinene |

Table 1 (continued)
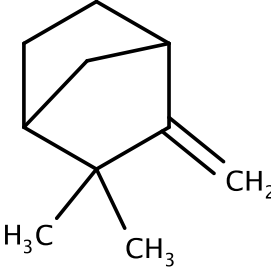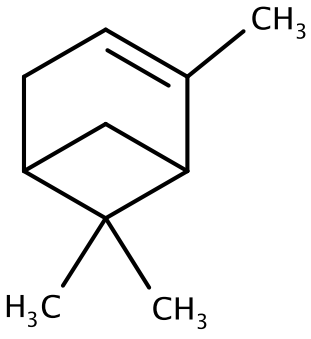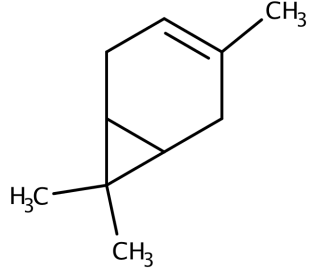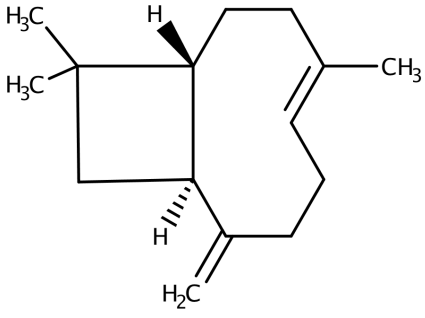
Bicyclic Monoterpenes		
 Camphene	 α-Pinene	 3-Carene
Bicyclic Sesquiterpene		
 t-Caryophyllene		

Table 1 (continued)
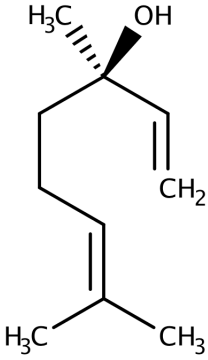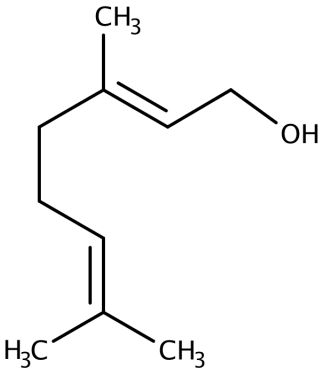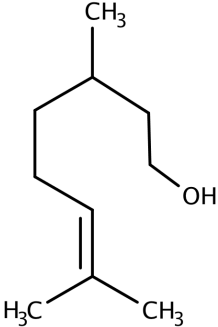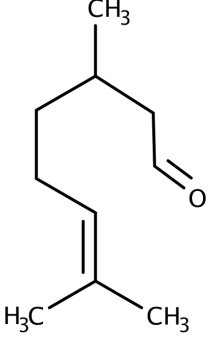
Terpenoids	
Acyclic Monoterpene Alcohols	
Allylic Alcohols	Linalool · Geraniol
Primary Alcohol	Citronellol
Acyclic Monoterpene Aldehyde	Citronellal

Table 1 (continued)
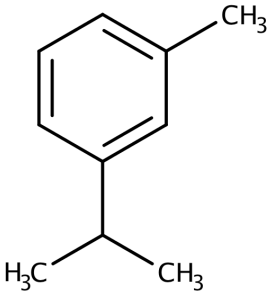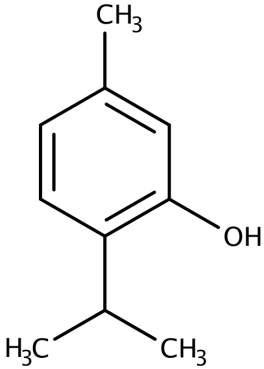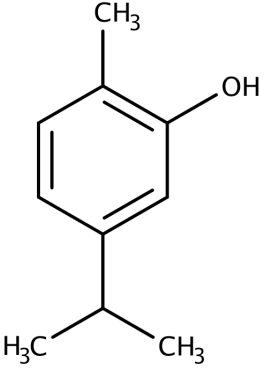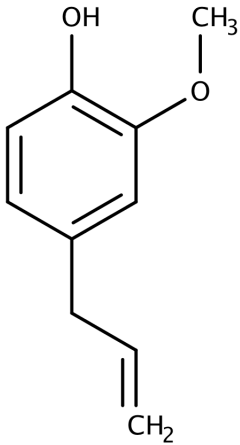
Monocyclic Aromatic Monoterpene	Cymene	
Monocyclic Monoterpene Phenols	Thymol	Carvacrol
Monocyclic Monoterpene Phenolic Ether	Eugenol	

Table 1 (continued)
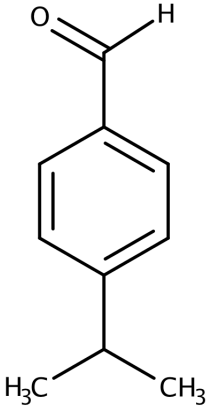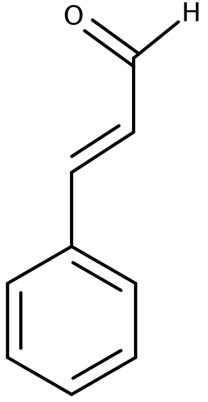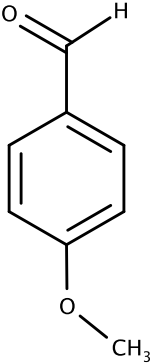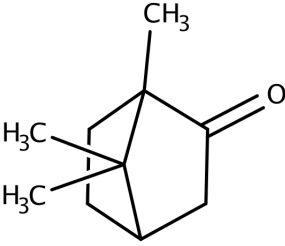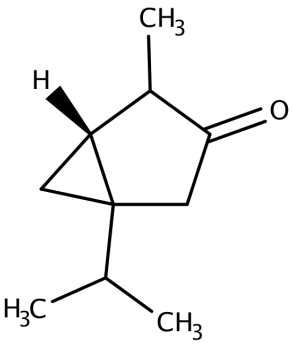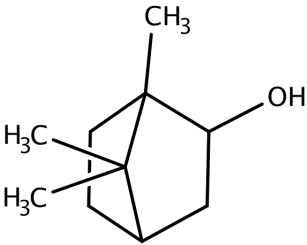
Monocyclic Monoterpene Aromatic Aldehydes	Cuminaldehyde	Cinnamaldehyde
Monocyclic Monoterpene Aromatic Methoxy-aldehyde	Anisaldehyde	
Bicyclic Monoterpene Ketones	Camphor	α-Thujone

Table 1 (continued)

Bicyclic Monoterpene Secondary Alcohol	Isoborneol

1.3.1 Activity of terpenes

 Some of the interesting effects that have been found for these terpenes include, but are not limited to, anti-oxidant and pro-oxidant [19-21], anti-fungal [22], anti-microbial [23-24] and anti-bacterial [25-27] activities. These effects have been examined using numerous methods. The antibacterial activity of six essential oils and 21 terpenoids was assessed against 25 different genera of bacteria [23]. This study found the phenolic compounds to be the most active with both the presence and location of the hydroxyl group determining the effectiveness of the antimicrobial agent.

 In somewhat contradictory results, the antibacterial activity of carvacrol and thymol against E. coli [27] was studied and the experiment found that while the presence of the hydroxyl group is important, there is no correlation between location of the hydroxyl group and the antibacterial strength. More importantly, Xu *et al.* proposed a mechanism for the antibacterial activity against E. coli. The study concludes that due to the hydrophobic capacity of these two phenolic monoterpenoids, they are able to permeabilize the membrane of the bacteria which affects membrane integrity allowing leakage of protons and eventually a complete

loss of membrane potential. It is suggested that the hydroxyl group present on these aromatic compounds is the functional group that enables them to transport proton across the membrane.

As to terpenes having both anti-oxidant and pro-oxidant activity, a review points to a study which determined that the concentration of the terpene is what determines this behavior with a higher concentration leading to pro-oxidant activity while low concentrations allow anti-oxidant reactivity [20, 28].

Other examples of methods used to study the effect of terpenes include an experiment which used 18 fungi species and a spectrophotometric absorbance test with tryptophan to show anti-fungal activity could be related to the LUMO (lowest unoccupied molecular orbital) energies of four monoterpenoid aldehydes. The study concluded that there is a correlation between aldehydes as electron acceptors and the corresponding antifungal activity [22].

Several studies have used model membranes composed of one (or more) phospholipids to measure antioxidant or antibacterial activity of terpenes [19, 25-26]. Two antibacterial studies utilized phospholipid LUVs (large unilamellar vesicles) by spectrophotometrically monitoring the release of trapped carboxyfluorescein [25-26]. Likewise, an antioxidant study was done with two lipid model systems – one using egg yolk homogenates as a source of lipid testing for lipid peroxidation and one using linoleic acid micelles testing for the formation of hydroperoxydienes [19]. This last study is the basis for our present study using fatty acid vesicles as model membranes to examine the activity of the terpene family of compounds.

1.4 Oleic Acid Vesicles

The term liposome generally refers to a bilayer membrane arranged in a

sphere as shown in Figure 3 [29]. Liposomes with biomimicry properties (or the
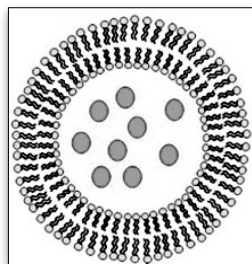
Figure 3 - Bilayer-membrane Liposome

ability to mimic biological membranes) are an advantage for *in vitro* studies into cell

membranes reducing the biohazard nature of biological studies. Most cellular

reactions depend on the structure of the cell membrane which is composed

primarily of phospholipids and proteins. Model membranes prepared from

phospholipids (example structure shown in Figure 4) are commonly used in

biological studies [31-32]. The effects of the addition of fatty acids (example

structure shown in Figure 5) to phospholipid liposomes have been studied [33-34].

However, membranes composed of exclusively fatty acids have only recently found

a place in studies looking at reactivities of cell membranes.
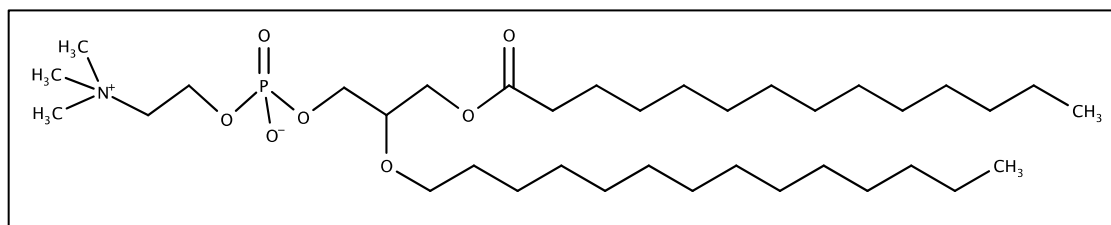
Figure 4 – Phospholipid (Dimyristoyl phosphatidylcholine)
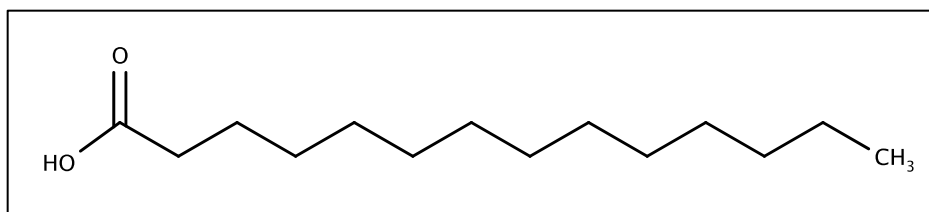
Figure 5 - Fatty Acid (Myristic Acid)

Gebicki and Hicks [30, 35-36] were the first to prepare and study membrane-enclosed bilayer vesicles composed of exclusively fatty acids which they called ufasomes because they were made out of unsaturated fatty acids. They were in search of a chemically homogeneous vesicle composed of only one type of compound in the bilayer membrane. Their defense of vesicle membranes made of fatty acids was that pure synthetic phospholipids are not readily available and the belief that the nonpolar fatty acids portion of the phospholipids determines the reactivities of the bilayer membrane rather than the polar head group. Fatty acid vesicles have been valued since then as biomimetic material and model membranes because of their simplicity. This ability of fatty acid vesicles to act in a biomimicry method is the basis for the present study.

1.4.1 Fatty Acid Vesicles as Protocells

A research group at Howard Hughes Medical Institute in the Department of Molecular Biology lead by Dr. Jack W. Szostak has been working with fatty acid vesicles as model protocells since 2001 [37]. This group has done a lot of work in analyzing the efficacy of these fatty acid vesicles as prebiotic protocells, a model for the origin of life, along with the properties associated with their formation and usage. They tested the formation [38-43], growth and division [44-48], osmoticity [49], stabilization [50-51], and reactivity [52-54]. A large body of the information

13

known today about fatty acid vesicles can be attributed to this group of researchers, including several chapters [40-42] in a book Methods in Enzymology which give the definitive method for forming and growing unilamellar vesicles.

1.4.2 Formation of Fatty Acid Vesicles

As mentioned previously, Gebicki and Hicks [35] are credited with the first preparation of fatty acid vesicles, experimenting with oleic acid and linoleic acid as the fatty acid base. Their study formed bilayer vesicles by dissolving the fatty acid in chloroform, evaporating the chloroform using a water vacuum pump and then a stream of nitrogen. The film of oleic acid formed was resuspended in 0.1 M Tris buffer, pH 8-9. Confirmation of a bilayer membranes was achieved using a freeze-fracture method [36].

pH dependence has been shown by Hargreaves/Deamer [55] and Haines [56] who performed titrations of fatty acids looking at the structures formed from pH 12 to pH 6. The structure-dependence was determined using phase-contrast microscopy by Hargreaves while Haines used ^{13}C NMR to determine the protonation state of the carboxyl group. They found that the titration curve shows two inflection points which they associate with phase changes from micelles structures above pH 9.45, liposomes from pH 9.45 to pH 7.15, and oil droplets below pH 7.15. Haines determined by NMR that the pKa of oleic acid is at pH 8.6. He further argues that the formation of oleic acid bilayer vesicles occurs at this pKa because of the stabilization afforded by alternating protonated carboxylic acid and anionic carboxylate molecules at the appropriate distance which leads to unusually strong, symmetrical hydrogen bonds as shown below (Figure 6).

14
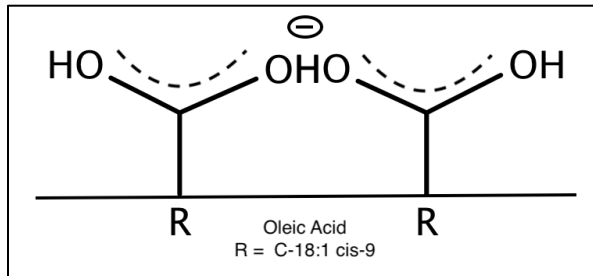
Figure 6 - Hydrogen Bonding of Fatty Acid Vesicles

The theory of the stabilization of fatty acid vesicle membranes by hydrogen bonding was modified in a study by Cistola *et al.* [57] that examined the stoichiometry of oleic acid to oleate in this lamellar phase. The ratio of oleic acid to unprotonated oleate at the pKa of the acid would be 1:1. However, the study concluded that because the stoichiometry can range from 1:1 to 1:3 (unionized to ionized), there is more at work than just hydrogen-bonding stabilization, including hydrocarbon interactions between the hydrophobic tails of the fatty acid molecules and charge repulsion between the polar headgroups.

1.4.3 Properties and Variables of Fatty Acid Vesicles

There are numerous variables in the formation, growth, stabilization and reactivity of fatty acid vesicles in general and oleic acid vesicles specifically. Pertinent aspects for our present study are reviewed below.

1.4.3.1 Size

There has been criticism [32, 58-59] on the usage of multilamellar liposomes as biological model membranes due to several concerns: the vast size distribution of these methods of formation; the reactive complexity of multiple layers of

membrane; and the relatively short half-life of these large liposomes. These concerns are addressed by adding an extrusion step to the formation process. After vesicles are formed in the aqueous buffer, the solution is extruded through polycarbonate membranes. The extrusion process creates a homogeneous size distribution of vesicles while retaining the efficacy of the bilayer membrane and the original contents of the vesicles.

1.4.3.2 Flip-Flop Effect

One of the advantages of fatty acid vesicles as model membranes is the dynamic equilibrium that occurs both between the individual molecules incorporated in the membrane and between the membrane and the surrounding environment. One such interaction is something known as the "flip-flop" effect. The flip-flop effect [30] is the ability of fatty acid molecules to rapidly flip from the outer layer of the bilayer membrane into the inner layer and vice versa as seen in Figure 7. This flip-flop dynamic is governed by the hydrophobicity of the lipid tail so is much more rapid for fatty acids than for phospholipids. The increase in speed of the flip-flop effect in fatty acid vesicle membranes allows for rapid growth of a fatty acid vesicle since as fatty acid molecules are incorporated into the outer layer from the surrounding solution, they can then flip to the inner layer making it possible for further introduction of molecules into the outer layer.
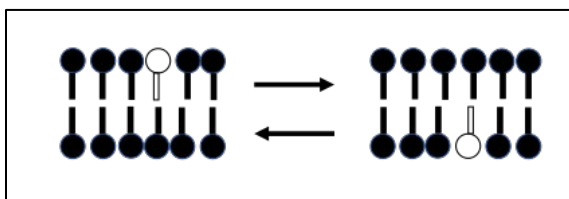
Figure 7 - The Flip-flop Equilibrium

The flip-flop effect can also account for several other aspects of the high degree of reactivity fatty acid vesicle membranes display. Membrane permeability is higher in fatty acid vesicles and can be accounted to this mechanism as flip-flop is utilized as a transport system. Unlike in phospholipid vesicles, pH gradients can also be achieved via the flip-flop effect due to cation permeability by the addition of an impermeant cation such as arginine [52].

1.4.3.3 Matrix Effect

Another interesting aspect of vesicle growth that has been studied is what is called the "matrix effect" [45, 60-62]. The matrix effect occurs when oleic acid micelles are added to a buffered solution of preformed vesicles that have been extruded to a specific size. The matrix effect process appears to be autocatalytic with the presence of the pre-formed vesicles speeding up the formation of new vesicles from the solution of micelles. There is evidence to support the theory that cooperative binding occurs between the micelles and the pre-formed vesicles causing an increase in the size of vesicles to a state where they split to form new vesicles. These splits result in an increase in the number of vesicles and, surprisingly, the newly-formed vesicles are indistinguishable from the preformed vesicles in size and content [63].

1.4.4 Reactivity of Fatty Acid Vesicles

The reactivity of fatty acid vesicles can be categorized into several areas: Permeability of the membrane can increase allowing the inner contents of the vesicle to leak out and/or compounds in the surrounding solution to leak into the

vesicle. <u>Fluidity</u> of the membrane can increase (or decrease) allowing more (or less) exchange between the solution inside the vesicle and the solvent in which the vesicle is suspended. Also, the attraction between vesicles can lead to <u>aggregation</u> and even <u>fusion</u>. Each of these reactivities will be examined more closely

1.4.4.1 Permeability

Permeability is the ability for the inner contents of a liposome to leak out and can be directly related to membrane tension and osmoticity [64]. The permeability of phospholipid membranes has been shown to increase upon the introduction of fatty acids into the membrane [30, 65]. This increase in permeability has been directly related to the dynamic ability of fatty acids to flip-flop allowing the fatty acid regions of the membrane to act as transport mechanisms [66]. The same flip-flop effect is seen in fatty acid vesicles [63]. This effect is analogous to proton transport and is the presumed reasoning behind the inability of fatty acid vesicles to maintain any kind of a pH gradient [52]. Several terpenes have been shown to disturb the equilibrium in phospholipid bilayers [25-27]. The terpenes studied were found to have strong hydrophobic capacities. As such, these terpenes will selectively embed themselves in the hydrophobic interior of the bilayer membrane. This perturbation of the membrane results in leakage of the interior solution through an increased permeability. A similar leakage has not been seen in fatty acid vesicles to date. Therefore, one aspect of the present study is to examine the permeability of fatty acid vesicles upon the addition of terpenes.

1.4.4.2 Fluidity

Fluidity is used as a measurement of the closeness of the packing of the inner hydrocarbon region of liposome membranes. Fluidity is measured in phospholipid vesicles using a non-polar fluorophore such as diphenylhexatriene (DPH) embedded in the interior of the membrane [26, 51, 55, 67-72]. The anisotropy of DPH is typically measured because of the extreme hydrophobicity of DPH which causes the molecule to burrow into the nonpolar inner region of the bilayer membrane. The confined space of the inner layer restricts the movement of DPH such that the fluorophore will give an anisotropy reading, or a difference in polarized fluorescence emission intensity.

In phospholipid bilayers, fluidity has been examined using anisotropy, showing an increase in fluidity upon the addition of fatty acids [73] or terpenes [26, 69]. This increase in fluidity was determined to be due to the perturbations the additions to the membrane cause in the hydrocarbon layer of the membrane.

Fluidity in fatty acid bilayer vesicles has also been studied using anisotropy of DPH to examine the stabilization of oleic acid vesicles using a cationic surfactant which causes a decrease in fluidity [72]. The results are hypothesized in the study to be related to the state of hydration of the surface of the membrane. Fluidity in the fatty acid vesicle upon the addition of terpenes has not been studied and is one aspect of the present study.

1.4.4.3 Aggregation

Extensive experimentation has been done on the aggregation of fatty acid molecules into micelles and vesicles, but less so on the aggregation of vesicles

themselves. Only very recently has this form of reactivity of fatty acid vesicles begun to be studied [74] and the findings are that one of the stabilizing factors in these vesicle solutions is "short-range hydration repulsion". The vesicles in a polar solution have been found to be largely hydrated which prevents them from grouping together or reacting with each other to form larger vesicles comingling their interior contents. Several studies have found methods that negate the stabilization effect of hydration however by using lysozyme [75], a salt [74], or even just temperature oscillations [76], although this last study also used aminopropyl triethoxysilane. The amine group of the amine additive most likely causes a reduction in hydration and is the reason aggregation can occur rather than solely the change in temperature.

Aggregation of vesicles in solution is routinely documented by observing an increase in turbidity measured in a visible absorbance increase. Aggregation is also often closely followed by fusion of vesicles with a corresponding decrease in turbidity [77].

1.4.4.4 Fusion

As with aggregation, fusion has been extensively studied using phospholipid vesicles [33, 64, 73, 77-85], ranging from experimentation on methods for determining if fusion has occurred, mechanisms by which fusion occurs and factors that can cause fusion to be more likely to occur. Very few studies have been reported on the fusion of pure fatty acid vesicles. The low likelihood of fusion of fatty acid vesicles is most likely due to the large hydration factor discussed previously with respect to aggregation. The improbability of fusion was confirmed

in the recent study [74] which used an amine group modification of oleic acid vesicles to reduce the hydration factor and then used NaCl to cause aggregation and fusion. They found that oleic acid vesicles without these modifications will not fuse.

There are two primary methods used to monitor vesicle fusion: The <u>complex-formation method</u> uses the formation of a complex ion (most commonly $Tb[DPA]_3^{3-}$) which fluoresces due to an internal energy transfer between the ligand and the metal ion. Alone the metal ion exhibits little to no fluorescent emission energy but with the ligand added, the emission energy increases dramatically. The metal ion and the ligand are placed inside separate solutions of vesicle membranes. These two solutions of membranes are subsequently brought together such that fusion can occur. This fusion can be detected by monitoring an increase in emission intensity of the metal complex ion.

The <u>Fluorescence Resonance Energy Transfer (FRET) method</u> utilizes a fluorescence pair of probes where the emission energy of one fluorophore (the donor) overlaps with the excitation energy of a second fluorophore (the acceptor) such that there is an energy transfer between the two. FRET is also called Förster Resonance Energy Transfer since the energy is not being transferred via fluorescence. This energy transfer is dependent on the proximity of the two probes and can be used to determine spacing in membrane. Several donor pair have been utilized, NBD/Rh (7-nitro-2,1,3-benzoadiazol-4-yl/Rhodiamine) and ANTS/DPX (8-aminonaphthalene-1,3,6-trisulfonate/p-xylylbis pyridinium bromide) being the most popular. There are two variations of the FRET method.

First, both fluorophores are placed in the same solution of vesicle membranes and none in a second solution of vesicle membranes. Fusion is monitored as an increase in donor fluorescence emission intensity based on the theory that as fusion occurs there is increased spacing between donor and acceptor fluorophore molecules reducing energy transfer to the acceptor fluorophore.

A second variation of FRET is to include the donor and acceptor fluorophore in separate solutions of vesicles. Fusion here is monitored as a decrease in donor fluorescence emission intensity based on the theory that mixing of membranes causes a closer proximity between the two fluorophore and increase in energy transfer.

One of the problems experienced with monitoring fusion of vesicles has to do with the mechanism involved. It is generally agreed that hemi-fusion (the combining of only the outer layer of the bi-layer membrane) is an intermediate step in the process of fusion of vesicle membranes. The first method of monitoring fusion by complex ion formation is more reliable for determining full fusion since the method monitors the mixing of the solutions inside the membranes rather than the membrane spacing.

1.4.5 Fatty Acid Vesicles and Terpenes

The properties and reactivities of fatty acid vesicles detailed above are the basis for the present study with the hypothesis that fatty acid vesicles show reactivities that can be utilized to study the mechanisms by which the terpene family of compounds show biological activity. This study proposes to form oleic acid vesicles and to utilize various fluorescent methods to view the degradation of these

vesicles upon the addition of a series of terpenes from the various families, e.g. monoterpenes - acyclic, monocyclic, and bicyclic; and monoterpenoids – alcohols, ketones, aromatic alcohols, and aromatic aldehydes.

1.5 Instrumentation

1.5.1 Gas Chromatography

Gas chromatography is a separation method which can used for samples which are readily volatilized without decomposing [86-87]. All chromatography methods use the idea of polar versus nonpolar compounds to separate mixtures of compounds. Regardless of the type of chromatography, all consist of a mobile phase which moves across or through a stationary phase. The stationary phase is either a liquid or a solid while the mobile phase can be either a gas or a liquid. The mobile phase is generally an inert gas such as hydrogen, helium or nitrogen for gas chromatography and the choice of gas is usually determined by the nature of the chemicals being separated, the availability of the inert gas, and by the detector used with the separation method. Helium is generally used in gas chromatography-mass spectrometry because helium is non-flammable and therefore safer than hydrogen and as a small molecule will therefore have less mass transfer effect than nitrogen. The stationary phase of gas chromatography is of vital importance in the performance of the separation of compounds, determining the efficiency of the separation. The first part of our study used a capillary column which has the stationary phase coated on the inside of the column.

The overarching equation that determines the performance of all forms of chromatography as a separation method is the van Deemter equation:

$$H = A + \frac{B}{\bar{u}} + C\bar{u} \qquad (1)$$

where H is the theoretical plate height, A is the eddy diffusion, B is the longitudinal diffusion, C is the resistance to mass transfer, and $\bar{u}$ is the average linear velocity of the gas mobile phase. The goal for optimal chromatographic separation is to minimize the theoretical plate height. In capillary column GC, there is no packing material in the column and therefore no eddy diffusion around the packing material so the A term of the van Deemter equation is equal to zero. The value of the B term is determined by the amount of time the analytes being separated spend interacting with the stationary phase and so a higher carrier gas flow velocity will reduce the B term very quickly as can be seen in Figure 8 [88]. The resistance to mass transfer in the C term is dependent on the carrier gas in GC with larger, heavier gases such as nitrogen increasing the resistance very quickly. Gases with smaller molecule sizes such as helium and hydrogen have much less resistance to mass transfer and therefore allow for higher gas flow velocity.
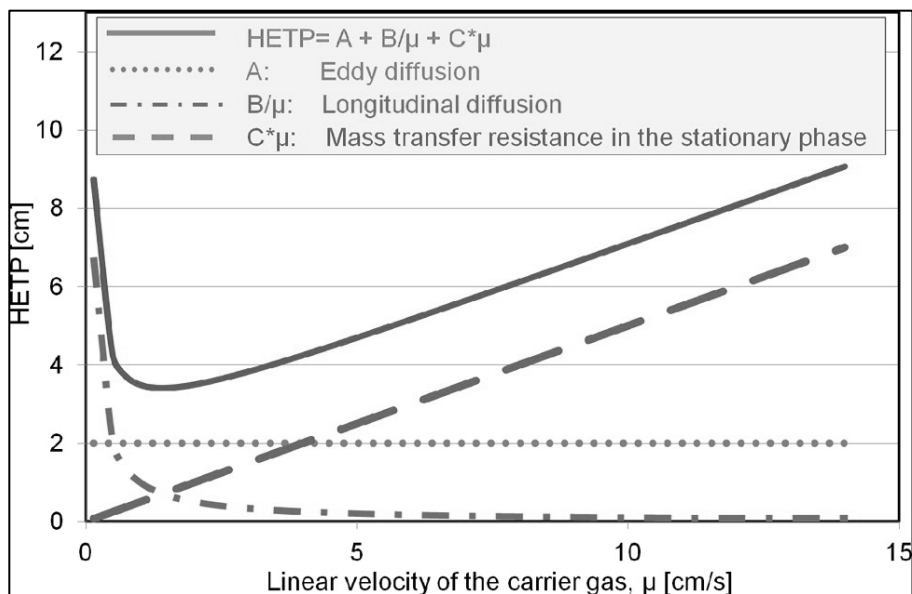
Figure 8 - van Deemter plot

Capillary GC uses a long, hollow fused silica tubing with a very narrow inner diameter and the stationary phase coating the inside of the tubing. The length of the column allows for a large surface area with no packing for minimal cross diffusion and a high number of theoretical plates to allow for highly efficient separation. The column used for the first part of this study was a Rxi-5ms (5% phenol, 95% polydimethylsiloxane). This type of column has a low-polarity phase with low bleed, improved signal-to-noise ratio and a high temperature limit and are commonly used for general purposes for semi volatiles, phenols and amines [89].

The experiment was performed in split injection mode so as to avoid overwhelming the column. The injection port was unpacked to prevent breakage of the SPME fibers (Figure 9) used in sample injection. Sample injection was achieved using solid phase microextraction fibers (SPME) chosen based on the polarity and volatility of the analytes. SPME is a solid phase extraction method in which a fiber was exposed to the smoke of the incense allowing for adsorption to the fiber and

followed by desorption into the injection port of the gas chromatograph. The SPME

fibers chosen for the first part of our study were DVB/CAR/PDMS

(Divinylbenzene/Carboxen on Polydimethylsiloxane fiber core). These are reported

to be more versatile for compounds with a larger range of molecular weights.
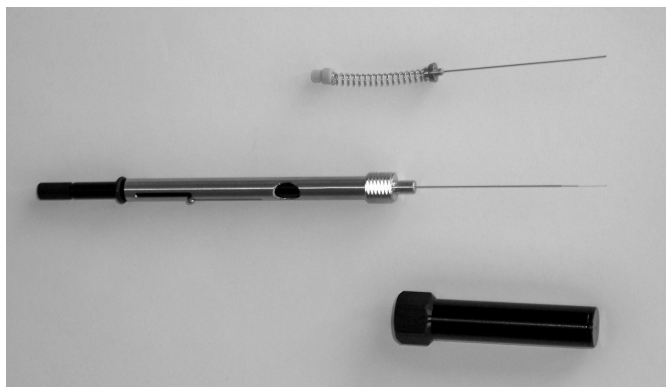
Figure 9 - SPME Fiber Assembly

1.5.2 Mass Spectrometry

Mass spectrometry was the detection system used in conjunction with gas

chromatography in the study of incense. A mass spectrometer operates as a detector

by analyzing the mass of each of the analytes as they emerge from the gas

chromatography column [87, 90]. The mass spectrometer in the first part of our

study used a quadrupole mass analyzer preceded by electron ionization.

Electron ionization is a process by which the incoming analytes are exposed

to a stream of highly energetic electrons [90]. When the electron field of an analyte

molecule resonates with a highly kinetic electron, ionization can occur removing an

additional electron from the molecule leaving behind a radical cation (Equation 2).

$$M + e^- \rightarrow M^{+\cdot} + 2e^- \qquad (2)$$
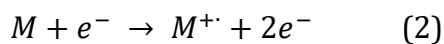
The radical cation is generally unstable and will often fragment into smaller ions

forming ion cloud which passes into the mass analyzer for separation of masses and

detection.

The quadrupole mass analyzer [91] consists of four cylindrical electrodes

arranged parallel to one another along the z-axis for a cross-sectional view as seen

in Figure 10.
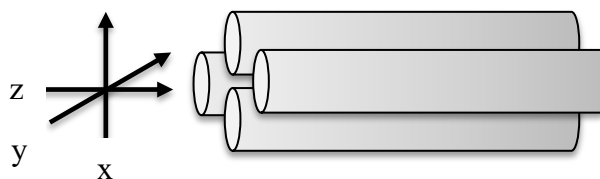
Figure 10 - Quadrupole Mass Analyzer

A time-independent (dc) potential and a time-dependent (ac) potential are placed

on the X-Z and Y-Z planes, respectively. The ac potential along the Y-Z plane

alternates between positive and negative potentials and ions oscillate between

being drawn towards the center between the poles and pushed toward the poles.

The dc potential along the X-Z plane is positive. The combined effect of these

potentials depends on the mass of the ion. High-mass ions will feel primarily the

effect of the positive dc potential and will be focused into the center while low-mass

ions will more fully be affected by the ac potential. This focusing effect may generate

enough acceleration towards a negative electrode to cause an ion to collide with the

electrode effectively neutralizing the molecule or fragment and removing it from the

process. Thus, the electrodes act as a bandpass mass filter, filtering out all ions

without the appropriate mass to maintain stability when passing through the

electrodes. By varying the magnitude of the potentials, a scan of masses can be done

very quickly, leading to a complete output of mass-to-charge readings for each

analyte as it passes through the detector. Alternately, the magnitude of the potentials can be focused to allow only select ions to pass through to the detector, known as Selective Ion Monitoring (SIM) mode.

1.5.3 Fluorescence Spectrophotometry

Fluorescence spectrophotometry was used in the second part of our study to examine the reactivities of oleic acid vesicles based on the absorption and emission of several chemical compounds known to fluoresce. Fluorescence [87, 92-93] occurs when absorbed energy is emitted at a lower energy and longer wavelength than absorption. Jablonski's diagram, shown below in Figure 11 [94], helps to illustrate these energy changes. When energy is absorbed, a fluorophore molecule is left in an excited energy state (S_1 or S_2 in the diagram) at any of the possible vibrational levels. In fluorescence, radiation-less internal conversion and vibrational relaxation down to the lowest vibrational level of the excited state S_1 occurs very quickly and are followed by an emission of light as the molecule loses energy back down to the ground state S_0.
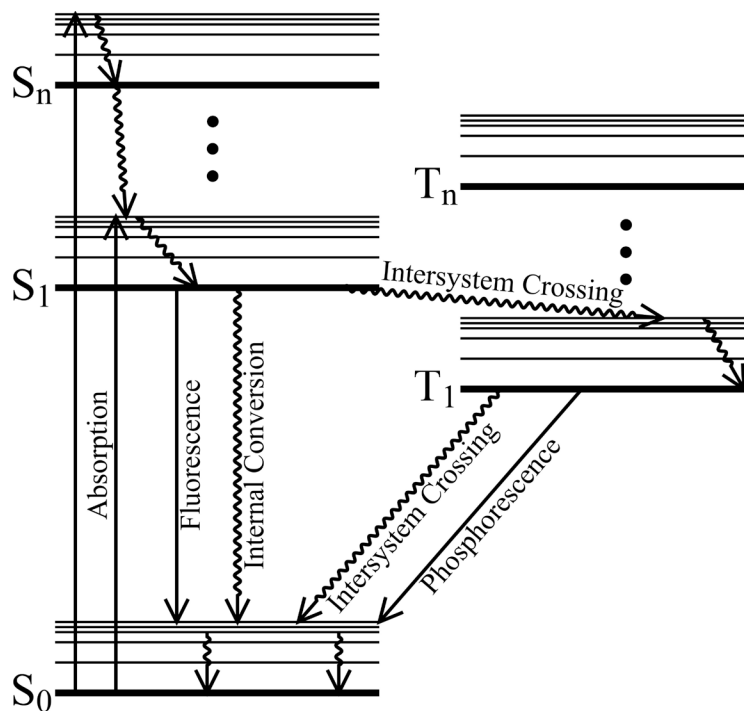
Figure 11 - Jablonski's Diagram

Typically, a fluorophore with a known high quantum yield will demonstrate a linear correlation between fluorescence intensity and fluorophore concentrations. Fluorescence is highly dependent on environmental effects [93] however so the linearity between emission intensity and concentration must be first established for the solvent system of choice.

Two additional aspects of fluorescence (anisotropy and FRET) will be used in the second part of our study. Fluorescence anisotropy is based on the principle that fluorophores will preferentially absorb light that is polarized in the same direction as the fluorophore molecule and is expressed by equation 3:

$$r = \frac{I\| - I\perp}{I\| + 2\,I\perp} \qquad (3)$$

29

where $I_\parallel$ and $I_\perp$ are emitted fluorescent intensities polarized parallel and perpendicular, respectively, to polarization of excitation beam as seen in the following diagram (Figure 12 [95]).
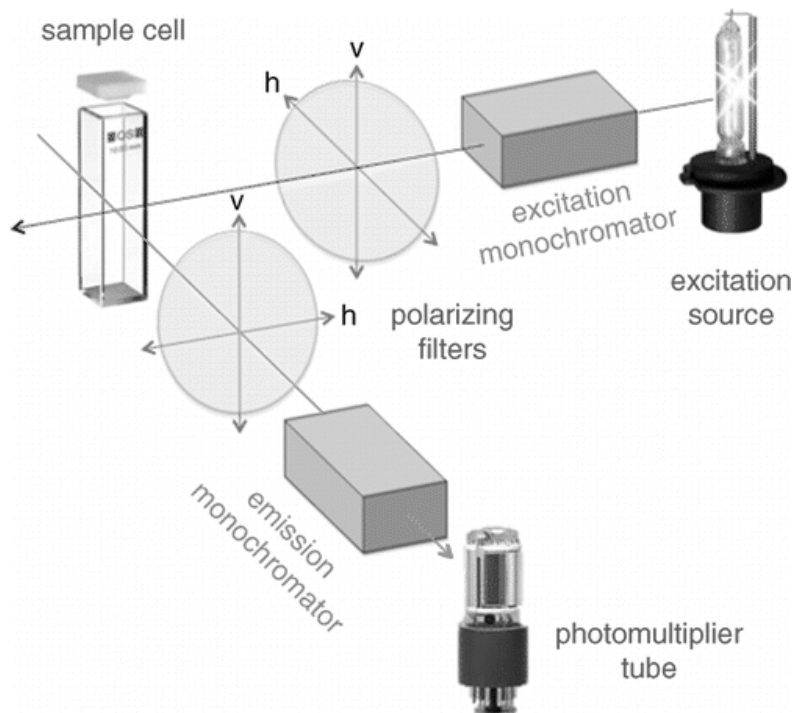
Figure 12 - Diagram of Fluorescence Anisotropy

In a solution of freely-moving fluorophore molecules, exciting with polarized light will give equal emission intensities when intensities are measured polarized parallel and perpendicular to the excitation polarization and resulting in an anisotropy calculation of zero. However, when the fluorophore molecules are bound, for example in a closely-packed membrane, the average movement of the molecules is more limited and a small but positive anisotropy will be seen.

Another aspect of fluorescence used in the second part of our study is known as fluorescent resonance energy transfer (FRET). FRET can occur between different fluorophore when the emission energy of one fluorophore (known as the donor) is

equal to the excitation energy of a different fluorophore (known as the acceptor). A pair of these molecules must be in close physical proximity to one another for the energy transfer to occur. FRET is usually observed by exciting the fluorophore at the excitation energy of the donor fluorophore and detecting the emission intensity of the acceptor fluorophore. FRET can be measured by calculating an efficiency of the energy transfer using equation 4 [45].

$$E = 1 - F_{da}/F_d \qquad (4)$$

where F_{da} and F_d are the donor emission intensity in the presence and absence of the acceptor, respectively.

Chapter 2 - Incense

2.1 Incense as used in ecclesiastical settings

Incense as used in the Catholic and Orthodox churches incense is burned on smoldering charcoal and the resulting smoke permeates everything in the space available. Incense consists of a base of frankincense resin with added essential oils to change the scent.

The first part of our study hypothesizes that incense as used ecclesiastically can be analyzed for content using GC-MS to create a library of compounds with special focus on a family of organic compounds known as the terpenes.

2.1.1 Terpene Content of Incense

Terpene chemistry [18] is integral to the study of incense because of the plant origin of frankincense. All terpene chemistry is based on the isoprene unit, C_5H_8 (Figure 2). The volatile and semi-volatile combinations of this unit are the smaller compounds – monoterpenes (two isoprene units, $C_{10}H_{16}$), sesquiterpenes (three isoprene units, $C_{15}H_{24}$) and some diterpenes (four isoprene units, $C_{20}H_{32}$).
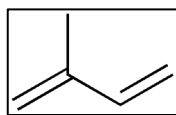
Figure 13 - Isoprene Unit

The terpene compounds commonly found in frankincense can be divided into acyclic and cyclic mono-, sesqui-, and di-terpene/terpenoid compounds as shown on the following pages (Table 2). Also shown is the mass spectra for each compound.

Table 2 - Monoterpenes and terpenoids
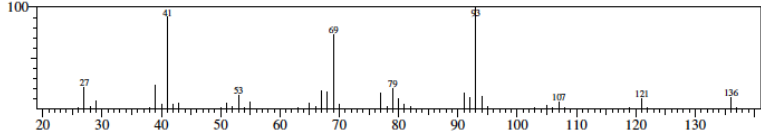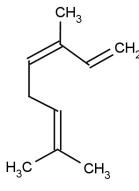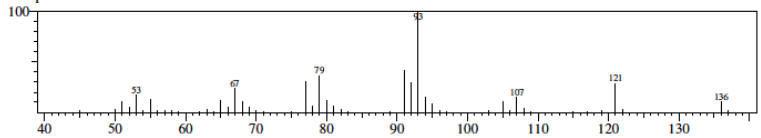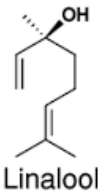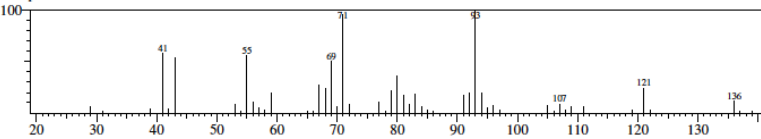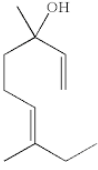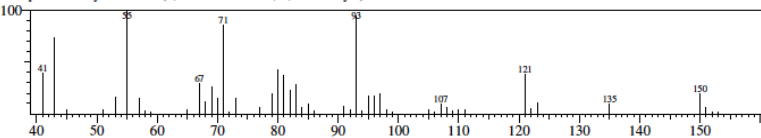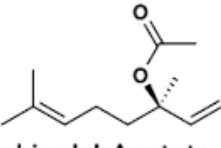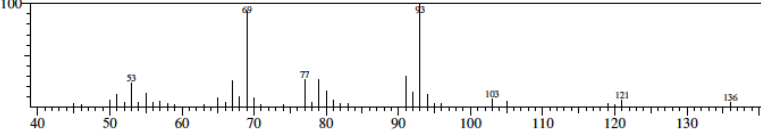
Acyclic monoterpenes	Mass Spectra of Modern Incense Components
α-myrcene	Formula:C10H16 CAS:123-35-3 MolWeight:136 RetIndex:68 CompName:.beta.-Myrcene
CH₃ CH₂ H₃C CH₃ β-ocimene	Formula:C10H16 CAS:3779-61-1 MolWeight:136 RetIndex:108 CompName:trans-B-ocimene
Acyclic monoterpenoids	
OH Linalool	Formula:C10H18O CAS:78-70-6 MolWeight:154 RetIndex:83 CompName:Linalool
OH Ethyl Linalool	Formula:C11H20O CAS:10339-55-6 MolWeight:168 RetIndex:98 CompName:Ethyl Linalool (1,6-Nonadien-3-ol, 3,7-dimethyl-)
O Linalyl Acetate	Formula:C12H20O2 CAS:115-95-7 MolWeight:196 RetIndex:131 CompName:Linalyl Acetate

Table 2 (continued)
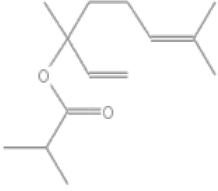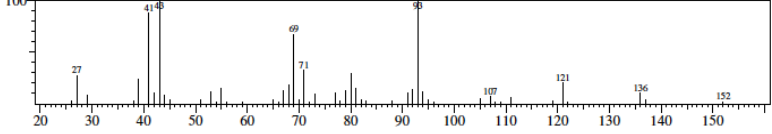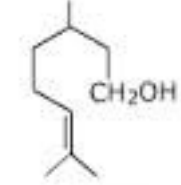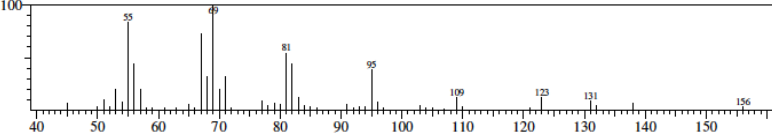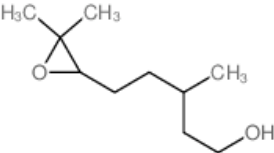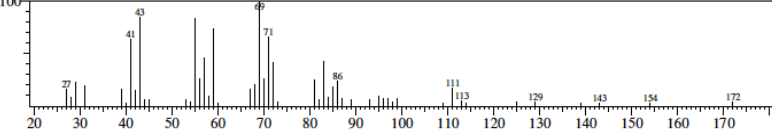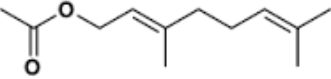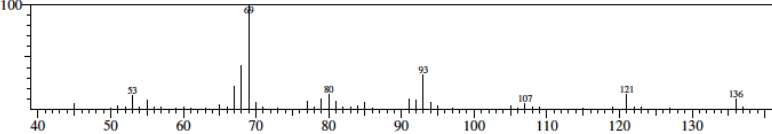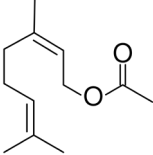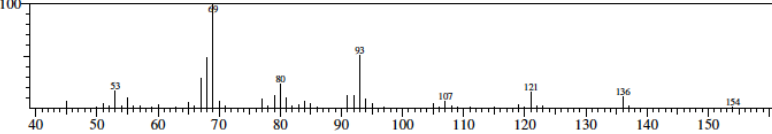
Linalyl Isobutyrate	Formula:C14H24O2 CAS:78-35-3 MolWeight:224 RetIndex:108 CompName:Linalyl isobutyrate
Citronellol	Formula:C10H20O CAS:1000149-87-3 MolWeight:156 RetIndex:103 CompName:a-Citronellol
Citronellol Epoxide	Formula:C10H20O2 CAS:1000163-92-8 MolWeight:172 RetIndex:132 CompName:Citronellol epoxide (R or S)
Geranyl Acetate	Formula:C12H20O2 CAS:105-87-3 MolWeight:196 RetIndex:130 CompName:Geranyl acetate
Neryl Acetate	Formula:C12H20O2 CAS:141-12-8 MolWeight:196 RetIndex:127 CompName:Neryl acetate

Table 2 (continued)
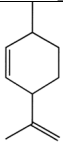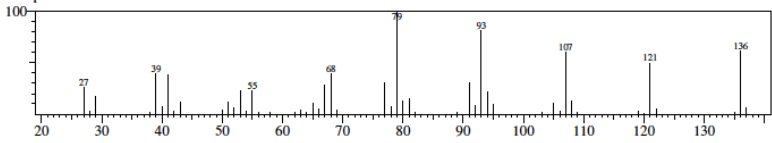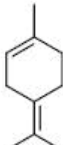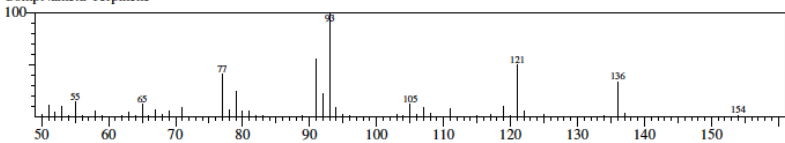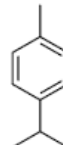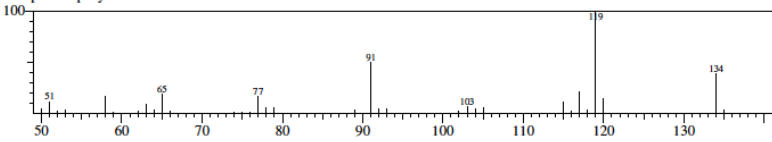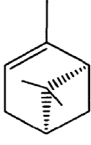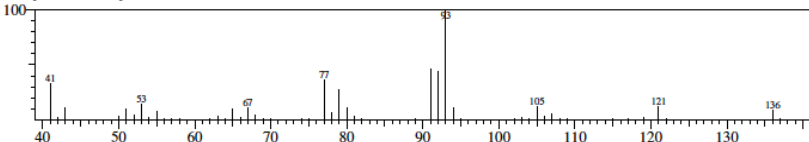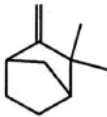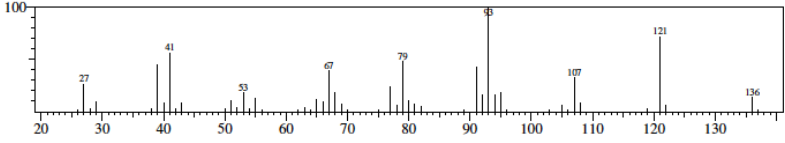
Monocyclic monoterpenes	
 isolimonene	Formula:C10H16 CAS:1000149-85-9 MolWeight:136 RetIndex:0 CompName:Isolimonene
 δ-Terpinene	Formula:C10H16 CAS:99-86-5 MolWeight:136 RetIndex:74 CompName:a-Terpinene
 p-Cymene	Formula:C10H14 CAS:99-87-6 MolWeight:134 RetIndex:74 CompName:p-Cymene
Bicyclic monoterpenes	
 (alpha-pinene).	Formula:C10H16 CAS:7785-70-8 MolWeight:136 RetIndex:61 CompName:1R-.alpha.-Pinene
 camphene	Formula:C10H16 CAS:79-92-5 MolWeight:136 RetIndex:64 CompName:Camphene

Table 2 (continued)
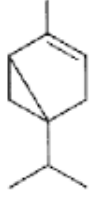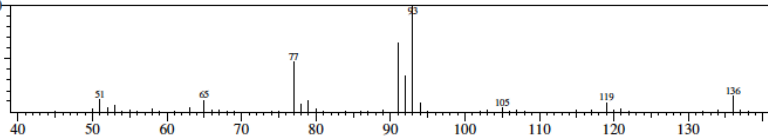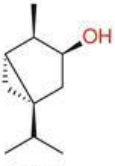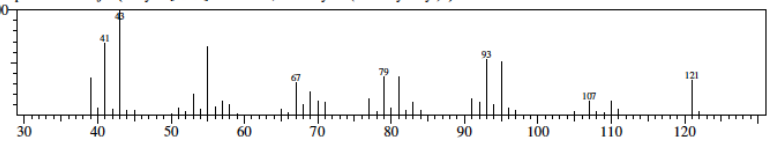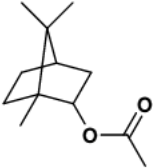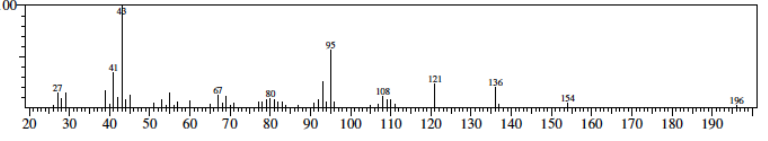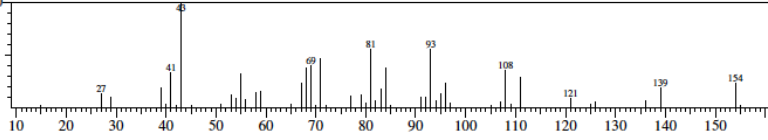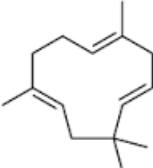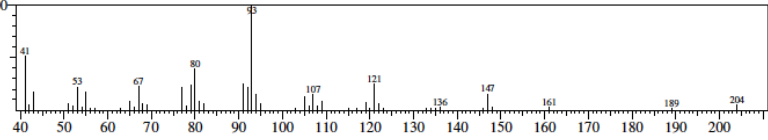
α-thujene	Formula:C10H16 CAS:2867-5-2 MolWeight:136 RetIndex:71 CompName:a-Thujene
Bicyclic monoterpenoids	
thujol	Formula:C10H18O CAS:513-23-5 MolWeight:154 RetIndex:96 CompName:Isothujol {Bicyclo[3.1.0]hexan-3-ol, 4-methyl-1-(1-methylethyl)-}
Bornyl Acetate	Formula:C12H20O2 CAS:1000245-86-9 MolWeight:196 RetIndex:116 CompName:Bornyl acetate
Eucalyptol	Formula:C10H18O CAS:470-82-6 MolWeight:154 RetIndex:74 CompName:Eucalyptol
Monocyclic Sesquiterpene	
Humulene (α-Caryophyllene)	Formula:C15H24 CAS:6753-98-6 MolWeight:204 RetIndex:141 CompName:,alpha.-Caryophyllene

Table 2 (continued)
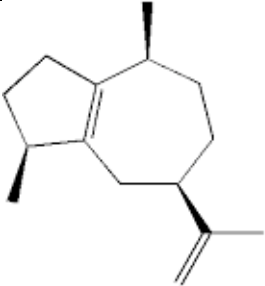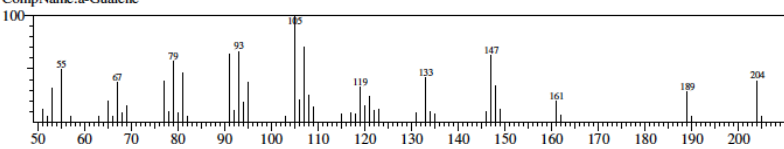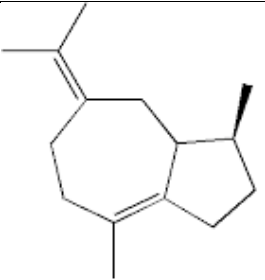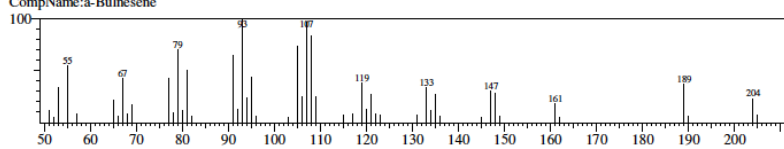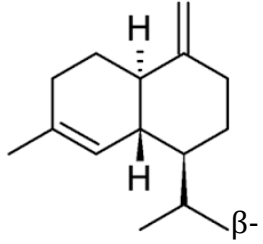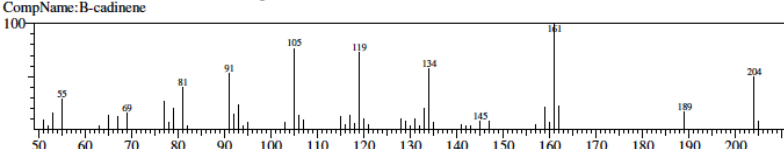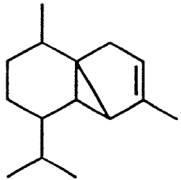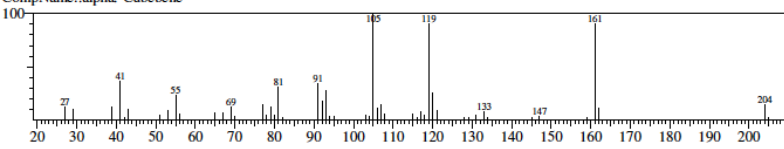
Bicyclic Sesquiterpenes	
α-Guaiene	Formula:C15H24 CAS:3691-12-1 MolWeight:204 RetIndex:143 CompName:a-Guaiene *(mass spectrum)*
α-Bulnesene	Formula:C15H24 CAS:3691-11-0 MolWeight:204 RetIndex:155 CompName:a-Bulnesene *(mass spectrum)*
β-Cadinene	Formula:C15H24 CAS:523-47-7 MolWeight:204 RetIndex:159 CompName:B-cadinene *(mass spectrum)*
Tricyclic Sesquiterpenes	
α-Cubebene	Formula:C15H24 CAS:17699-14-8 MolWeight:204 RetIndex:127 CompName:.alpha.-Cubebene *(mass spectrum)*

Table 2 (continued)
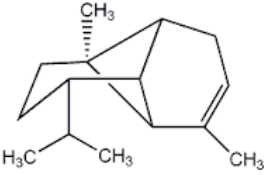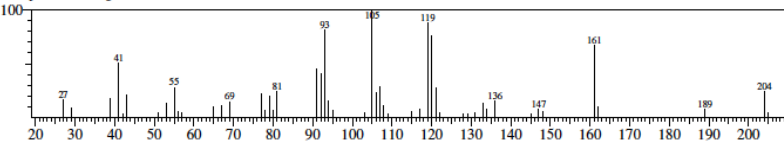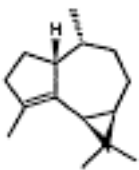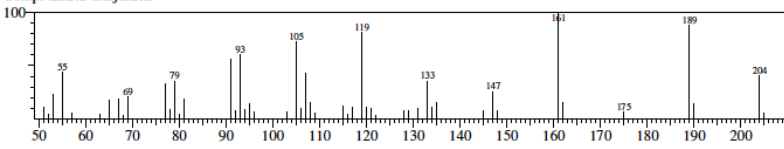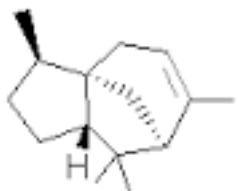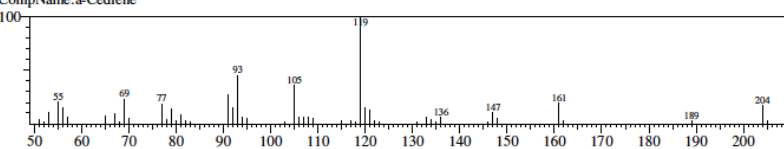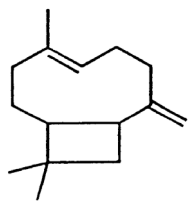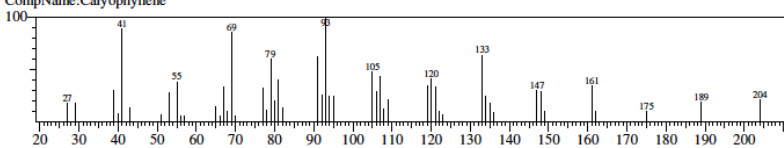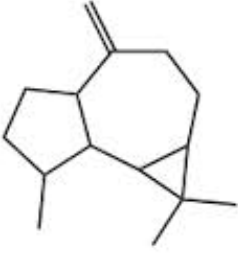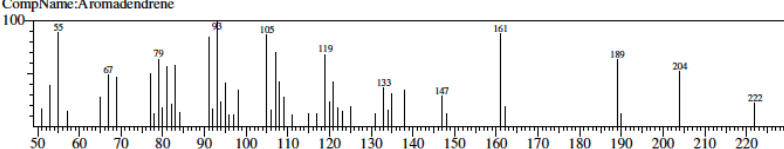
 Ylangene	Formula:C15H24 CAS:14912-44-8 MolWeight:204 RetIndex:0 CompName:Ylangene
 (-)-α-gurjunene	Formula:C15H24 CAS:489-40-7 MolWeight:204 RetIndex:134 CompName:a-Gurjunene
 α-cedrene	Formula:C15H24 CAS:469-61-4 MolWeight:204 RetIndex:140 CompName:a-Cedrene
 β-Caryophyllene	Formula:C15H24 CAS:87-44-5 MolWeight:204 RetIndex:141 CompName:Caryophyllene
 Aromadendrene	Formula:C15H24 CAS:72747-25-2 MolWeight:204 RetIndex:185 CompName:Aromadendrene

Table 2 (continued)
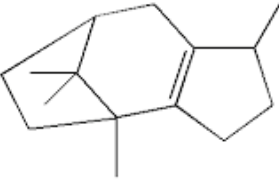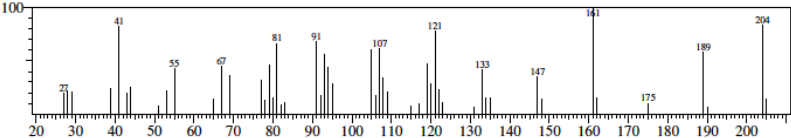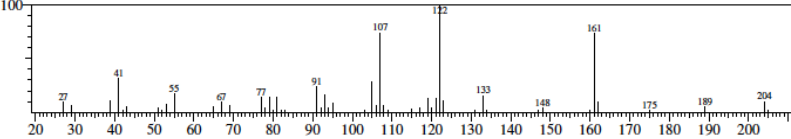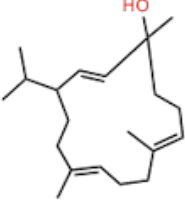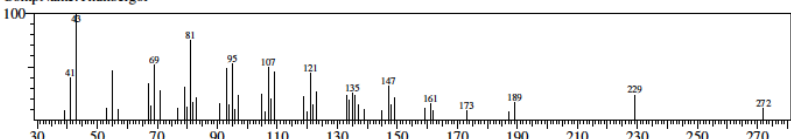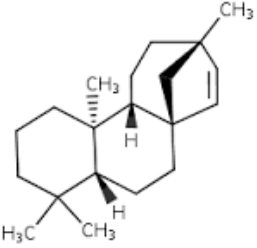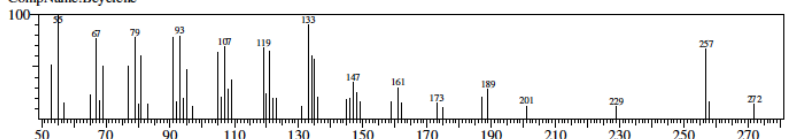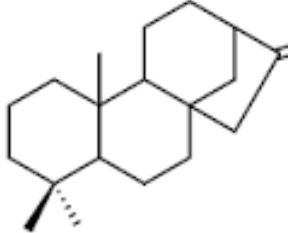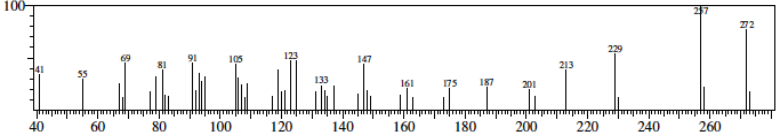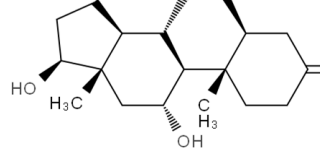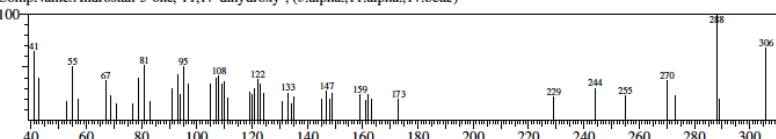
 β-Patchoulene	Formula:C15H24 CAS:1405-16-9 MolWeight:204 RetIndex:149 CompName:Patchoulene
 α-Panasinsen	Formula:C15H24 CAS:1000157-62-7 MolWeight:204 RetIndex:146 CompName:(-)-.alpha.-Panasinsen
Monocyclic Diterpenoid	
 Thunbergol	Formula:C20H34O CAS:25269-17-4 MolWeight:290 RetIndex:264 CompName:Thunbergol
Tetracyclic Diterpenes	
 Beyerene	Formula:C20H32 CAS:3564-54-3 MolWeight:272 RetIndex:234 CompName:Beyerene

39

Table 2 (continued)

Kaurene	Formula:C20H32 CAS:562-28-7 MolWeight:272 RetIndex:255 CompName:Kaur-16-ene
Tetracyclic Diterpenoid	
Androstan-3-one, 11,17-dihydroxy-, (5a,11a,17b)-	Formula:C19H30O3 CAS:25788-56-1 MolWeight:306 RetIndex:263 CompName:Androstan-3-one, 11,17-dihydroxy-, (5.alpha.,11.alpha.,17.beta.)-

2.2 Analysis of Incense

Hamm *et al.* [5] used headspace SPME GC-MS on several species of frankincense and compiled a database of 131 compounds. They then applied these findings to a Mt. Athos "traditional incense" or an incense as traditionally used in the Orthodox church. Their method will be the starting point for the method development in the first part of our study. There are two aspects of the ecclesiastical usage of incense that their database does not address: the addition of other scents to the frankincense and the contents of the smoke emitted as a result of burning the incense.

40

The special scents that are added to frankincense can be analyzed using the same method as for frankincense as has been shown in several studies. SPME fiber headspace analysis was utilized in the analysis of the essential oils of grapefruit and lavender [96] and the honeysuckle flower at different stages of life [97] using the same SPME fiber collection method as we propose to use for frankincense.

The other aspect of concern to our study is the content of the smoke released from the incense. While the volatiles released from the smoke of several variations of incense sticks have been studied [6], these were not frankincense based. They do report that the smoke samples show almost 100 more compounds than the headspace analysis. We propose to use the SPME GC-MS method used in headspace analysis [98] to build a library of compounds present in modern incense smoke.

Optimal temperature and optimal equilibrium time are a balancing act when using SPME fibers to analyze terpenes. Hamm's study sites competition for the active sites on the coating of the SPME fiber, where lower-volatility compounds can displace high-volatility compounds given a longer time to reach equilibrium. In spite of the site competition, SPME fiber analysis has several advantages: SPME is a non-destructive and non-invasive method; analysis can be performed on only the volatiles, eliminating the pretreatment necessary for traditional GC of resin-type materials; there are numerous types of SPME fibers available which can be chosen based on the specific compounds to be studied; and finally, while optimal experimental times and temperatures peak intensities may not be at maximum for all compounds, they are large enough to ensure detection of the compounds of interest.

We propose to optimize the SPME fiber collection method for the burning of incense, adjusting the equilibrium time as needed.

2.2.1 Incense Analysis Method

Chemicals and reagents used include: Incense (More than two dozen scents) and Charcoal (Three Kings) provided by St. Athanasius Orthodox Church (Nicholasville, KY) and Hermitage of the Holy Cross Monastery (Wayne, WV); Octyl Acetate, >99% (Sigma-Aldrich, Milwaukee, WI); SPME fibers – DVB/CAR/PDMS, 50/30um (Supelco, Bellefonte, PA).

Charcoal was cut into smaller pieces ($\sim$1 cm^3) and lit using a Fisher burner or a handheld lighter until smoldering and placed in an evaporating dish. A single piece ($\sim$0.5 cm^3) of incense was placed on top of the charcoal. Once smoke began to visibly rise from the incense, the SPME fiber was exposed for five seconds in the smoke stream 2-4 cm above the incense.

The SPME fiber was then immediately injected for 2 min into a Shimadzu GC-MS QP5000 using a Rxi-5ms column (length 30 m, thickness 0.25 um, diameter 0.25 mm) under the following conditions: split injection (29:1 split ratio, 29.3 mL/min total flow, 0.9 mL/min column flow) Injector port at 210°C; Oven at 50°C for 2 min, 30°C/min to 110°C, 8°C/min to 270°C, hold 5 min; Detector at 240°C. Mass spectra were collected using electron ionization operating in the full scan mode, scanning m/z 45 to 550 at 1 sec interval to produce a total ion chromatogram (TIC) for each compound that came through the capillary column. Gas chromatogram peaks were identified using the data provided by the TIC and the NIST98 library of mass spectral data for each of the incense scents listed in Table 3. This table represents a

wide range of scents while not comprising the entire body of incense available for

usage in ecclesiastical settings.

Table 3 - List of Incense Scents Analyzed

Bethlehem
Burning Bush
Cassia
Coptic
Cypress
Ethiopian Frankincense
Evergreen & Embers
Gethsemene
Honeysuckle
Hyssop
Orange Blossom
Rose
Sarov
Shepherd's Field
Somolian Frankincense

A library specifically for our study was developed with retention times

relative to octyl acetate, present in most samples of incense. When octyl acetate was

not present, a SPME fiber was exposed to the headspace of pure octyl acetate for 1-2

seconds before being exposed to the incense to confirm the retention time of the

octyl acetate and develop a library of retention times for the other compounds

detected.

In the cases when multiple SPME fibers were exposed either to the same

piece of incense or to be transported to the GC-MS instrument, the fiber was

transported in a sealed glass test tube. A travel blank was analyzed frequently to

ensure no contamination from the storage test tubes.

SPME fibers were conditioned between each run on a Varian 3400 GC without a detector for 45 min at: Injector port – 250 °C; Oven – 150 °C with fiber exposed for the entire time. Blanks were tested on a regular basis to ensure complete removal of all compounds during conditioning.

2.2.2 Optimization of SPME Method

Temperature and equilibrium time are a balancing act when using SPME fibers to analyze terpenes. The temperature must be high enough to vaporize the larger, less volatile diterpenes. The more volatile, smaller monoterpenes begin to be desorbed from the SPME fiber however, if the temperature is too high. The same kind of balance must be found for equilibrium time.

2.2.2.1 SPME Fiber Equality Experiment

Equality in the absorption of different SPME fibers exposed to the same incense smoke must first be assured before testing the equilibrium time of SPME fibers. An atrium gate, purchased from Home Depot, was used to hold the SPME fibers close together as seen in the pictures (Figure 14). The atrium gate was placed directly on top of the burning incense holding four similar SPME fibers. The fibers were exposed for 15 sec as 60 mg of Honeysuckle incense was burned on a hotplate set at maximum power. The fibers were stored in glass test tubes until analysis by GC-MS as previously reported.
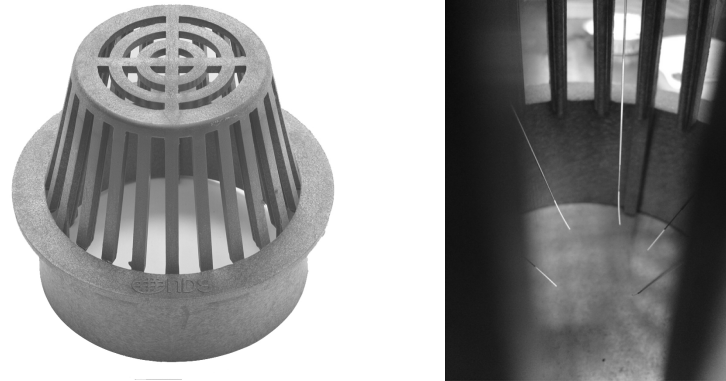
Figure 14 - Atrium Gate

Shown below in Table 4 is the data from one trial of four similar SPME fibers exposed to the same stream of incense smoke for the same amount of time using the atrium gate. The four SPME fibers were analyzed by GC-MS about 30 minutes apart in numerical order, and stored in capped glass test tubes until analysis. The following line graph in Figure 15 shows the variations of peak areas versus each of the peak times. An interesting trend demonstrated is the higher concentration of the later, heavier compounds in the first SPME fibers run on the GC, while the fibers analyzed last show higher concentrations in the earlier, smaller compounds. This trend confirms the need for a consistent equilibrium time for SPME.

Table 4 – Comparison of Peak Areas in SPME Equality

Comparison of Peak Areas for 4 SPME Fibers					
Peak Time	SPME 1	SPME 2	SPME 4	SPME 5	RSD
8.5	24944822	62439110	56690900	45896351	34.789
11.4	20906350	35483623	31918891	30601068	20.964
15.5	68392608	93151596	83768554	87329123	12.720
21	78160339	76490642	68344580	75050270	5.775
22.7	67921335	60501017	50775901	67786166	13.108
23	97722562	74525043	64414117	82727950	17.628
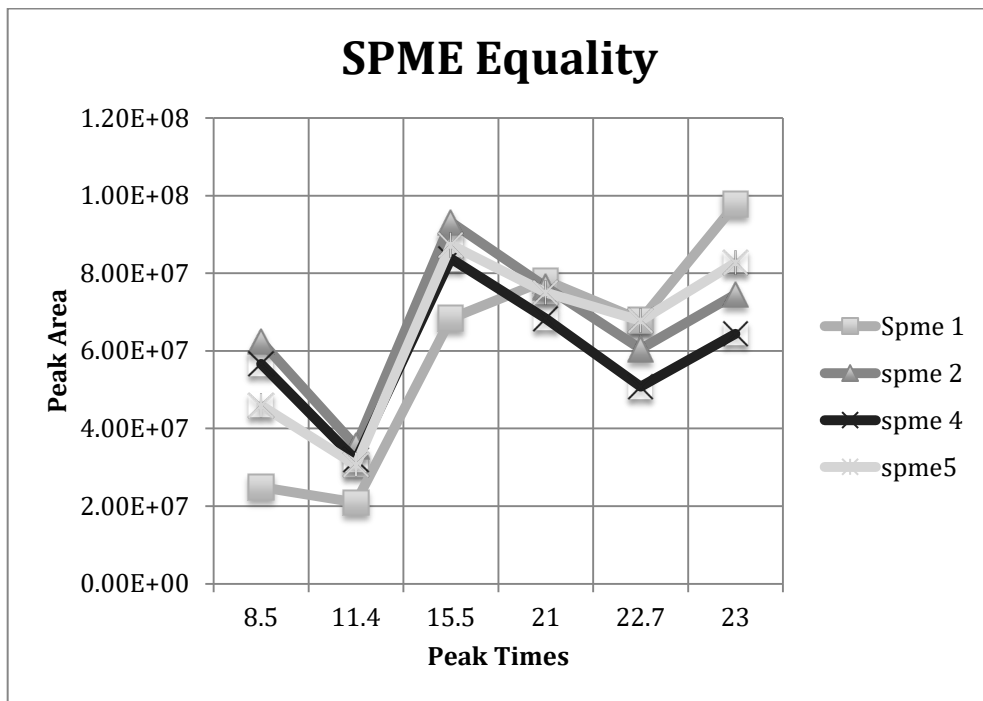
Figure 15 - Graph of SPME Equality

2.2.3 Temperature

The majority of SPME analysis of frankincense performed to date [5-6, 99] has absorbed and analyzed the VOC content of the headspace of the sample at <100 °C. This low-temperature analysis is also true for the analysis of other essential oils [96-97, 100] that are used for the various scents of ecclesiastical incense. A comparison of incense smoke components to literature values is unreliable at best and may be impossible due to the difference in temperatures at which the incense is burned.

The burning of incense in the church can be compared to the "pyrolysis" performed by Assefa [13]. Pyrolysis in this literature study refers to the melting and vaporization of frankincense at varying degrees: 400 °C on a hotplate, <1000 °C in a can on red-hot charcoal and 1000 C-1200 °C directly on red-hot charcoal. At each temperature, only the time, odor, color and physical appearance were recorded. The smoke was not tested for identification or quantification of the compounds emitted.

We propose to analyze the smoke of vaporizing incense at the temperatures achieved on red-hot charcoal as is typical in ecclesiastical settings versus a more controlled burn on a hotplate. The hypothesis is that the compounds released by the incense will vary depending on the temperature at which the incense is heated/burned.

2.2.3.1 Charcoal Analysis

Red-hot charcoal is reported to achieve a temperature of >1000°C [13], The charcoal tested reached a maximum of 350°C. Our reading however, was limited by

47

the temperature testing method which consisted of an infrared thermometer with a maximum of 350°C so the actual temperature most likely was much higher.

SPME fiber samples of the smoke of charcoal-burned Honeysuckle incense were taken at the beginning of the burn (as melting/vaporization began); after the incense had been smoking for a bit and the powder on the outside was visibly gone but the incense piece was not yet turning black (full vaporization); and at the end of the burning process when the incense was completely black (vaporization complete, combustion begun). All SPME were analyzed by GC-MS as previously reported.

Samples taken from beginning of burn, middle of burn and end of burn show similarities in the beginning and middle of burn but a completely different composition at the end of the burn when the incense has turned black. The following gas chromatograms in Figure 16 show the results of SPME sampling at the beginning, middle and end of the burn. While the first two chromatograms are very similar in content, the end of the burn shows a noticeably lower concentration of the

smaller, more volatile compounds and similar intensities for the larger, heavier compounds detected in the last third of the run.
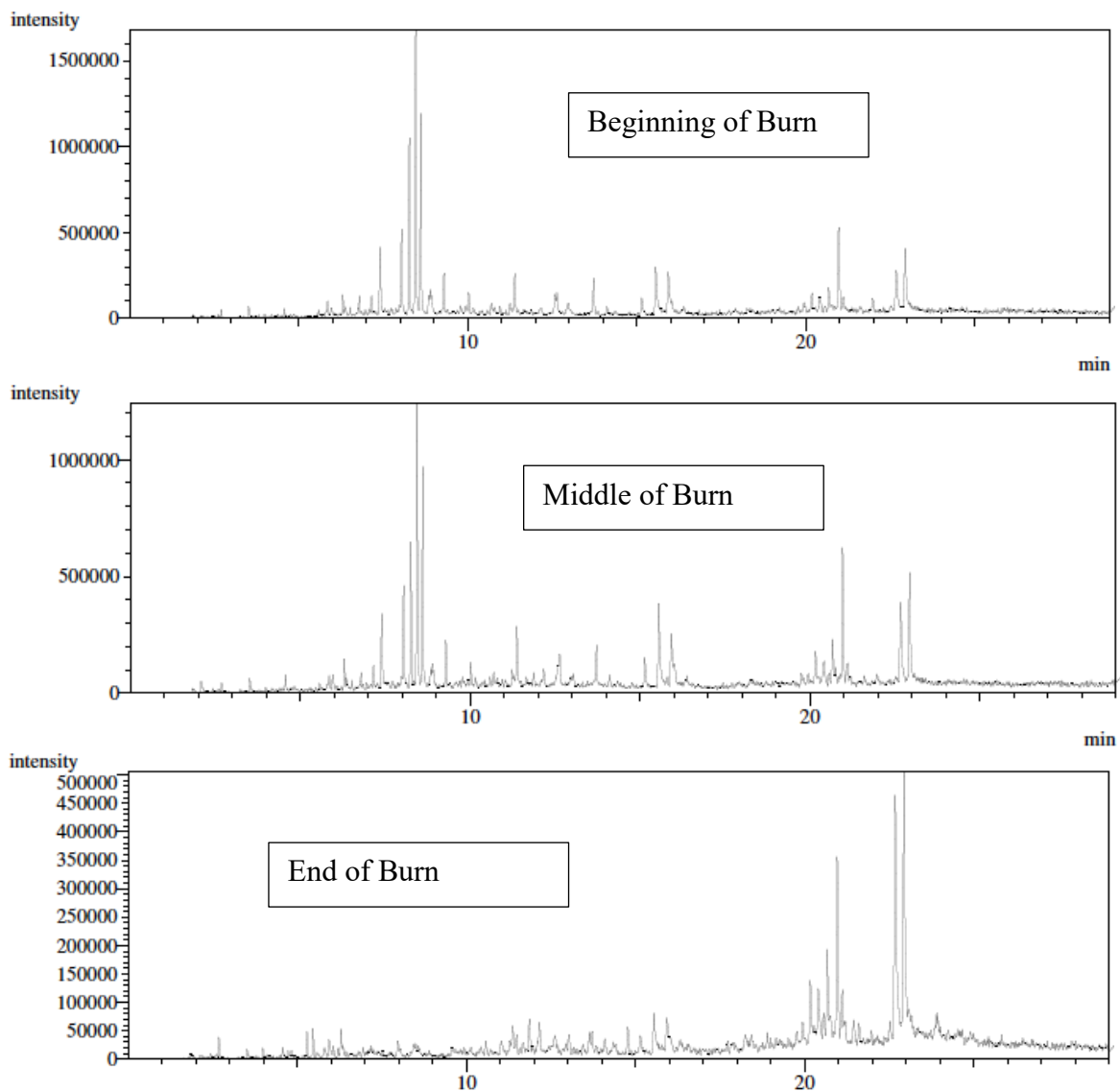
Figure 16 - Chromatograms of Honeysuckle Incense

The conclusion of the stages of burning test from visible data is that melting/vaporization does take place as the incense is first heated. Then combustion of the non-volatile components takes place as the incense turns black after the volatile components have all evaporated. The semi-volatile diterpenes that

elute between 21-23 minutes are present in all three samples while the more volatile monoterpenes are seen in very small intensities in the 'end of burn' data.

It is interesting to note that incense burned in the church is generally not allowed to burn to black according to a representative of St. Athanasius Orthodox Church with experience in the process. Rather the incense is scraped off the charcoal and fresh incense applied to prevent the "bitter smell" that comes as the end of the burn.

2.2.3.2 Hotplate Analysis

Honeysuckle incense was ground and 50 mg weighed out in a 3-in diameter aluminum weighing boat. The boat was placed on a hotplate once maximum temperature was achieved. A maximum temperature of 340°C was seen at 50% power. Maximum power reached a temperature of 450°C.

Quantitative amounts of incense could be burned with the pieces ground smaller and melting and evaporation is clearly visible. One problem with the hotplate at maximum power is that the incense is completely vaporized very quickly and combustion of non-volatile compounds is almost unavoidable. The following chromatograms in Figure 17 compare honeysuckle incense burned on the hotplate versus 'middle of burn' on charcoal.
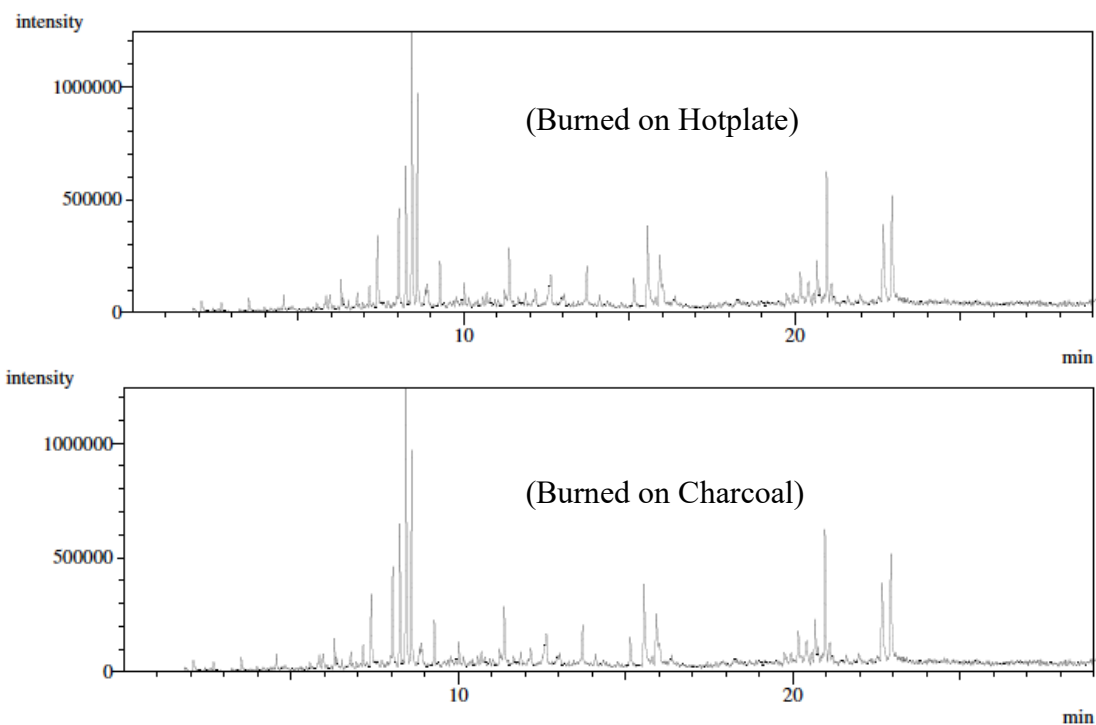
Figure 17 - GC Chromatogram of Hotplate Analysis

The conclusion drawn from the charcoal-hotplate experiment is that hotplate burning is comparable to charcoal burning for basic content analysis. Additionally, 50% power does not achieve complete vaporization very quickly and so prolongs the melting/vaporization process to allow for testing the equilibrium process of the SPME fibers.

2.2.4 Frankincense vs. Added Scent Experiment

Samples of the components of Honeysuckle incense (Ethiopian Frankincense, Honeysuckle fragrance, and China powder), along with a new sample of Honeysuckle incense (not yet fully cured) were obtained from Holy Cross Monastery. Each was individually burned on charcoal and analyzed by SPME-GC-MS as reported previously. The china powder that coats the incense to prevent sticking

was not analyzed by GC-MS because it did not react when placed on the red-hot charcoal and no smoke was emitted.

Ethiopian frankincense, honeysuckle fragrance and honeysuckle incense were tested as the components of Honeysuckle incense and the following chromatograms (Figure 18) clearly show the components that can be attributed to Ethiopian Frankincense and those of the Honeysuckle scent. These chromatograms also show that these two components, frankincense and added honeysuckle scent, do indeed account for all the compounds found in honeysuckle incense.
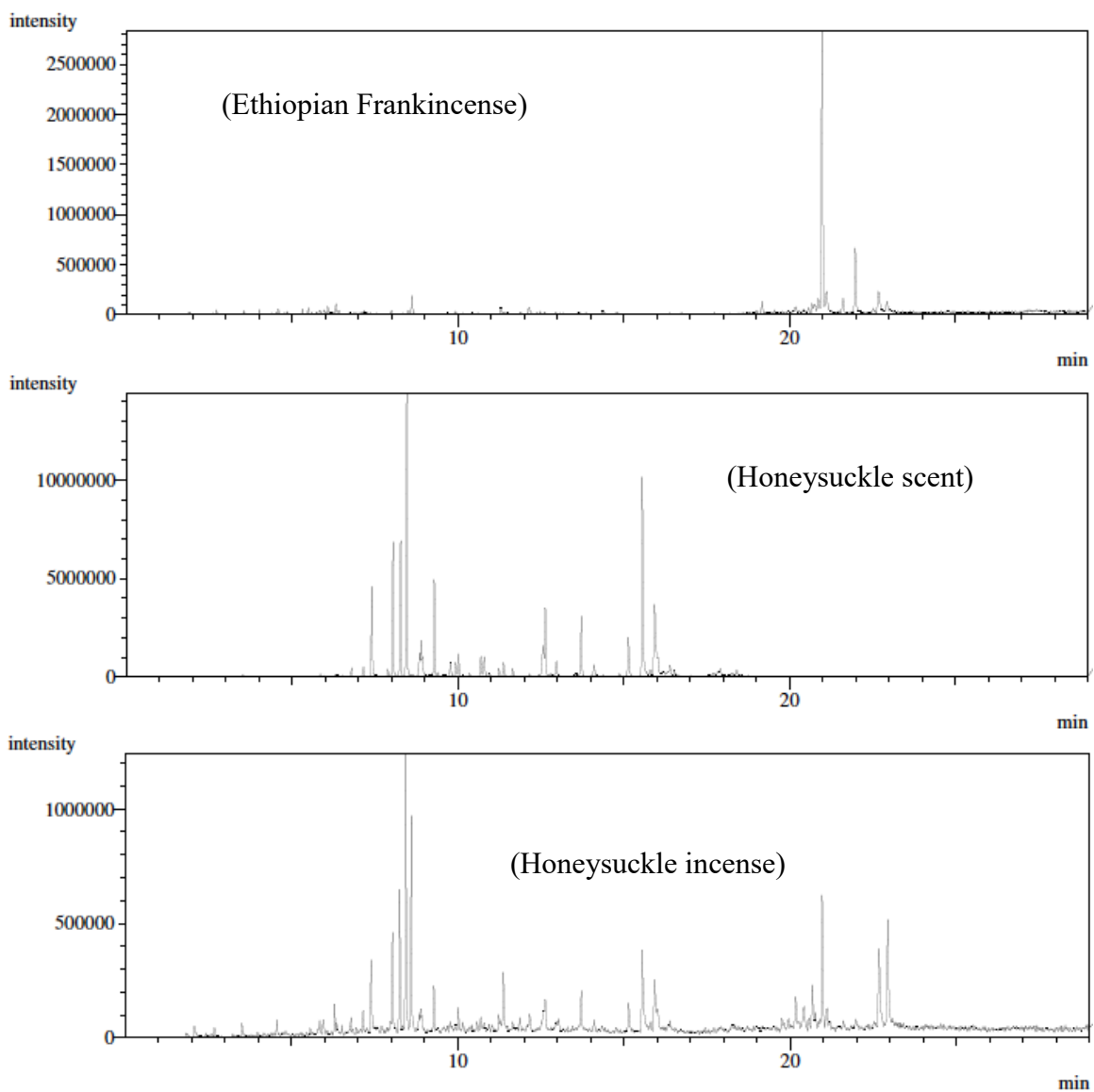
Figure 18 - GC Chromatograms of Components of Honeysuckle Incense

2.3 Results and Discussion

A library was constructed of 73 compounds identified from the incense
tested. They are listed in the following table (Table 5) along with their CAS number,
and retention time relative to octyl acetate. There are several compounds,
specifically several terpenes of interest, that are commonly found in frankincense

that were not detected in our present study. These are the compounds that show no retention index in the table, e.g. B-pinene and limonene. Also, there are several compounds, which were detected in the tested incenses but they have not yet been identified. The unidentified peaks are particularly those in the latter part of the chromatogram (Retention Indices 1700-2400). A longer separation time as optimized by Hamm *et al.* [98] could be the answer to detecting the missing smaller compounds and to identifying the larger ones.

The 15 incenses examined by SPME-GC-MS all show different combinations of these compounds (Table 6). Some are clearly of the Athonite style, showing frankincense components as well as other compounds due to the additional scents. Shown below are the components of the 15 incenses tested. The terpenes and terpenoids are highlighted. Notice that there are two columns side-by-side for the incense Honeysuckle with very different components listed. These are two samples obtained at different times that had the same name but show different components when analyzed by SPME-GC-MS.

Table 5 – Retention Times of Incense

Incense Library		
Compound	CAS Number	Rel. RI
a-Pinene	80-56-8	612
Camphene	79-92-5	640
B-Myrcene	123-35-3	680
B-Pinene	127-91-3	
a-Thujene	[2867-05-2	710
Dipropylene glycol, #1	110-98-5	723
Cymene	99-87-6	740
Eucalyptol	470-82-6	745
Dipropylene glycol, #3	106-62-7	753
1-Octanol	111-87-5	786
Linalool	78-70-6	830
Limonene	138-86-3	
Phenethanol	60-12-8	860
Phenylmethylacetate	140-11-4	934
Isothujol	513-23-5	960
Ethyl linalool	10339-55-6	980
a-Terpineol	98-55-5	990
Ocytlacetate	112-14-1	1000
a-Citronellol	106-22-9	1036
Ocimene (Dimethyloctatriene)	502-99-8 (a-); 3338-55-4 (cis-B); 3779-61-1 (trans-B)	1081
Linalyl isobutyrate	78-35-3	1078
Naphthalene	91-20-3	
Cinnamaldehyde	104-55-2	1123
Isopulegol	7786-67-6	1140
Benzyl-t-butanol	103-05-9	1162
Bornyl acetate	1000245-86-9	1161
Isobornyl acetate	125-12-2	
4-t-Butylcyclohexylacetate	32210-23-4	1230
Aminomethylbenzoate	134-20-3	1249
Neryl acetate	141-12-8	1260
Eugenol	97-53-0	1270
a-Cubebene	17699-14-8	1271
Geranyl acetate	105-87-3	1300
Linalyl acetate	115-95-7	1307

Table 5 (continued)

Citronellol epoxide	1000163-92-8	1320
Ylangene	14912-44-8	1326
a-Gurjunene	489-40-7	1338
Vanillin	121-33-5	1360
Diphenyl ether	101-84-8	1365
Methyl cinnamate	103-26-4	
a-Cedrene	469-61-4	1400
Caryophyllene	87-44-5	1412
a-Guaiene	[3691-12-1	1435
Hydroxycinnamic acid	583-17-5	1447
Ethyl vanillin	121-32-4	1460
a-Panasiene	10000157-62-7	1460
a-Caryophyllene (a-Humulene)	6753-98-6	1476
Patchoulene	1405-16-9	1488
a-Isomethylionone		1510
a-Bulnesene	3691-11-0	1555
1-ethoxy-naphthalene	[5328-01-8	1590
B-Cadinene	523-47-7	1590
3-Buten-1-ol, 2-methyl-4-(2,6,6-trimethyl-1-cyclohen-1yl)	62924-27-8	1637
Hexyl octanoate	1117-55-1	1670
Diethyl phthalate	84-66-2	1700
Acetonaphthone	941-98-0	1754
Isocitronellol	1000149-89-1	1810
		1848
Aromadendrene	72747-25-2	1852
Hexyl cinnamaldehyde	101-86-0	1977
Benzyl benzoate	120-51-4	2012
Isopropyl myristate	110-27-0	2074
		2149
Benzyloxybenzoic acid	1486-51-7	2191
Beyerene		2338
		2366
Beyerene	3564-54-3	2428
Kaur-16-ene	562-28-7	2546
Androstan-3-one, dihydroxy	25788-56-1	2633
Thunbergol	25269-17-4	2639
4,8,13-Duvatriene-1,3-diol	7220-78-2	2660

Table 6 - Components of Examined Incense

Components of liturgical incense (in retention order)	Bethlehem	Burning Bush	Cassia	Coptic	Cypress	Eth. Frank.	Evgrn & Emb	Gethsemene	Honeysuckle (old)	Honysuckle (new)	Hyssop	Orange Blossom	Rose	Sarov	Shpd's Field	Som. Frank.
a-Pinene	X			X										X		X
Camphene	X													X		X
B-Myrcene				X				X								X
B-Pinene																
a-Thujene	X															
Dipropylene glycol, #1			X		X											
Cymene		X		X				X				X		X		X
Eucalyptol				X							X					
Dipropylene glycol, #3			X		X											
1-Octanol		X	X											X		
Linalool		X						X			X			X		
Limonene																
Phenethanol		X							X	X		X	X	X		
Phenylmethyl-acetate			X							X						
Isothujol										X						
Ethyl linalool										X						
a-Terpineol																
Ocytlacetate	X	X	X	X	X	X	X	X	X	X	X	X	X	X	X	X
a-Citronellol	X	X											X	X		
Ocimene (Dimethyl-octatriene)											X			X	X	
Linalyl isobutyrate								X								
Naphthalene																
Cinnamaldehyde		X	X													
Isopulegol																
Benzyl-t-butanol														X		
Bornyl acetate						X										
Isobornyl acetate																
4-t-Butyl-cyclohexylacetate					X						X				X	

Table 6 (continued)

Aminomethyl-benzoate							X								
Neryl acetate							X			X					
Eugenol		X	X												
a-Cubebene															X
Geranyl acetate				X			X			X					
Linalyl acetate													X	X	
Citronellol epoxide								X	X					X	
Ylangene															X
a-Gurjunene		X													
Vanillin															
Diphenyl ether		X											X		
Methyl cinnamate															
a-Cedrene						X								X	
Caryophyllene		X											X	X	X
a-Guaiene		X				X				X				X	
Hydroxycinnamic acid													X		
Ethyl vanillin															
a-Panasiene		X							X						
a-Caryophyllene (a-Humulene)															X
Patchoulene		X													
a-Isomethylionone															
a-Bulnesene		X												X	
1-ethoxy-naphthalene															
B-Cadinene															X
3-Buten-1-ol, 2-methyl-4-(2,6,6-trimethyl-1-cyclohen-1yl)															
Hexyl octanoate						X			X						
Diethyl phthalate	X	X				X									
															X
Acetonaphthone									X		X				
Isocitronellol									X						
C15H22O2						X			X						
Aromadendrene		X													

Table 6 (continued)

Hexyl cinnamaldehyde									X						
Benzyl benzoate									X						
Isopropyl myristate								X							
								X							
Benzyloxybenzoic acid								X							
Beyerene			X				X				X		X		
Beyerene	X				X	X		X		X					
Kaur-16-ene					X										
Androstan-3-one, dihydroxy			X			X	X	X	X		X	X		X	
Thunbergol															X
4,8,13-Duvatriene-1,3-diol			X			X	X	X	X		X	X		X	

In conclusion, the goal for the first part of our study was to create a library of components found in incense with particular interest paid to the compounds known as the terpenes after optimizing a SPME-GC-MS method for their analysis. Our goal was partially achieved. The SPME-GC-MS method was optimized for the analysis of incense as used in ecclesiastical settings. The method devised was used to create a library of compounds, with corresponding retention indices and mass spectra, as can be found in a selection of incense used in ecclesiastical settings. However, vast differences in the components of incense were found dependent on the species of frankincense used as the base and the essential oils added for scent. Identification of all the compounds found in all the variations of incense available commercially for ecclesiastical use and, furthermore, absolute quantitation of the components of

incense was deemed too large a project for the present study but may be pursued in the future.

A turn in the direction of research for our study was proposed because of the large number of terpenes found in these incense samples. Much research has been published in literature on the harmful effects of VOC's found in the burning of incense. However, many of the terpene family of compounds are known to have positive health effects. The release of these terpenes upon the burning of incense and their possible health benefits has not been previously studied and was suggested as a continuation of the study of incense.

A chemical *in vitro* method of studying the reactivity of fatty acid vesicles upon the addition of terpenes was proposed as a potential model system to begin to examine the biological activity of this family of compounds found in frankincense and the essential oils added to make ecclesiastical incense. It was hypothesized that by studying the effect the terpene family has on oleic acid vesicles, we can take a step towards better understanding the role terpenes play in essential oil health benefits.

Chapter 3 – Formation of Oleic Acid Vesicles

3.1 Introduction

The history, benefits and uses, formation and reactivities of fatty acid vesicles were presented in section 1.4. Continuing from that introduction, we propose to prepare oleic acid vesicles in a reproducible manner that can then be utilized to analyze for the possible reactivities as presented in chapter 1. We hypothesis that these reactivities will be instigated by the terpenes that were found in incense in chapter 2. The effect these terpenes will have on oleic acid vesicles should depend on the functional groups each terpene contains. Functional groups such as aromatics, alcohols, and aldehydes are of particular interest because of the biological effects these terpenes have demonstrated in studies found in the literature as detailed in section 1.3 of the present document.

Our study seeks to utilize a model membrane made of oleic acid to demonstrate the reactivity of vesicles in an *in vitro* manner. The first step to this goal is to form oleic acid vesicles that will serve this purpose. Gebicki and Hicks [30, 35-36] were the first to prepare and study membrane-enclosed bilayer vesicles composed of exclusively fatty acids. There are several variables that must be controlled in the formation of these oleic acid vesicles.

First, the vesicles need to be bilayer and unilamellar. The vesicles also need to be of a relatively narrow size range to ensure consistency in their reactivities. The most commonly used method of forming these vesicles is thin-film rehydration [40]. In the rehydration process, oleic acid is dissolved in a non-polar solvent in a round-bottom flask and the solvent is evaporated leaving a thin-film layer of the fatty acid.

The thin film of fatty acid is resuspended in an aqueous buffer at the appropriate pKa and cvc (critical vesicle concentration) of the fatty acid. Vesicles will not form outside these parameters. Micelles form at pH higher than the pKa of the fatty acid and an oily film at lower than the pKa. Only micelles and free oleic acid molecules are present in concentrations less than the cvc. These critical values for oleic acid are a pKa of 9.8 and a cvc of 80 mM. After brief vortexing, the solution is allowed to mix overnight. The resulting solution is a mixture of multilamellar vesicles of various sizes. Extrusion through a porous membrane forces these vesicles to become unilamellar and of a standard size [32, 60].

Several reactivities are detected with these vesicles using fluorescence spectroscopy as detailed in the next chapter. The vesicles need to be able to contain a fluorophore either in the encapsulated solution or embedded in the bilayer itself so that these reactivities can be studied. Permeability can be detected by leakage of a polar fluorophore encapsulated in the solution interior to the vesicle membrane, while fluidity and fusion require fluorophore in the nonpolar region of the bilayer membrane itself. These fluorophores are added with the aqueous rehydrating solvent if the desired location is to be encapsulated inside the vesicle and added with the organic solvent before the formation of the thin film if the desired location of the fluorophore is the non-polar region of the membrane.

3.2 Materials & Methods

3.2.1 Vesicle Formation Method

Oleic acid, analytical grade (All chemicals and reagents obtained from Sigma-Aldrich, Milwaukee, WI) was weighed out to give an 80-100 mM final concentration, was dissolved in a chloroform:methanol (2:1) solvent at a 1:40 (oleic acid:solvent) ratio in a round-bottom flask. Fluorophore (DPH or Nile Red) dissolved in an organic solvent (THF or methanol, respectively) was added at this point in the method to form vesicles with fluorophore embedded in the bilayer membrane. All organic solvents were evaporated using rotary evaporation for 30 minutes and then dried under a stream of nitrogen for 30 minutes. The drying process allowed the oleic acid molecules to organize in layers and to form a film on the surface of the round-bottom flask, incorporating the fluorophore into the bilayer when present. After removal of organic solvent, 0.20M bicine buffer, pH 9.8 was added to the oleic acid in order to achieve an 80-100 mM solution. The bicine buffer was prepared by dissolving bicine (N,N-Bis(2-hydroxyethyl)glycine) in deionized water to a concentration of 0.2 M. The pH was then adjusted using a pH meter to pH 9.8 by adding aqueous NaOH dropwise. The resulting solution was vortexed for 10 seconds and placed on a horizontal shaker overnight, or a minimum of 12 hours.

For experiments involving fluorescence trapped inside the vesicle, fluorescein sodium salt was dissolved in bicine buffer to a concentration of 1.0 μM. This bicine-fluorescein solution was used as the solvent to form vesicles instead of the solvent with only bicine in order to trap fluorescein inside the vesicles. After vortexing and mixing overnight, dialysis was performed to remove fluorescein

molecules not trapped inside the vesicles by placing the vesicle solution in dialysis tubing and soaking in a 10-15 mM oleic acid:bicine buffer solution. Four steps of dialysis were performed allowing time (4 hours twice, overnight, and 24 hours) for equilibrium to be established each time before replacing the oleic acid:bicine buffer with fresh dialysis buffer.

Sizing of the vesicles was done by extruding through a Whatman polycarbonate membrane with a pore size of 5 microns. Extrusion was done manually and repeated five times.

Opacity of 80-100 mM oleic acid solutions was too high to transmit light. In order to reduce opacity to an instrument-readable level, all final solutions of vesicles were diluted 1:10 with the bicine buffer before reading visible absorbance or fluorescent emission.

3.3 Results & Discussion

Formation of unilamellar vesicles was supported by fluorescence microscopy using an Olympus microscope with a 561 nm excitation filter and 60X water objective. Oleic acid vesicles were prepared as described above with the nonpolar fluorophore Nile Red (excitation at 550nm and emission at 625 nm) added at a concentration of 20 mM relative to the oleic acid. The fluorophore was added with the organic solvent used to dissolve the oleic acid before drying and re-solvating with bicine buffer so as to embed the fluorophore inside the bilayer membrane. The picture below (Figure 15) shows the resulting vesicles formed.
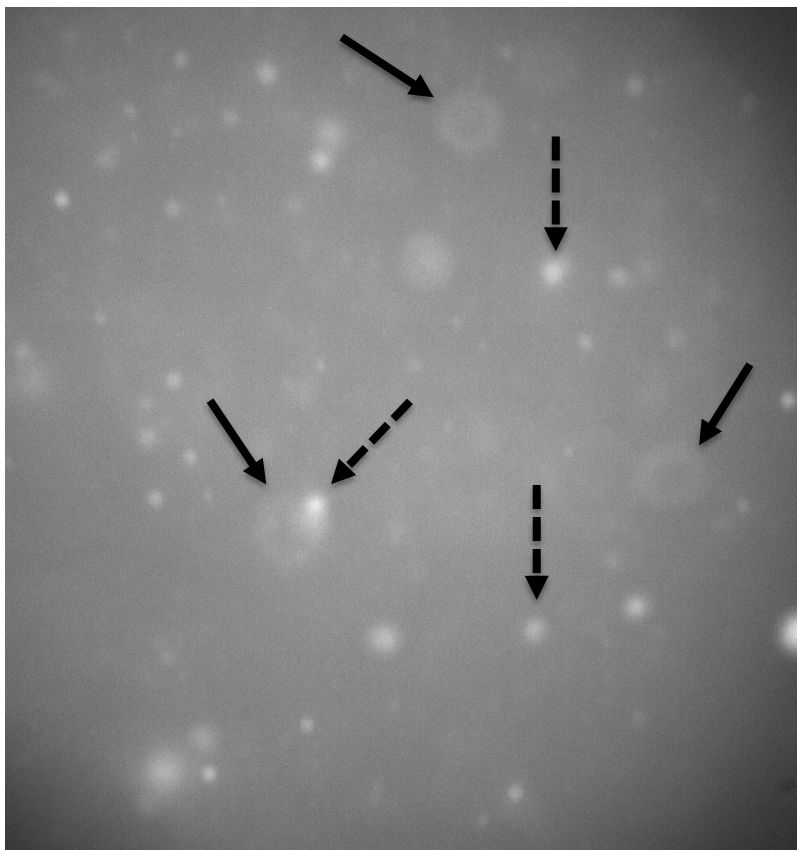
Figure 19 - Fluorescence Microscope Photo of Bilayer Nature of Vesicles

The bright spots indicated by the dashed arrows are at a different focal level than the circles with the darker centers indicated by the solid arrows. These bright spots become circles with darker centers as the focus is varied. The nature of the visibility of fluorescence supports the idea of a bilayer nature of the spherical vesicles with the fluorophore embedded in the bilayer.

3.3.1 Fluorescence Baselines

As introduced in section 1.5 on the instrumentation of fluorescence spectroscopy (28), Beer's Law allows us to relate the emission intensity of the fluorophore with the concentration of the fluorophore. However, the method of fluorescence spectroscopy can be "strongly influenced" [93] by the environment in

which the fluorophore is being viewed. A number of control experiments were performed to establish baselines for the three fluorophores (Fluorescein, DPH, and Nile red) used in our study. These three fluorophores were each chosen to test a specific reactivity of the oleic acid vesicles as is detailed in chapter 1.4.4. Positive and negative controls for each fluorophore were examined to compare with the results obtained from reactions with the terpenes of interest.

All fluorescence spectroscopy was read on one of two instruments: PTI Fluorescence Spectrophotometer or Agilent Cary Eclipse Fluorescence Spectrophotometer with Xenon lamp.

3.3.1.1 Fluorescein

Fluorescein is a polar fluorophore which was trapped with the aqueous solution interior to the membrane and as such must have baselines established specific to the aqueous buffer used - 0.2 M Bicine buffer, pH 9.8.

3.3.1.1.1 Linearity of Fluorescein Emission Intensity in Bicine Buffer

Increasing amounts of 1 μM fluorescein were added to 1 mL bicine buffer. Linear regression analysis of resulting emission intensities is shown in Figure 20. Emission intensity of fluorescein increases on a linear basis with the concentration of fluorescein.
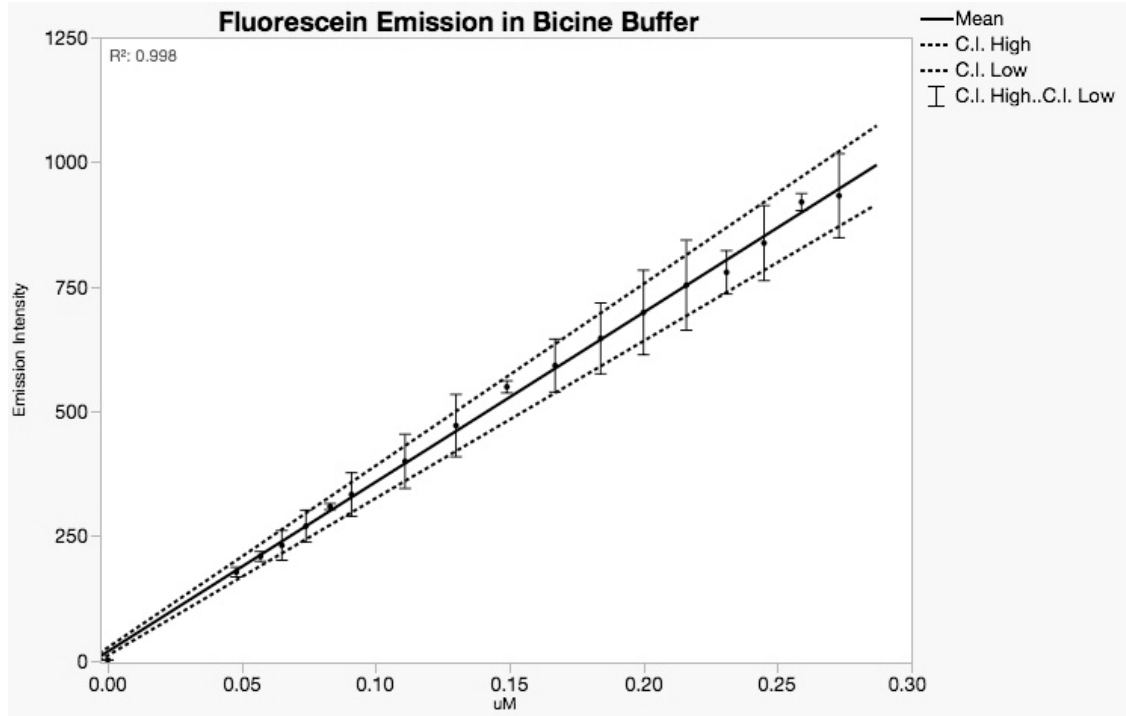
Figure 20 - Linearity Graph of Fluorescein in Bicine Buffer

3.3.1.1.2 Linearity of Fluorescein Emission Intensity in 10 mM Oleic acid/Bicine
buffer

Different concentrations of fluorescein were added to 10 mM oleic acid in
bicine buffer to account for the effect of the opacity of the solutions. Regression
analysis shows that much higher concentrations of fluorescein are within range of
instrument detection due to the opacity of oleic acid in bicine buffer. However,
higher concentrations reduce the linearity of the regression fit and in fact show a
quadratic relationship as seen below (Figure 21). Linearity is preserved in the same
concentration range (0 - 0.3 uM) as was seen with fluorescein in only bicine buffer
(Figure 22).
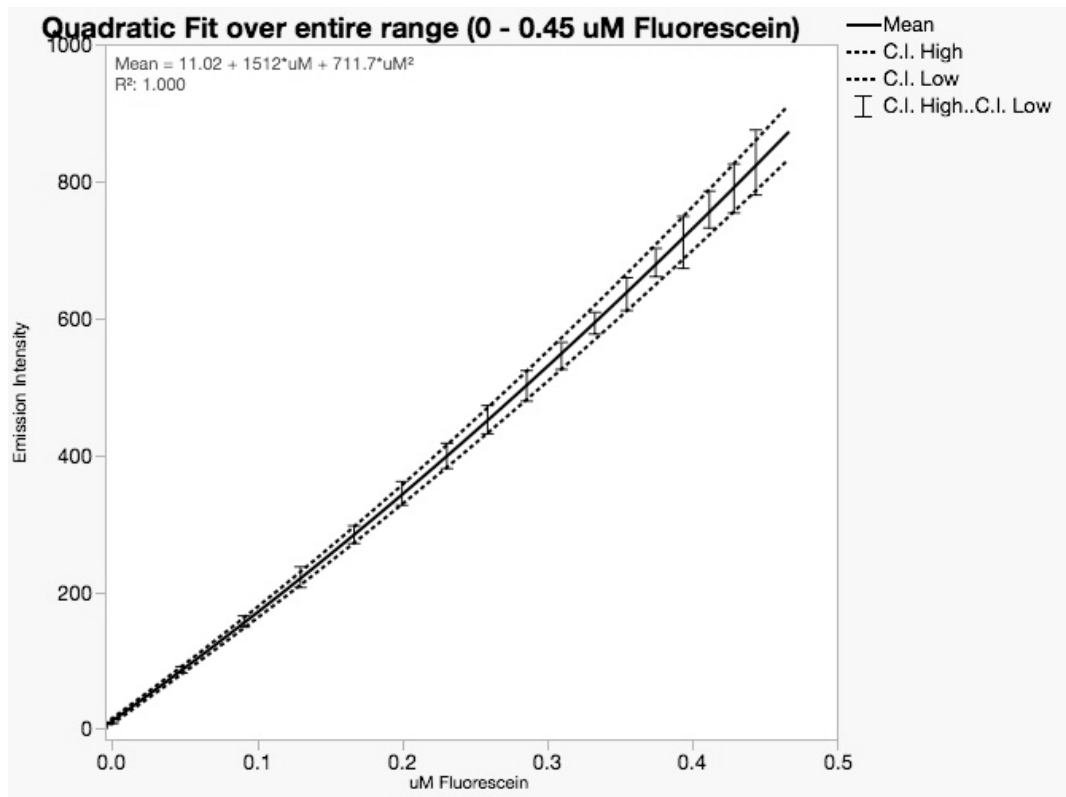
Figure 21 - Graph of Entire Range of Fluorescein Concentrations in 10 mM Oleic Acid
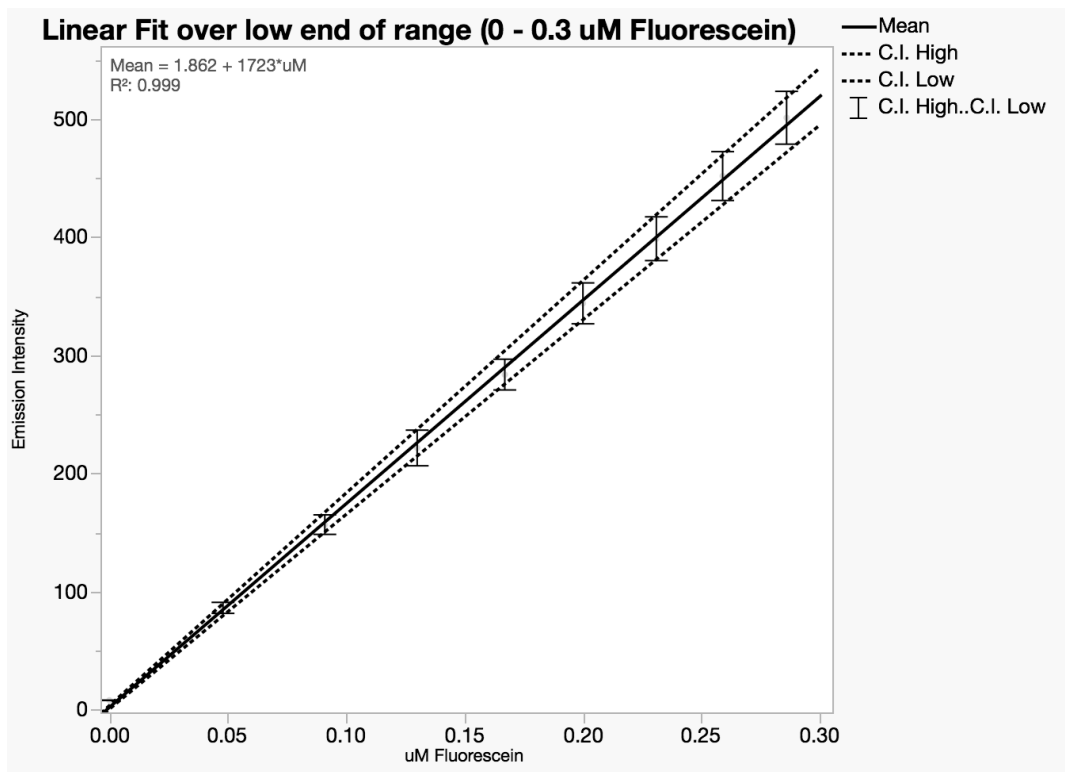
Figure 22 - Graph of Partial Range of Fluorescein Concentrations in 10 mM Oleic Acid

3.3.1.1.3 Linearity of Fluorescein Emission Intensity upon Dilution of Oleic Acid

Vesicles

Because of the high opacity of 80-100 mM oleic solutions, all vesicle solutions had to be diluted before reading emission intensity of fluorescein. Creating a series of dilutions of vesicles (5-30 mM) insured linearity of the dilution process as could be seen Figure 23. The emission intensity of these solutions was also tested at various times (30 sec – 4 hours) after dilution to ensure these intensities do not change as time progresses. Results show (Figure 24) that while, initially there are minor changes observed in the intensities, they stabilize and remain constant after the first hour.
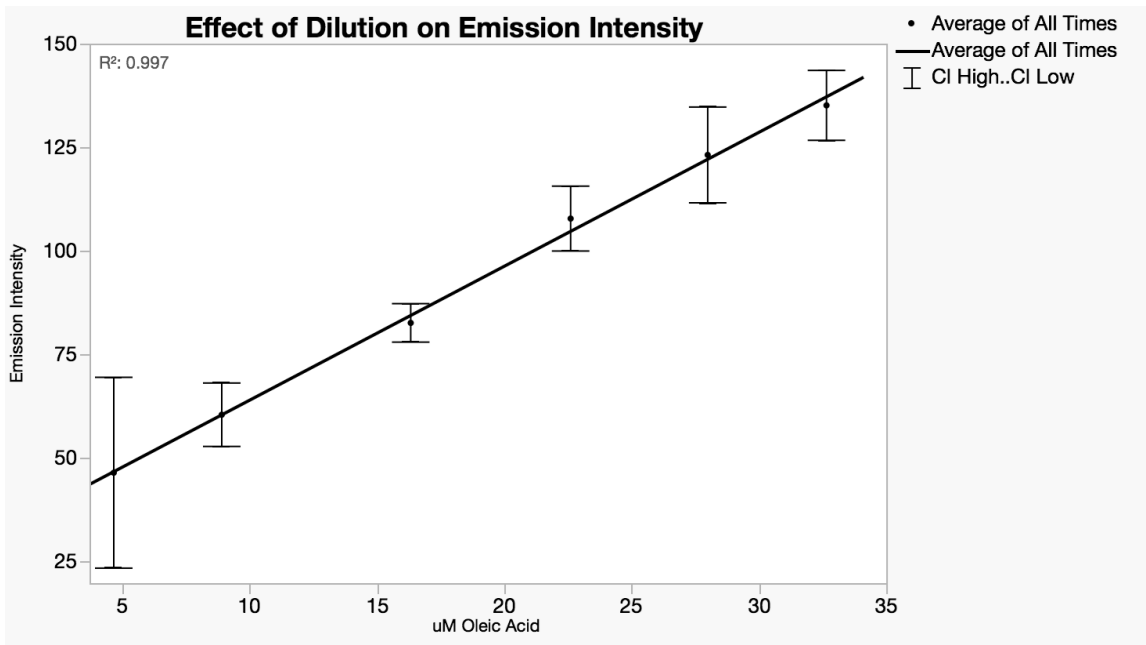
Figure 23 - Graph of Fluorescein in Diluted Oleic Acid Vesicles
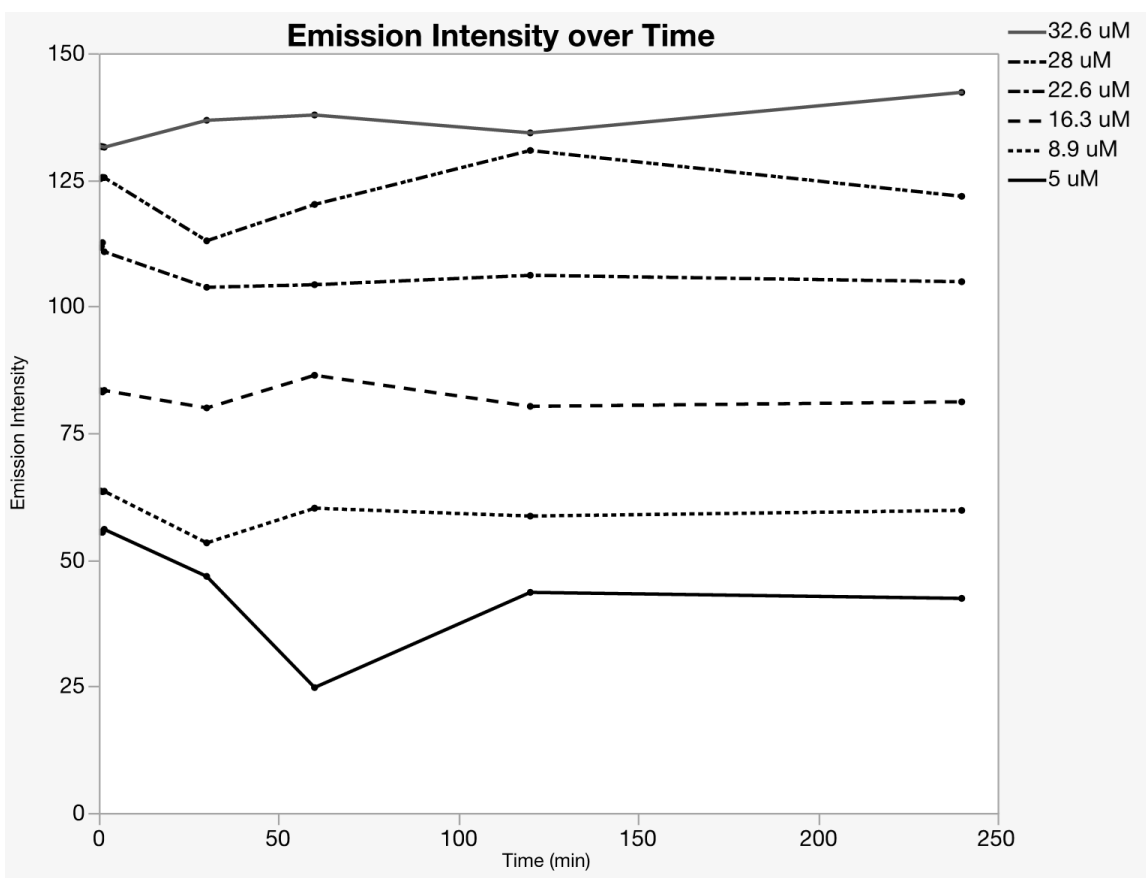
Figure 24 - Graph of Fluorescein in Oleic Acid Vesicles over Time

3.3.1.2 DPH (1,6-Diphenyl-1,3,5-hexatriene)

DPH is a nonpolar fluorophore trapped inside the bilayer membrane so the aqueous buffer is not among environmental factors affecting its fluorescence. The oleic acid in the bilayer vesicle however does have an effect on the environment of the DPH fluorophore and must be examined to establish a baseline.

3.3.1.2.1 Linearity of DPH Emission Intensity in Oleic Acid

A series of concentrations of DPH (1-50 uM) were added to a series of oleic acid solutions (10-100 mM) to determine the linearity of DPH emission. All solutions were diluted to 10 mM oleic acid before fluorescence readings were taken to reduce opacity.

Figure 25 reveals that DPH emission intensity is linear at the higher concentrations of oleic acid (50-100 mM).
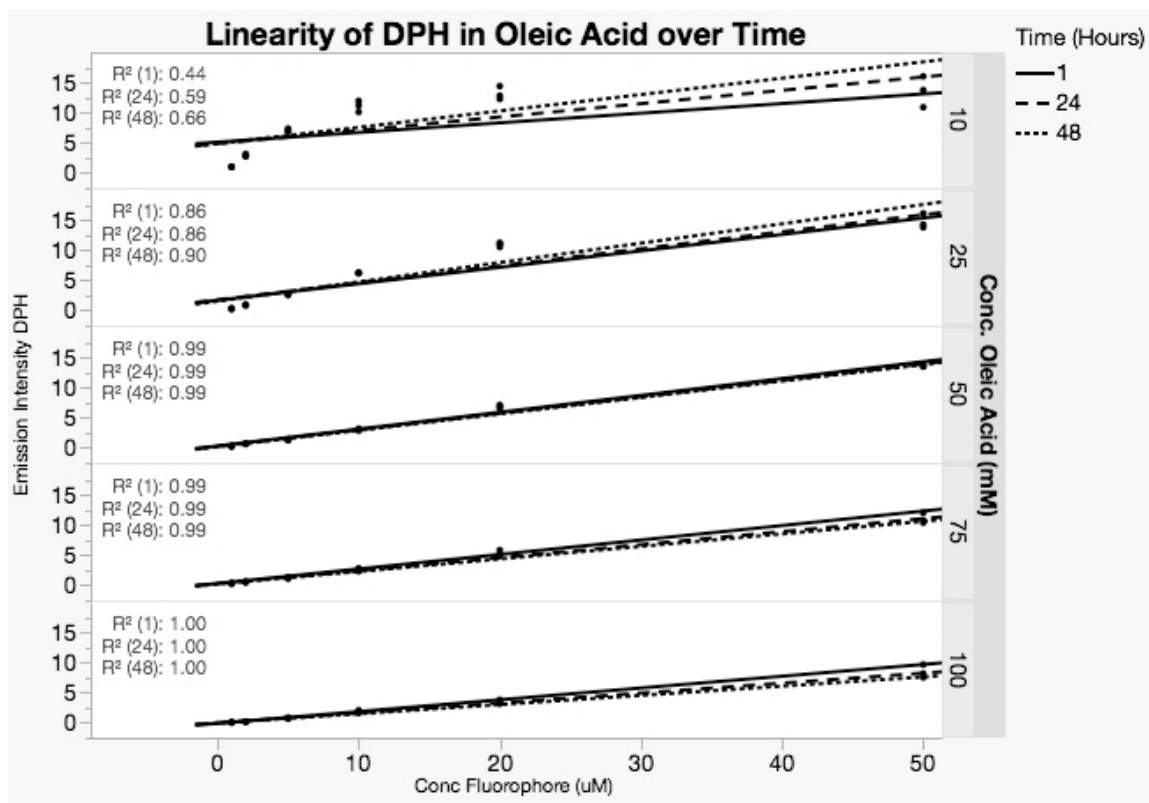
Figure 25 - Graph of Linearity of DPH Emission in Oleic Acid

3.3.1.2.2 Linearity of DPH Emission Intensity in Dilutions of Oleic Acid Vesicles

All oleic acid vesicle solutions were diluted before reading emission intensity of DPH to reduce opacity of the solutions. A series of dilutions of vesicles (2.5-17.5 mM final oleic acid concentration) insured linearity of the dilution process as can be seen in Figure 26. The emission intensity of these solutions was also tested at 48 hours after dilution to ensure these intensities do not change as time progresses. Linearity actually improves over time.
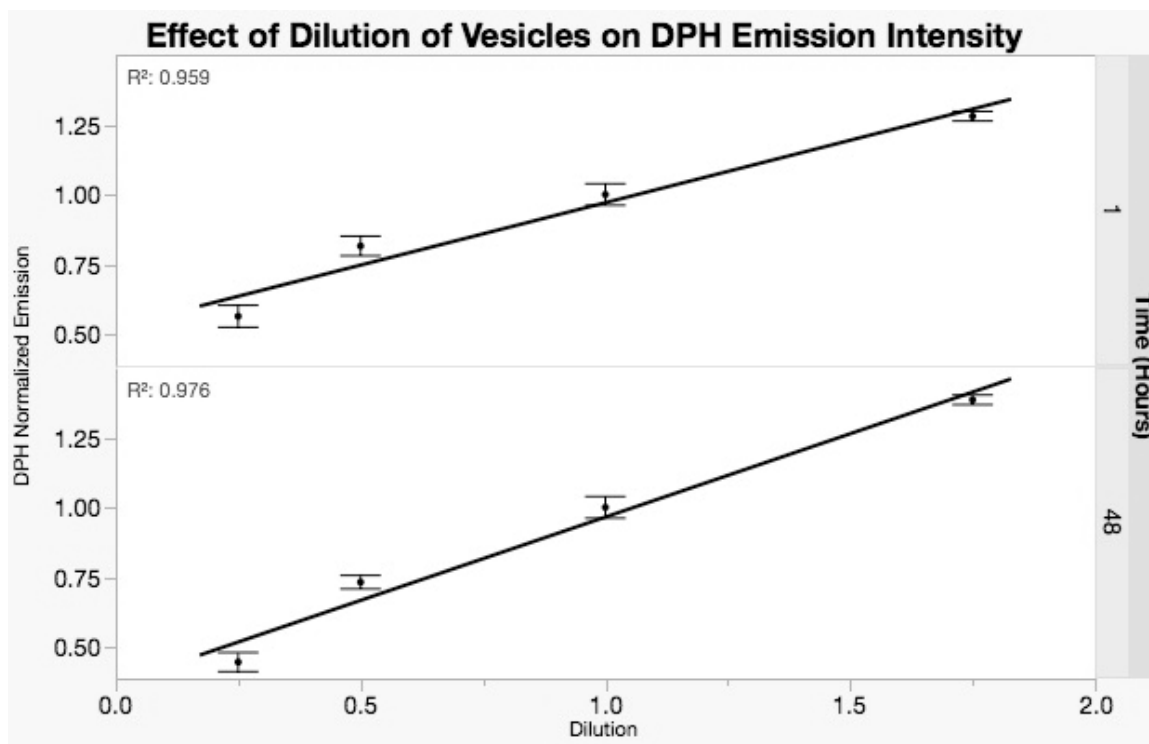
Figure 26 - Graph of DPH Emission upon Dilution of Oleic Acid Vesicles

3.3.1.3 Nile Red

Nile Red is also a nonpolar fluorophore trapped inside the bilayer membrane. Again, the aqueous solvent of the vesicles does not affect the fluorescence results. The fluorescence is detected only in the bilayer membrane so a baseline in this environment must be established.

3.3.1.3.1 Linearity of Nile Red Emission Intensity in Oleic Acid

As with DPH, a series of concentrations of Nile Red (1-50 uM) were added to a series of oleic acid solutions (10-100 mM) to determine the linearity of Nile Red emission intensity. All solutions were diluted to 10 mM oleic acid before fluorescence readings were taken to reduce opacity. All solutions were read at 1, 24 and 48 hours for Nile Red emission intensity.

73

The series of graphs shown below reveal that similar to DPH readings, Nile Red emission intensity is linear at all but the lowest concentrations of oleic acid for up to 48 hours (Figure 27). A closer look at the readings for the 75 mM oleic acid solutions (Figure 28) shows that while the emission intensities do decrease at higher concentrations of fluorophore over 48 hours, linearity is still maintained.
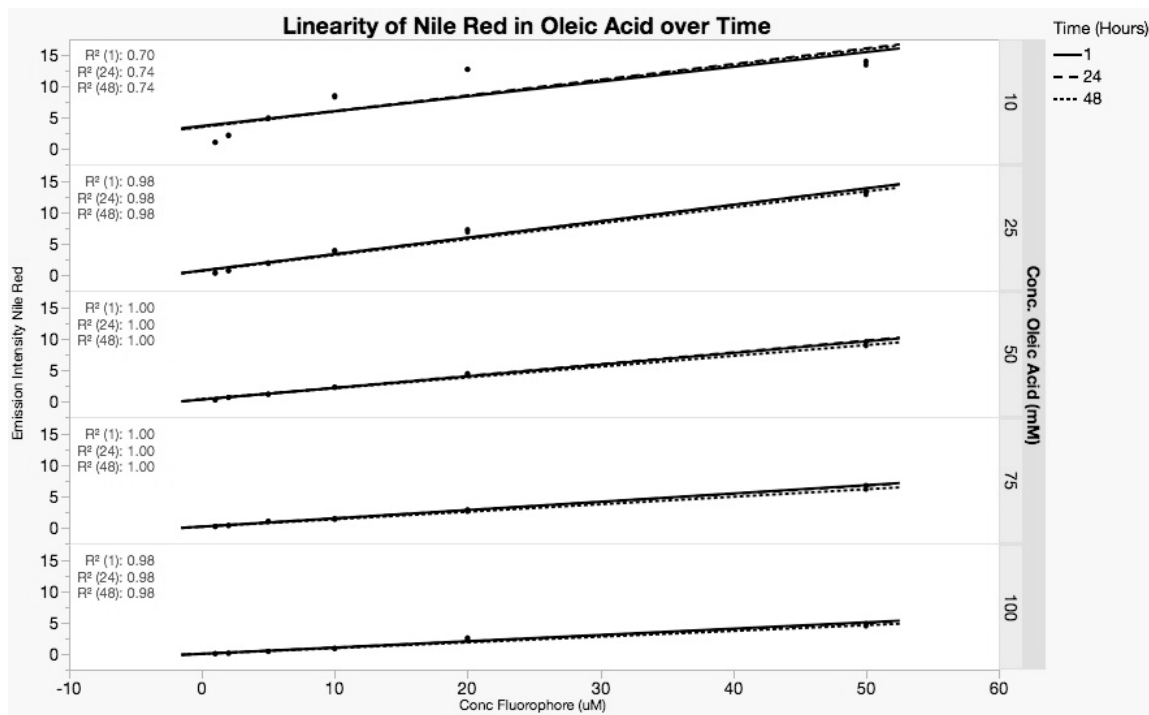
Figure 27 - Graph of Linearity of Nile Red Emission in Oleic Acid
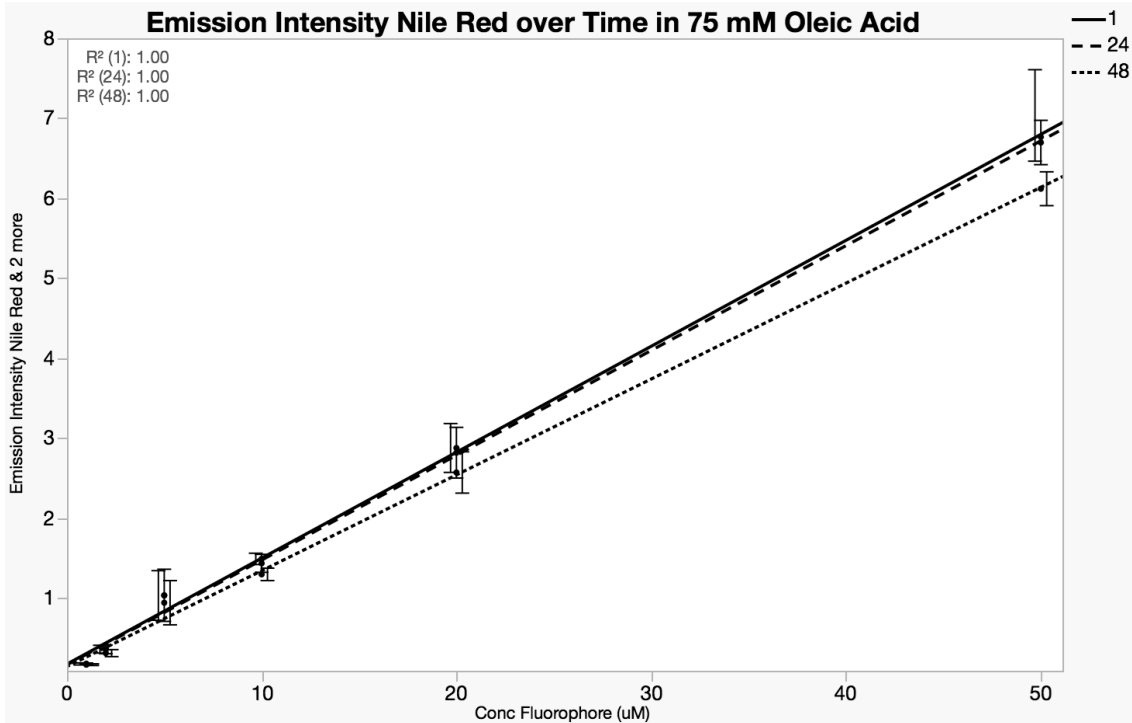
Figure 28 - Graph of Linearity of Nile Red Emission in 75 mM Oleic Acid over Time

3.3.1.3.2 Linearity of Nile Red Emission Intensity in Dilutions of Oleic Acid Vesicles

All oleic acid vesicle solutions were diluted before reading emission intensity of Nile Red to reduce opacity of the solutions. A series of dilutions of vesicles (5-17.5 mM final oleic acid concentration) showed that the dilution process is not linear as can be seen in Figure 29. The emission intensity of these solutions was also tested at 48 hours after dilution to ensure these intensities do not change as time progresses.
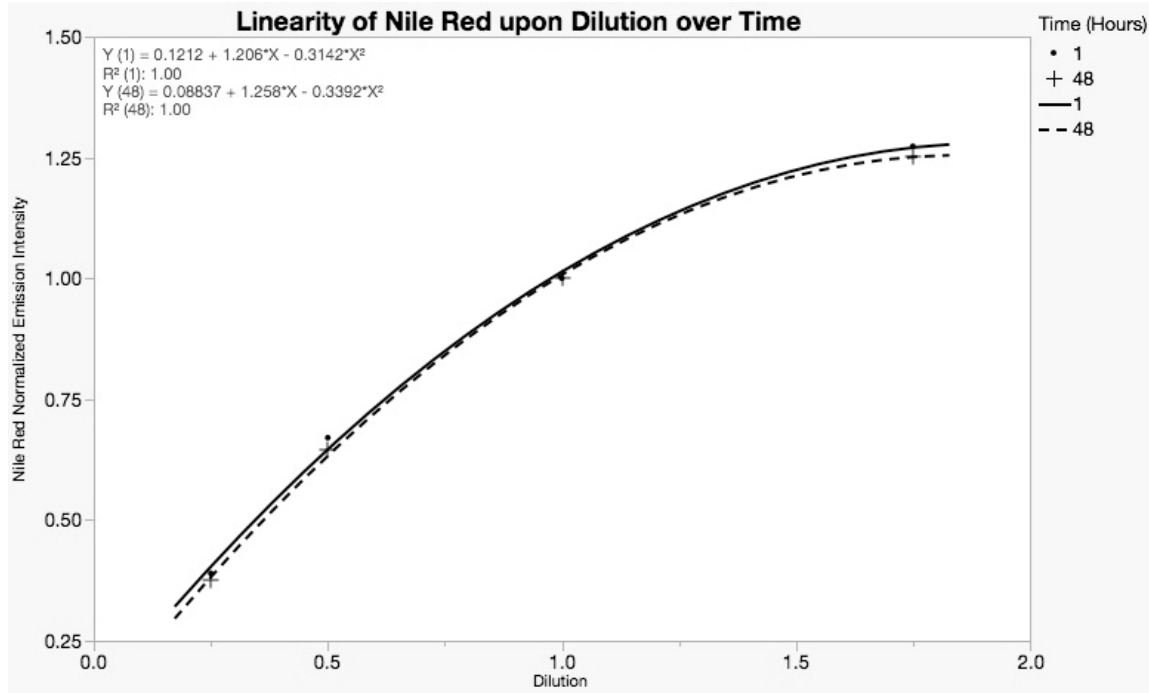
Figure 29 - Graph of Linearity of Nile Red Emission in Dilutions of Oleic Acid Vesicles

3.3.2 Experiments on Variables of Vesicle Formation Procedure

A high degree of variability in intensity was seen across batches of vesicles in the process of analyzing the emission data from these fluorophores. Several variables in the vesicle formation process were studied to eliminate, or at least reduce, the variability.

3.3.2.1 Oleic Acid Concentration and Flask Size

The process of forming an oleic acid film in the flask during organic solvent evaporation has two possible variables – the surface area of the glass flask as measured by the size of the flask and the amount of oleic acid available to coat the surface. A series of vesicle solutions were made to experiment with these variables by varying the amount of oleic acid relative to the size of the flask. Fluorescein was

76

included with the bicine buffer and both were held constant in each trial. The emission intensity of fluorescein after dialysis was read as an indication of the effect of the concentration of oleic acid and the size of the flask.

The following graph (Figure 30) represents 14 batches of oleic acid vesicles prepared by varying the amount of oleic acid added to 10 mL of bicine buffer in two different size round-bottom flasks. This graph does show a correlation between increasing amounts of oleic acid and increasing fluorescein emission intensity. The line fit is not great but is the same for either size of flask examined, however the slope of the line is not the same. Thus, the conclusion of the flask size experiment is that, while the size of the flask in which the oleic acid vesicles are formed does make a difference, that difference can be eliminated by consistently using the same size flask for each batch of vesicles.
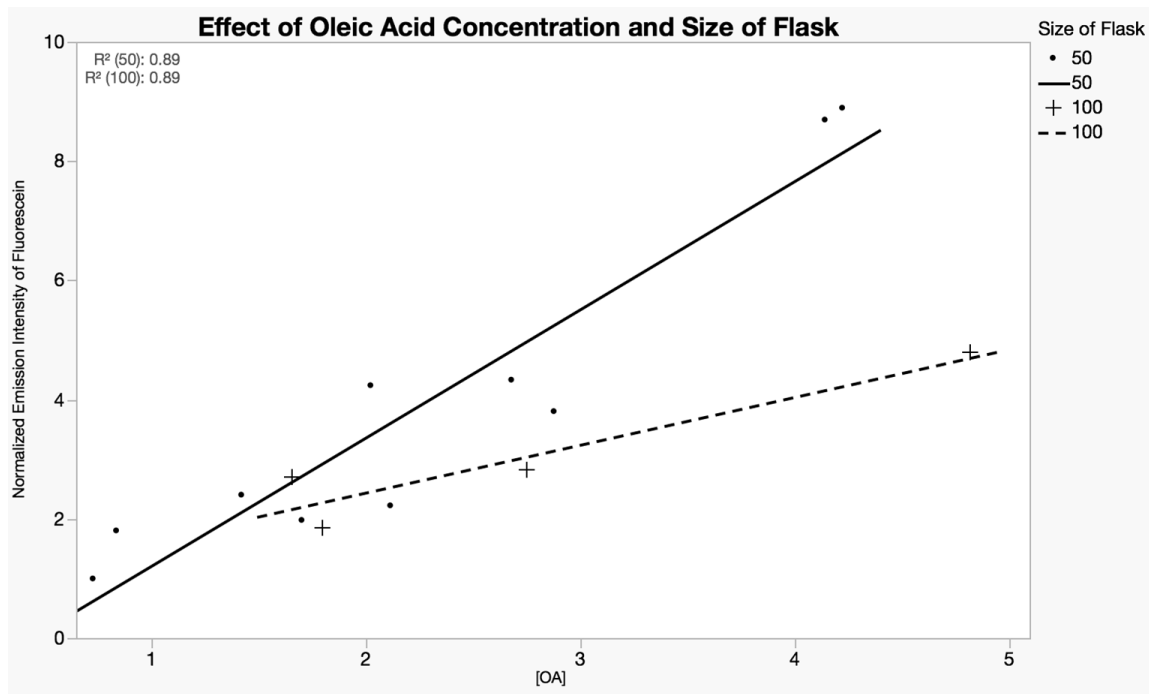
Figure 30 - Graph of the Effect of Concentration of Oleic Acid and Size of Flask on Vesicle Formation

3.3.2.2 Extrusion and Vesicle Size

Another variable in the vesicle formation process is the size of vesicles formed which can be controlled by extrusion through a polycarbonate membrane. Fluorescence microscopy was used to show the effect of extrusion upon the uniformity of vesicle sizes. Comparison of the following picture (Figure 31), taken after extrusion, with the previous picture (Figure 19), taken before extrusion, shows that bilayer vesicles form in many different sizes but are reduced to a fairly uniform distribution upon extrusion.
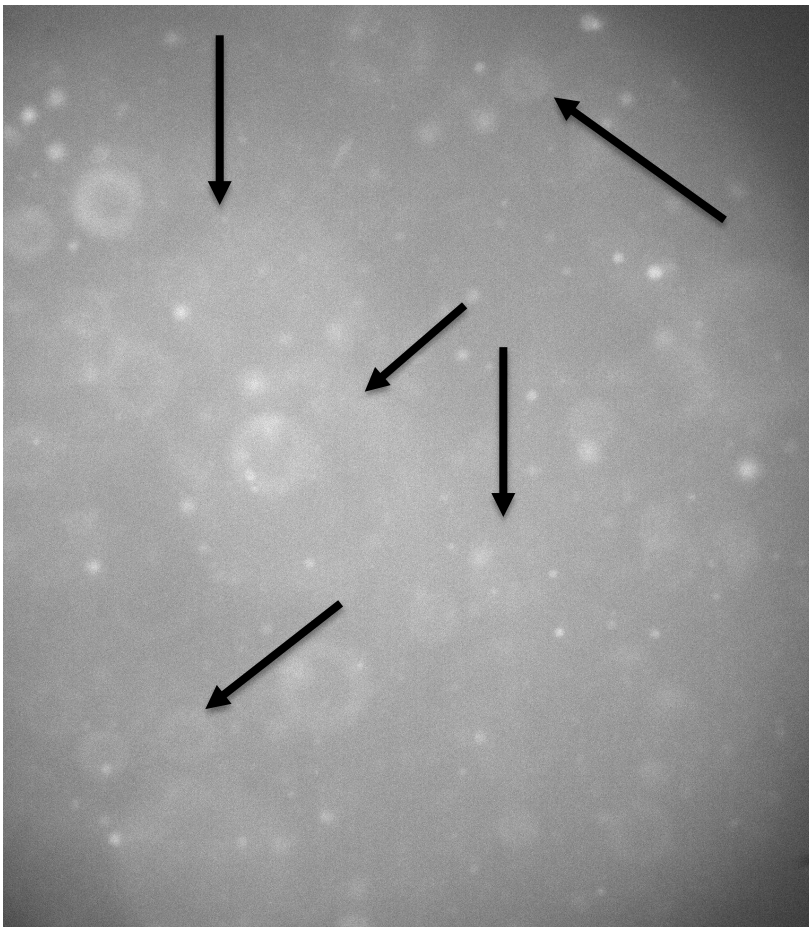
Figure 31 - Oleic Acid Vesicles before Extrusion

3.3.3 Effect of Complete Dispersion of Oleic Acid from Vesicles

Vesicles were destroyed to release all trapped fluorescence as a positive control. A surfactant, Triton-X, was added to the oleic acid vesicles to further understand how the fluorophore molecules which have been encased inside the vesicles are released upon dispersion of the oleic acid molecules. The initial results showed a remarkably large concentration of Triton-X was necessary to fully disperse the oleic acid from the vesicles.

Methanol was then added to vesicle solutions at various concentrations of methanol to determine the amount needed to fully disperse the oleic acid molecules. The same unexpected results were seen with methanol as with the surfactant, requiring up to 40% methanol to fully disperse the oleic acid. Further experiments were performed to better understand the phenomenon of why such relatively high concentrations of dispersant were needed and to examine the hypothesis that leakage, or permeability, from the vesicle increases on a linear basis as the methanol concentration increases and the vesicle is destroyed.

Several baselines were examined to determine the effect on the fluorescein emission of including methanol in the solvent because of the high degree of influence the environment has on fluorescence.

3.3.3.1 Effect of Methanol on Fluorescein Emission in Bicine Buffer

A portion of the bicine buffer was replaced with methanol and emission intensity of 0.167 μM fluorescein (200 μL in 1 mL bicine buffer/methanol solvent) was tested

as in the first baseline experiment described previously. Scans were performed in excitation (450 – 500 nm, emission at 513 nm) and emission (500 – 550, excitation at 489 nm) to detect any shifts methanol might cause in peak wavelength. There was no peak wavelength shift seen in excitation scan. The emission scan over 500 – 550 nm did show a red shift in peak wavelength with the shift starting at 50% methanol (Figure 32). A decrease was seen in emission intensity beginning at 50% methanol and is most likely due to the shift in emission peak wavelength (Figure 33). An approximate linear correlation between increasing concentration of methanol and emission intensity is seen up to 50% methanol (Figure 34).
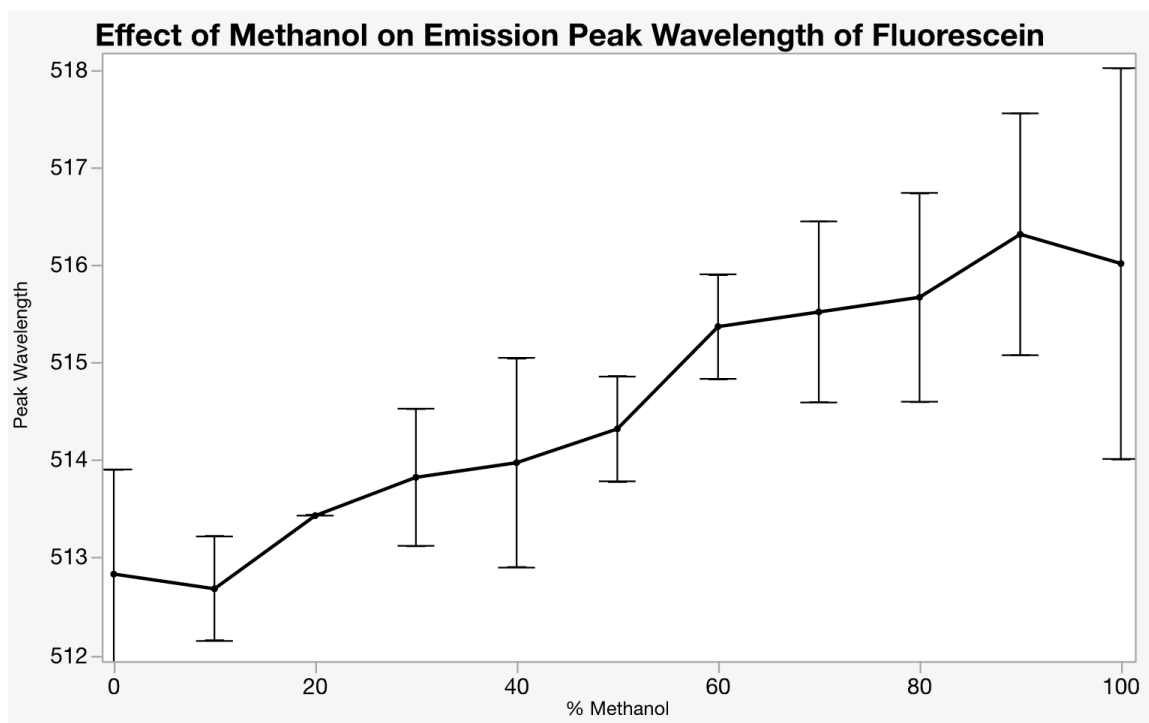
Figure 32 - Graph of the Effect of Methanol on Fluorescein Emission Peak Wavelength in Bicine Buffer
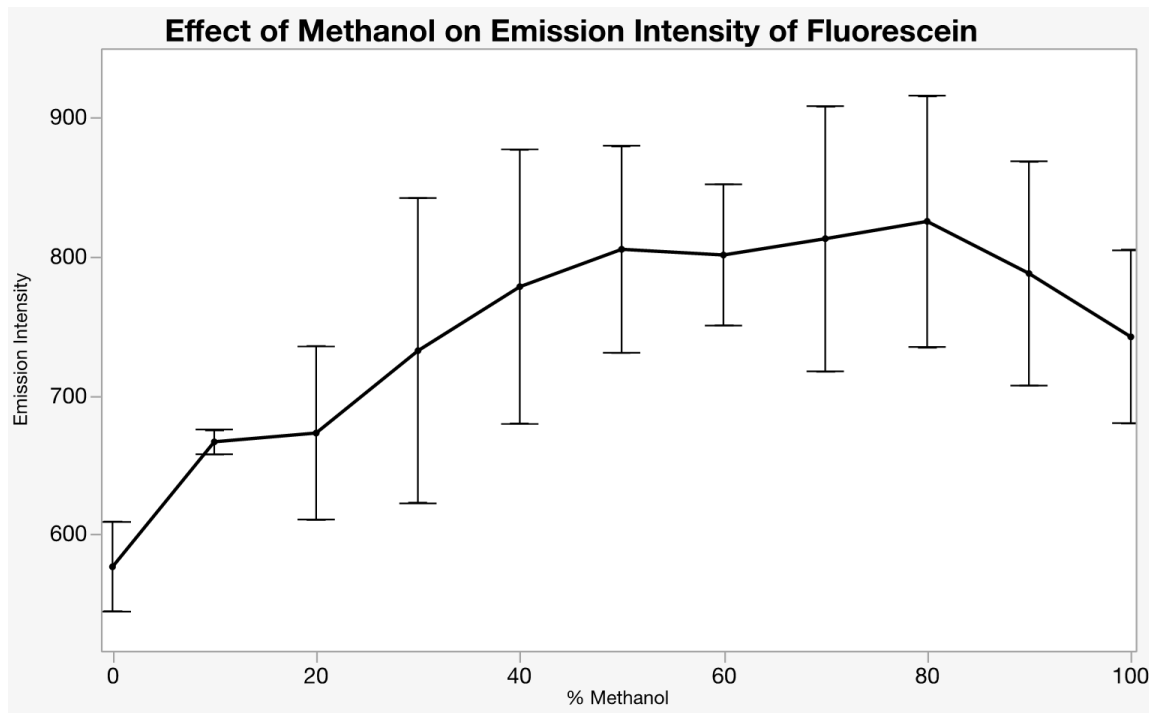
Figure 33 - Graph of the Effect of Methanol on Fluorescein Emission Intensity in Bicine Buffer
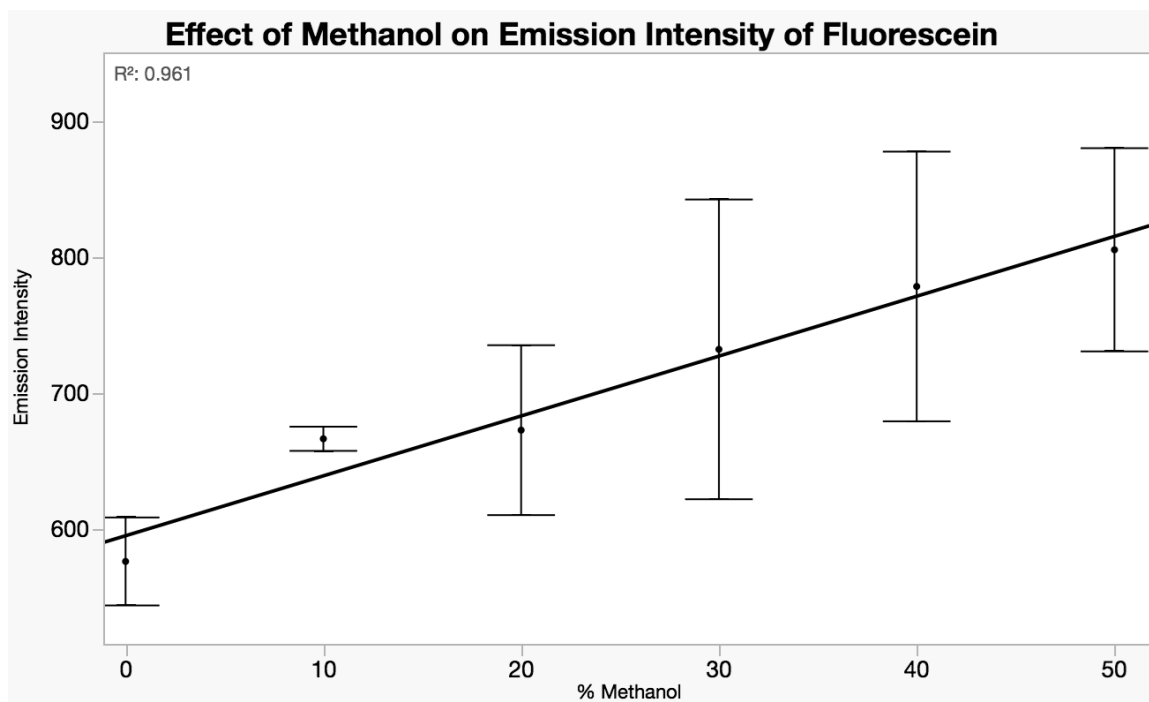
Figure 34 - Graph of the Effect of <50% Methanol on Fluorescein Emission Intensity in Bicine Buffer

3.3.3.2 Effect of Methanol on Fluorescein Emission Intensity in Oleic acid and Bicine

Buffer

The same experiment was performed using 10 mM oleic acid in bicine buffer to

determine if the same effect is seen with oleic acid present in the solution. These

solutions do have an opacity not seen in solutions of only bicine buffer due to the

dispersion of oleic acid in aqueous solvents, however the concentration of oleic acid

is low so no vesicles have been formed.

Fluorescein in oleic acid and bicine buffer shows results similar to fluorescein in

only bicine buffer with the red shift in emission peak wavelength starting at about

40% methanol (Figure 35).
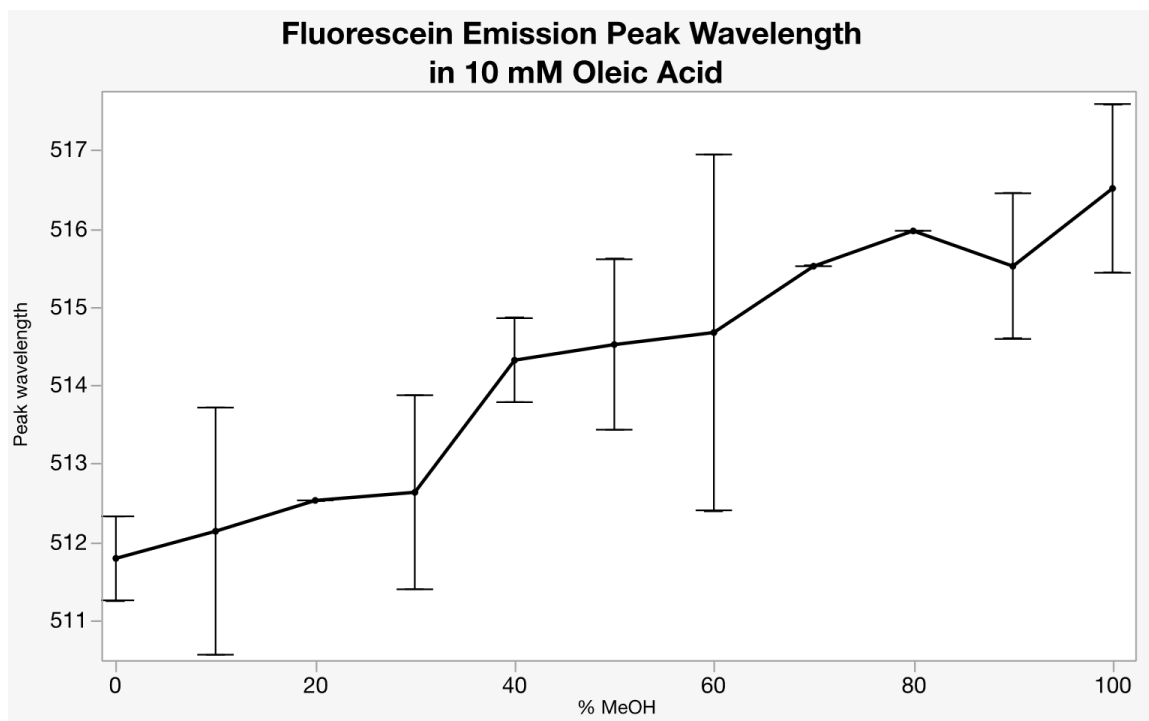
Figure 35 - Graph of the Effect of Methanol on Fluorescein Emission Peak
Wavelength in Oleic Acid Solutions

82

There is a corresponding large increase in emission intensity at this same concentration of methanol (40%) while the emission intensity is relatively constant as methanol concentration increases for less than 40% methanol (Figure 36). Visible opacity changes drastically at 40% methanol as well. All higher concentrations of methanol appear clear rather than the opaque solution associated with a dispersion of oleic acid in an aqueous solvent. The slight reduction in emission intensity at 20% methanol and the high degree of uncertainty at 30% methanol both demonstrate anomalies in expectations of the effect of methanol on oleic acid. These results are for low concentrations of oleic acid (below the cvc) so no conclusions can be made concerning the effect of methanol on oleic acid vesicles. However, these results should be kept in mind in the next step of analyzing the effect of methanol on oleic acid vesicles.
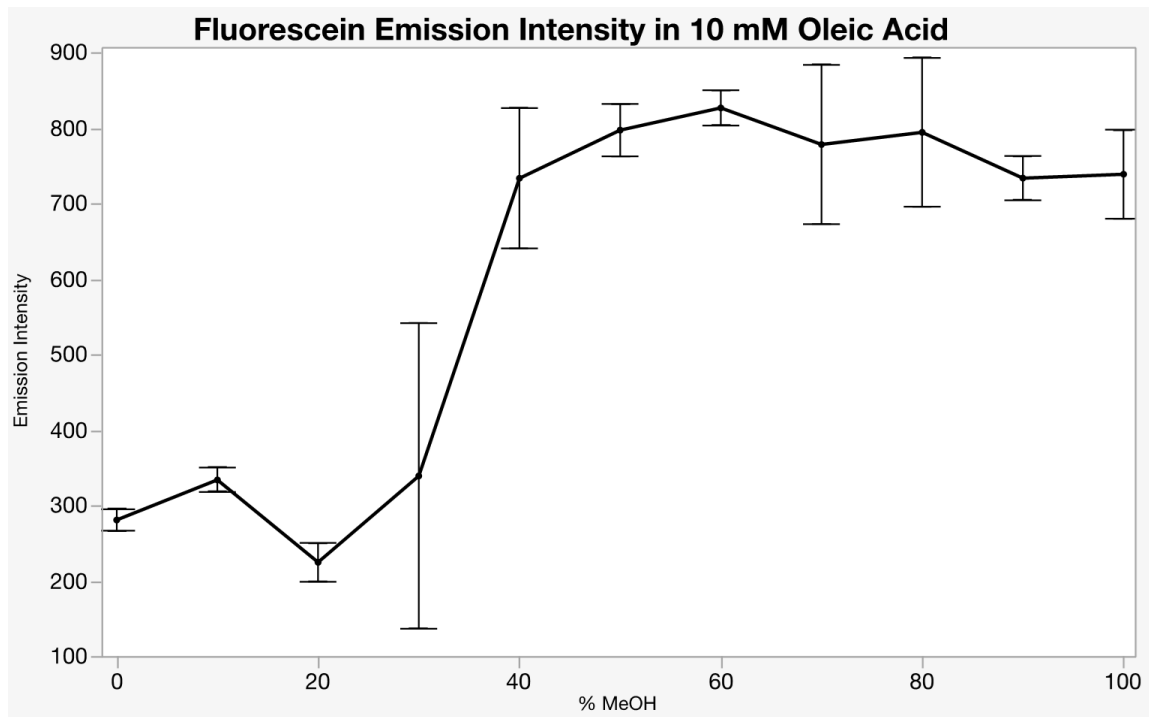
Figure 36 - Graph of the Effect of Methanol on Fluorescein Emission Intensity in Oleic Acid Solutions

3.3.3.3 Effect of Methanol on Fluorescein Emission Intensity in Oleic Acid Vesicles

The effect of increasing concentrations of methanol on oleic acid vesicles was examined by changing the ratio of methanol to bicine buffer (0-100% methanol) in the solvent used to dilute oleic acid vesicle solutions (1:10) down to an opacity that allows for fluorescent readings. Each tested concentration of methanol was a separate experiment done in triplicate trials to triple batches of vesicles.

This experiment was done to determine the maximum amount of fluorescein emission intensity obtainable as the vesicle membrane is disrupted and eventually completely destroyed with the resulting complete dispersion of the oleic acid molecules. The expectation is that fluorescein emission intensity will increase steadily until the vesicle is completely disrupted and all the fluorescein trapped inside the vesicle is released.

A scan of emission peak wavelength was obtained as with previous solutions of fluorescein in bicine buffer and low concentrations of oleic acid in bicine buffer. Results show the same red shift in emission peak wavelength at 40% methanol (Figure 37).
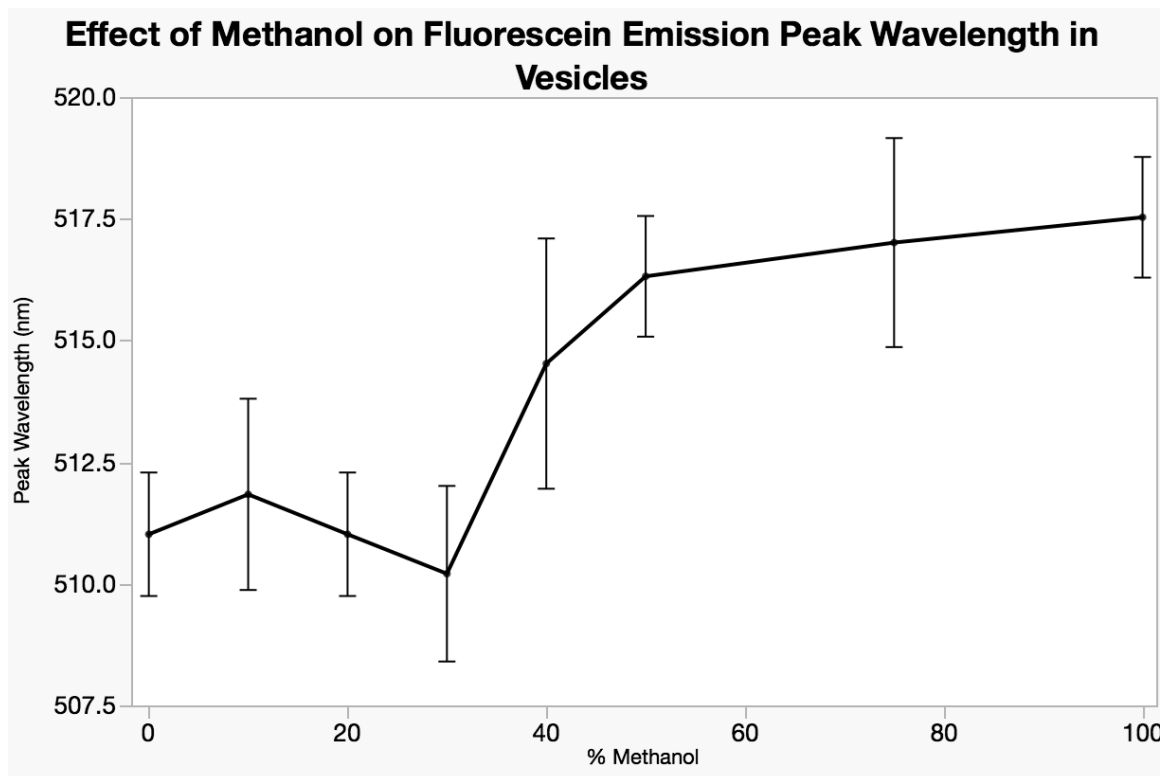
Figure 37 - Graph of the Effect of Methanol on Fluorescein Emission Peak Wavelength in Oleic Acid Vesicle Solutions

The corresponding fluorescein emission intensity shows some very interesting and unexpected deviations from expectations (Figure 38) similar to the previous results which require a closer look. One-way ANOVA was performed on the data with post-hoc multiple comparison. All concentrations of methanol higher than 5% show a statistically significant difference from 0% methanol. Upon expansion of

the graph in the 0-40% range (Figure 39), the emission intensity shows no change as the concentration of methanol increases for vesicles diluted in up to 10% methanol. An initial increase in emission intensity is seen as the concentration of methanol is increased and passes 10% methanol which confirms the initial theory that vesicles increase in permeability as they degrade. However, this increase in intensity is followed by an unexpected decrease in emission intensity in the 20 to 35% methanol range, just as was seen when solutions of 10 mM oleic acid (below the cvc) were dispersed in 20% methanol. The solutions in this 20-35% methanol range also show a visible increase in opacity. The increase in opacity means that the decrease in emission intensity is more likely related to a decrease in transmission of light into and through the solution. The results from the experiment with methanol and oleic acid vesicles are unexpected based on the initial hypothesis that vesicles increase in permeability as they degrade releasing fluorescein in a linear correlation. These results suggest that mechanistically there must be an alternate explanation for how oleic acid vesicles degrade.
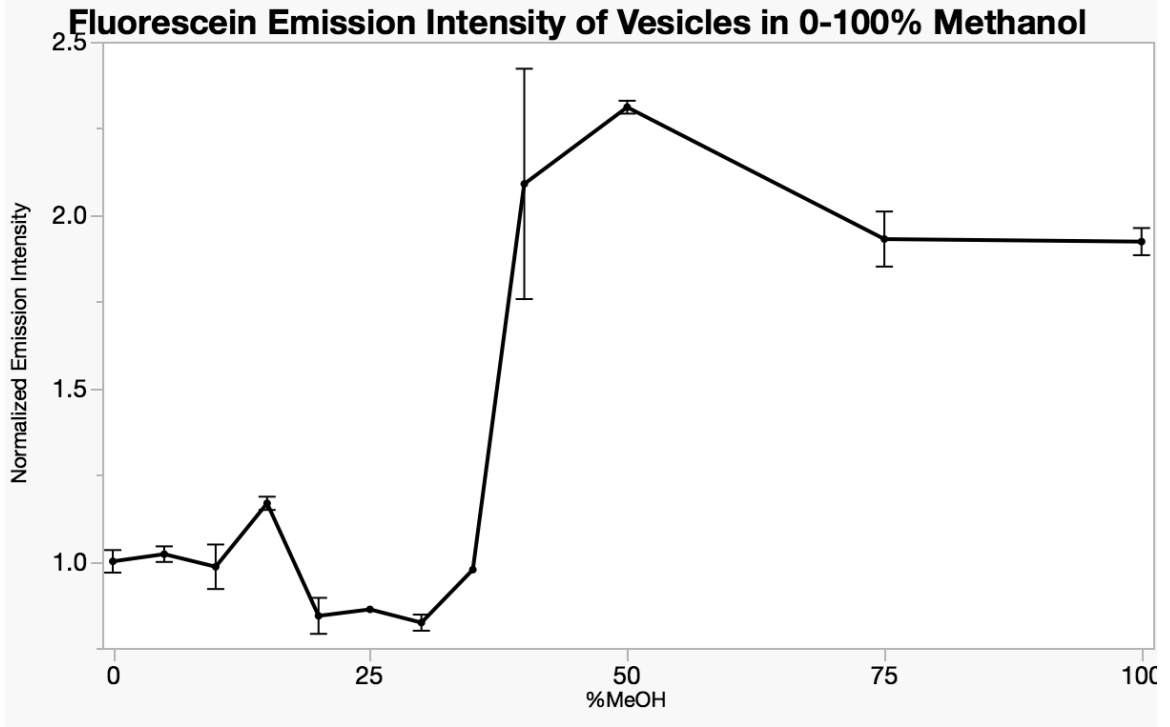
Figure 38 - Graph of the Effect of Methanol on Fluorescein Emission Intensity in Oleic Acid Vesicle Solutions
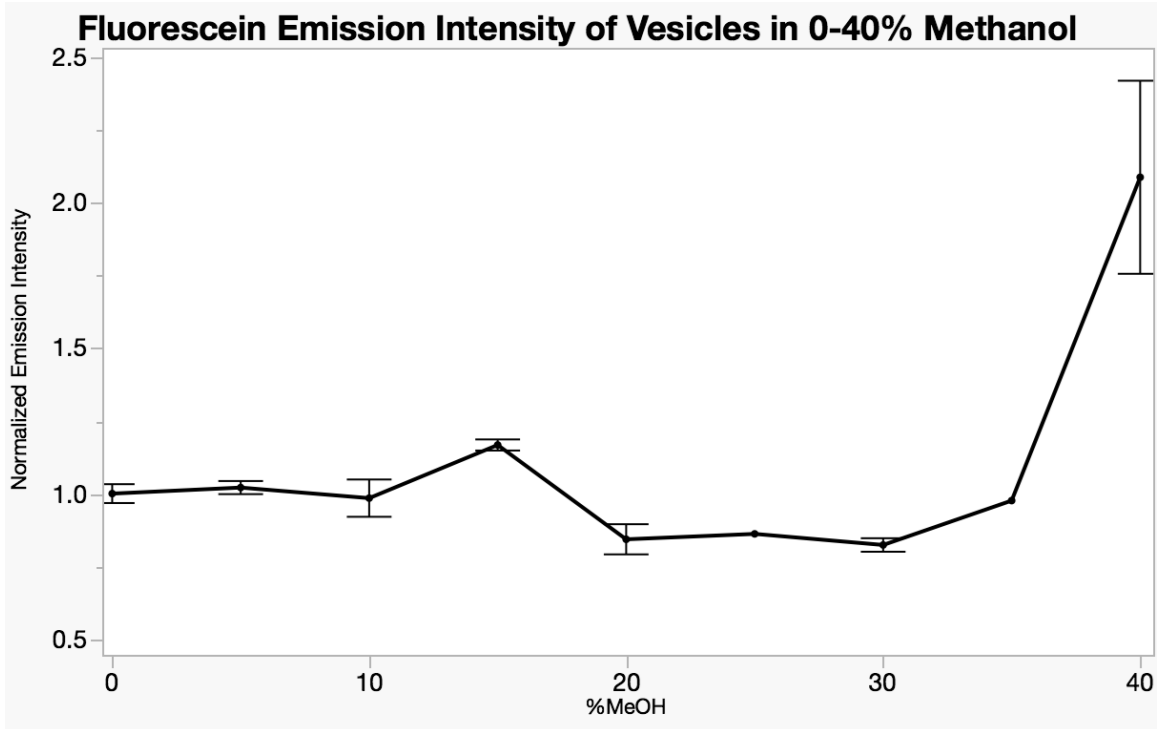
Figure 39 - Graph of the Effect of <40% Methanol on Fluorescein Emission Intensity in Oleic Acid Vesicle Solutions

87

Chapter 4 –Oleic Acid Vesicle Reactivities and Terpenes/Terpenoids

4.1 Introduction

Fatty acid vesicles are valued as biomimetic material and model membranes because of their simplicity and reactivity [76]. Our study seeks to utilize the reactivity of fatty acid vesicles to examine the effect of the terpene family on oleic acid vesicles specifically.

The oleic acid vesicles formed in the previous experiments demonstrate this sensitivity to reactions. The unexpected departure from a linear increase in permeability upon degradation of oleic acid vesicles caused by increasing concentrations of methanol leads to modifications of the theory of fatty acid vesicle reactivity.

There are several departures from expectation which must be addressed. First, a larger concentration of dispersant is necessary to have any effect on oleic acid vesicles than expected. This departure from expectations can be attributed to the strong hydration shell of vesicles in an aqueous solution. The methanol is hypothesized to simply be replacing the water in the protective hydration shell around vesicles and is also hypothesized to be driven by entropy and not by polar binding. Our hypothesis would be supported if the effects of methanol are reversible. For example, if the solutions with higher opacity formed with 20% methanol can be reversibly driven back to a lower opacity through dilution of methanol, we can conclude that entropy and not polar binding is the driving force for the results seen.

No change to fluorescein emission intensity is seen in solutions up to 10% methanol suggesting no change in permeability of vesicle membranes. However, an increase in fluidity is theorized to occur at low concentrations of methanol as the methanol replaces the water surrounding the vesicles. This hypothesis could explain the reactivity at the initial degradation of oleic acid vesicles. Perhaps initially oleic acid vesicles lose some rigidity and become more fluid rather than the membranes developing holes and leaking. This hypothesis can be examined through the use of anisotropy of a fluorophore trapped in the membrane of the vesicles.

There is a point in the degradation of vesicle membranes when leakage does occur as seen at 10-15% methanol in the previous experiment. This leakage of fluorescence validates fluorescein as a continued experiment to test for permeability of oleic acid vesicle membranes.

Fluorescein emission intensity decreases rather than increasing between 20-35% methanol. Opacity of the oleic acid vesicle solutions also increases in these solutions. While permeability may still be occurring and simply cannot be observed through an increase in fluorescein emission intensity, a hypothesis for this increase in opacity is that aggregation of the vesicles is occurring. Aggregation can be tested by examining the turbidity of the solution spectrochemically.

Several possibilities can result once aggregation and adhesion of vesicles to one another occurs - no change in either vesicle; leakage from one vesicle to another without full fusion; and full fusion of vesicles are all possible if aggregation is occurring. The hypothesis that partial or full fusion follows aggregation can be examined in several ways building off of the fluorescent models previous discussed.

4.1.1 Terpenes/Terpenoids

One hypothesis for our study is that the effect on membranes of the terpene family of compounds as found in incense can be studied in an *in vitro* model of oleic acid vesicles. This hypothesis becomes accessible by examining the reactivities of these vesicles as outlined. Each of these reactivities can be examined using the terpenes/terpenoids of interest (Table 7) in the place of the dispersant methanol. We propose a dual hypothesis that (1) terpene/terpenoids with similar structural properties will cause similar reactions in the oleic acid vesicle solutions and that (2) inferences can be made concerning the mechanism by which these incense compounds cause these reactions in oleic acid vesicles. The second part of our hypothesis is theorized to depend on the pKa of the terpene/terpenoid relative to water as shown in the following table. The ability to either donate protons (low pKa's) or accept protons (high pKa's) is hypothesized to cause an interference with the protective hydration shell of the oleic acid vesicles allowing them to react in one or more of the four previously stated ways: fluidity, permeability, aggregation, and fusion.

Table 7 - Families of Terpenes

Family of Terpenes	Compound Name	pKa
Acyclic Monoterpenes	Ocimene	N/A
Monocyclic Monoterpenes	Limonene	N/A
	a-Phellandrene	N/A
	a-Terpinene	N/A
Bicyclic Monoterpenes	Camphene	N/A
	a-Pinene	N/A
	3-Carene	N/A
Bicyclic Sesquiterpene	t-Caryophyllene	N/A
Acyclic Terpene Alcohols	Linalool	18.46
	Geraniol	16.33
	Citronellol	17.11
Acyclic Terpene Aldehyde	Citronellal	18.32
Monocyclic Aromatic Terpene	Cymene	N/A
Monocyclic Aromatic Alcohols	Thymol	10.62
	Carvacrol	10.42
	Eugenol	10.19
Monocyclic Aromatic Aldehydes	Cuminaldehyde	-7.1
	Anisaldehyde	15.96
	Cinnamaldehyde	-4.4
Bicyclic Monoterpene Ketones	Camphor	-7.5
	a-Thujone	-7.4
Non-Terpenes	Water	14
(relevant to our study)	Methanol	15.5
	Octyl acetate	-7

4.2 Materials and Methods

4.2.1 Vesicle Formation Method

Vesicles were formed as described in the previous section: Oleic acid, weighed out to give an 80-100 mM final concentration, was dissolved in a chloroform:methanol (2:1) solvent at a 1:40 (oleic acid:solvent) ratio in a round-bottom flask. Solvent was evaporated using rotary evaporation for 30 minutes and then dried under a stream of nitrogen for 30 minutes. This drying process allowed the oleic acid molecules to organize in layers.

After removal of organic solvent, 0.20M bicine buffer, pH 9.8 was added to the oleic acid in order to achieve 80-100 mM solution. The resulting solution was vortexed for 10 seconds and placed on a horizontal shaker overnight, or a minimum of 12 hours to allow for equilibrium to be established.

4.2.2 Terpene/Terpenoid Solutions

Various terpenes/terpenoids were prepared in bicine buffer solution. The terpenes shown represent the range of terpene chemistry and the terpenes/terpenoids found in incense (Table 7). Octyl acetate is counted among these chemicals, not because it is in the terpene family but because it is present in high quantities in almost all incense examined.

The terpenes/terpenoids used were dissolved first in methanol at a concentration of 0.5 M due to low solubility in aqueous solutions. These terpene/methanol solutions were then added to 0.2 M bicine buffer, pH 9.8 at a ratio of 1:100 for a final methanol concentration of 1% and final terpene concentrations of 5 mM. These terpene/methanol/bicine buffer solutions were used to dilute the oleic acid vesicles 1:10 so opacity was not too high for fluorescence detection. The resulting dilutions were allowed to sit undisturbed for 48 hours at room temperature to allow equilibrium to be established and for maximum reactivity time.

4.3 Fluidity of vesicle membranes

An increase in the fluidity of the oleic acid vesicle membrane is a hypothesized explanation for why low concentrations of methanol seem to not

92

disrupt the membrane allowing leakage and increasing permeability. An increase in fluidity, a loosening of the molecules in the membrane, would not result in leakage of the inner contents of the vesicle but would be a possible reactivity resulting in a less discernable disruption of the membrane.

Fluidity of the vesicle membrane was studied by using 1,6-diphenyl-1,3,5-hexatriene (DPH). DPH is a nonpolar fluorescence compound that is used as a membrane probe, embedding itself deep inside the nonpolar region of the bilayer membrane [71]. The limited space in the bilayer restricts the movement of the fluorophore and allows for anisotropy to be examined. Fluorescence anisotropy is studied by comparing the emission intensities of light polarized parallel and perpendicular to the direction of the polarized excitation source. A decrease in anisotropy indicates an increase in fluidity.

4.3.1 Fluidity Method

DPH was dissolved in THF at 0.1 mM. This DPH-THF solution was added to the oleic acid with the organic solvent, chloroform:methanol before drying by rotary evaporation and N_2 stream. Oleic acid vesicles were formed as previously described by adding 0.2 M bicine buffer, pH 9.8 to make an 80-100 mM solution, vortexing for 10 seconds and horizontal mixing overnight. No dialysis is needed due to the non-polar nature of DPH.

Fluorescence anisotropy was determined by exciting at wavelength 350 nm, filtering excitation beam polarized vertically and reading emission intensities polarized vertically and horizontally at wavelength 452 nm. Polarization was done

using a manually adjusted polarizer, an equipment addition to the Agilent Cary Eclipse Fluorescence Spectrophotometer.

As previously described, all vesicle solutions were diluted 1:10 with bicine buffer, bicine buffer/methanol solutions or terpene/terpenoid solutions before determining emission intensities.

4.3.2 Results of Fluidity Study

DPH is a nonpolar fluorophore which embeds itself inside the bilayer membrane and has no discernable fluorescence in polar compounds [67]. Baseline linearity need not be established in the polar bicine buffer used as solvent for this reason. This assumption was confirmed by attempting to test for DPH emission intensity in the buffer. However, DPH would not go into solution and no emission intensity was seen in a scan of emission wavelengths at either the excitation wavelengths for DPH or fluorescein.

4.3.2.1 Linearity of DPH Emission Intensity and Anisotropy in Oleic Acid

Linear regression of DPH emission intensity and anisotropy show that 5-20 μM DPH show the best linearity of both emission intensity (Figure 40) and anisotropy (Figure 41) with the least variance over the 10-100 mM range of concentrations of oleic acid.
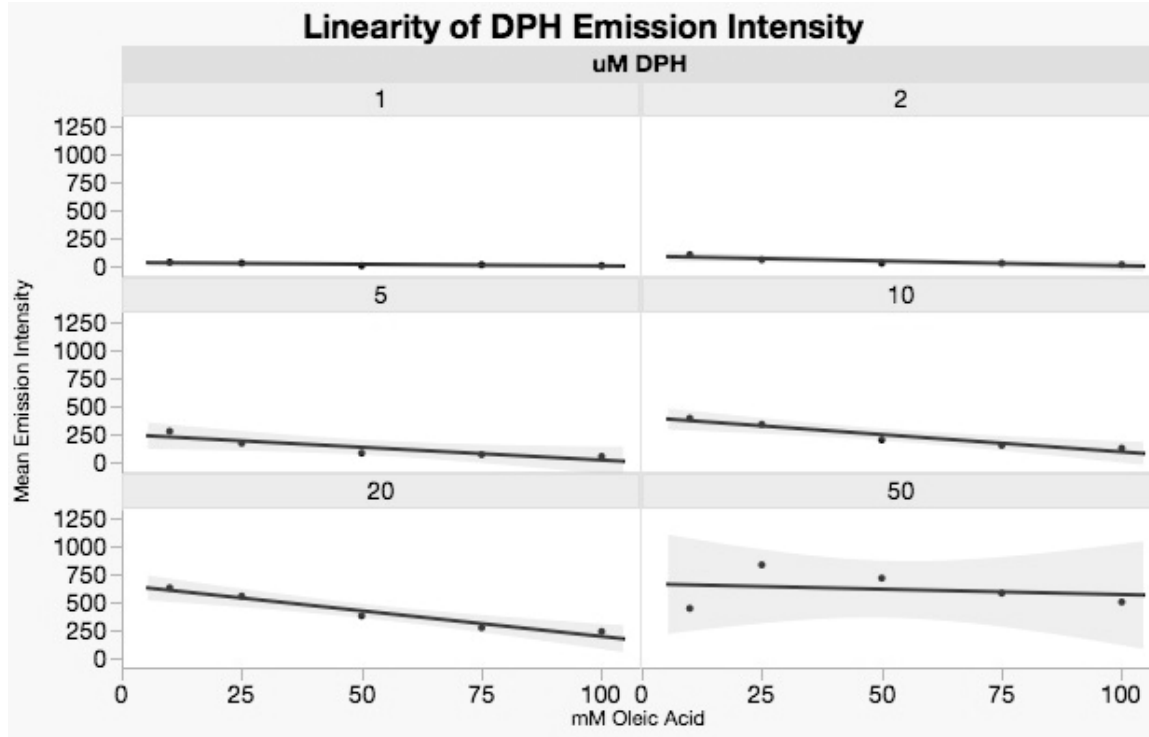
Figure 40 - Graph of the Linearity of DPH Emission Intensity in Oleic Acid Solutions
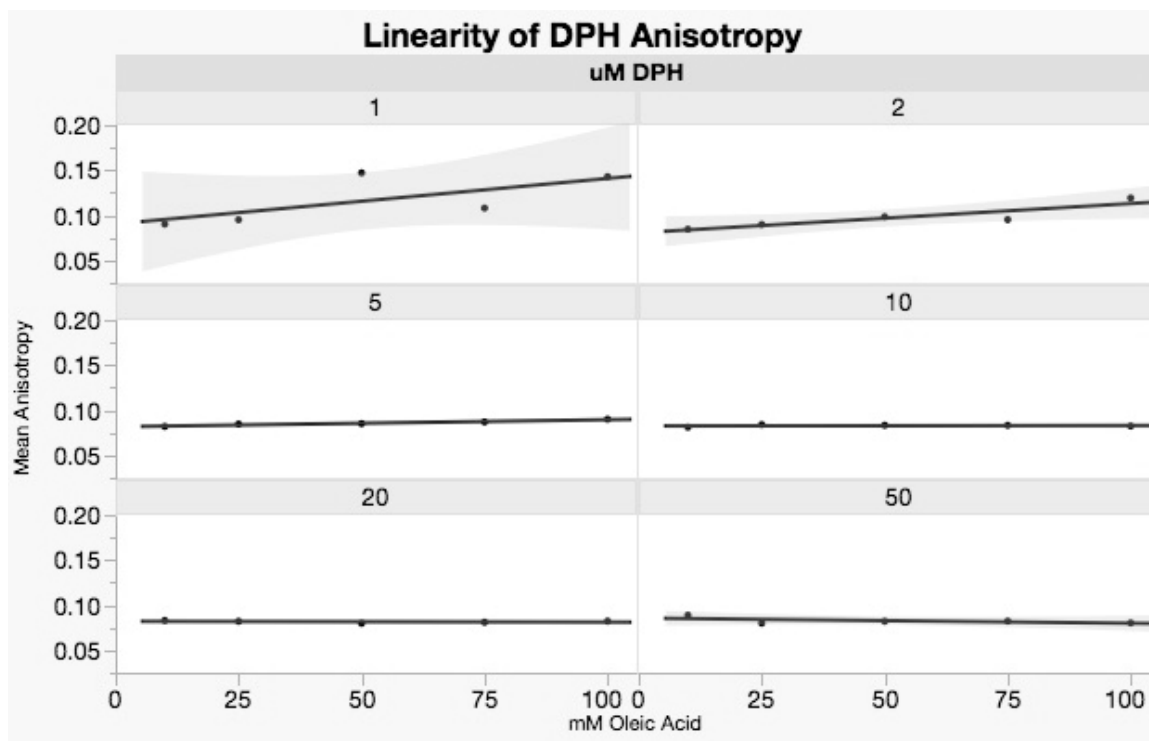
Figure 41 - Graph of the Linearity of DPH Anisotropy in Oleic Acid Solutions

The addition of terpene/terpenoids experiments, which are allowed 48 hours to react, necessitate background linearity studies to be assessed over the same time span. The emission and anisotropy of DPH was examined over the course of 48 hours to ensure that they are stable for the duration. Solutions were diluted 1:10 in bicine buffer before reading for opacity reasons. As can be seen, there is some shift in both emission (Figure 42) and anisotropy (Figure 43) over the first hour as the dilution equilibrates. However, by 48 hours the emission (Figure 44) and anisotropy (Figure 45) readings have stabilized especially for 20 μM DPH. For these reasons, 20 μM was chosen as the optimum concentration of DPH for all further anisotropy experiments.
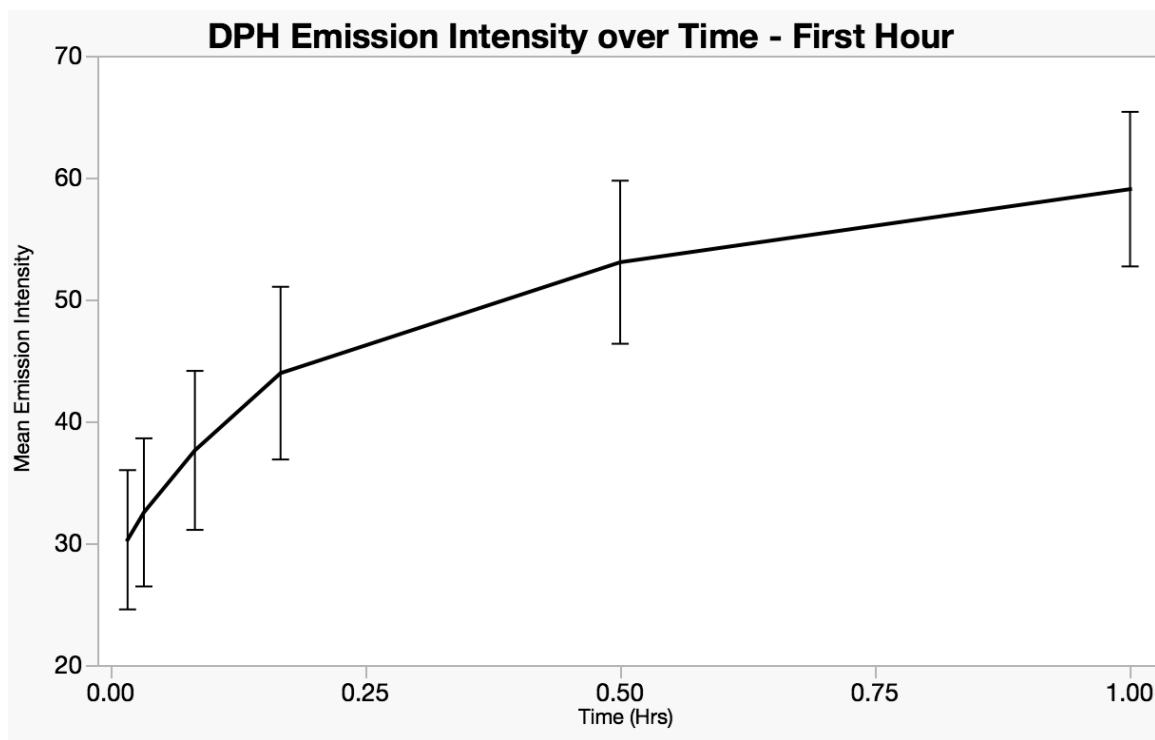
Figure 42 - Graph of DPH Emission Intensity over the First Hour
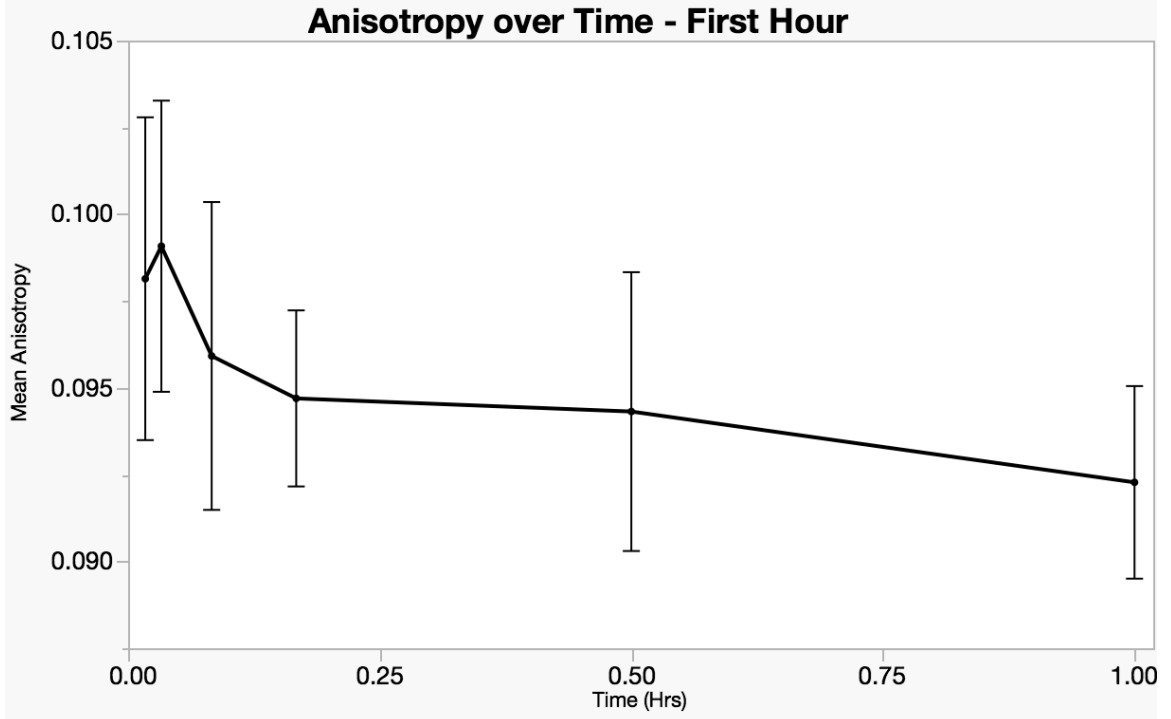
Figure 43 - Graph of DPH Anisotropy over the First Hour
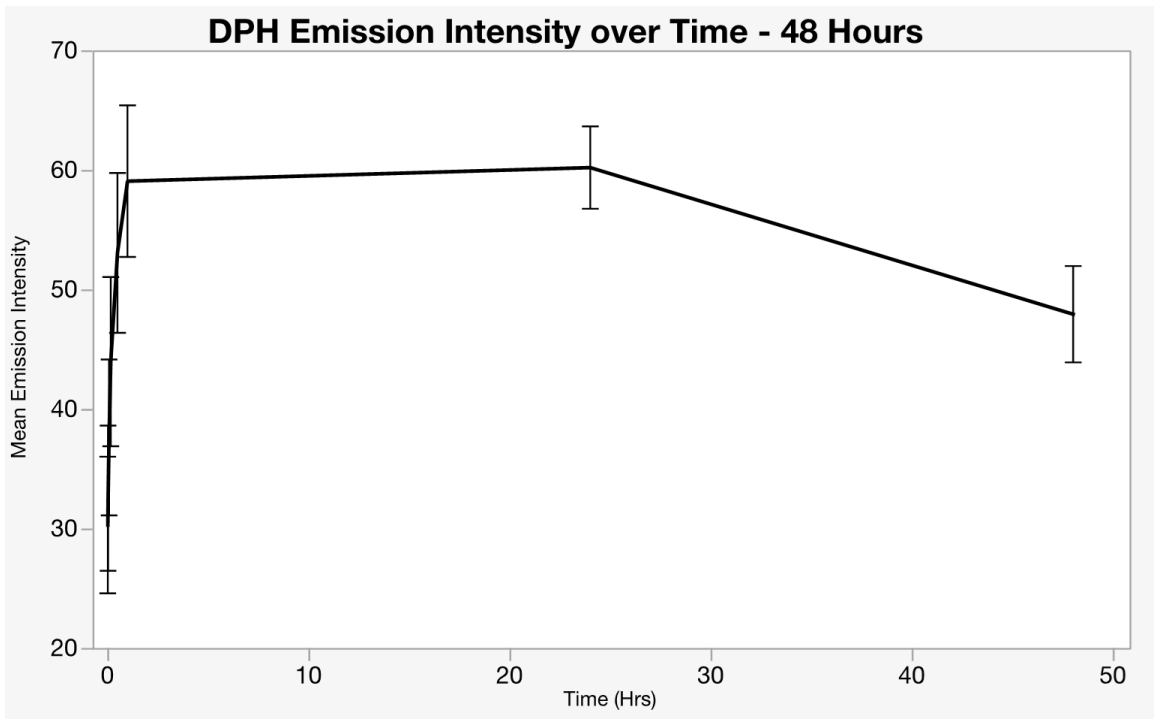
Figure 44 - Graph of DPH Emission Intensity over 48 Hours
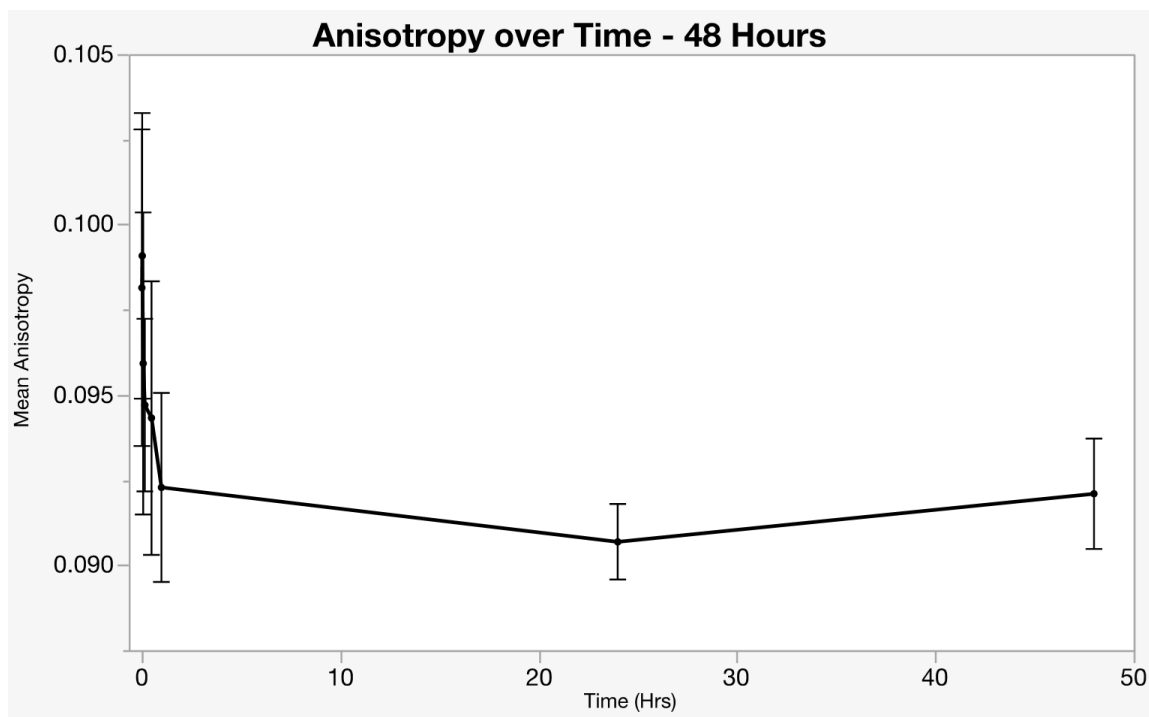
Figure 45 - Graph of DPH Anisotropy over 48 Hours

4.3.2.2 DPH Emission Intensity and Anisotropy in Oleic Acid Vesicles

DPH anisotropy in oleic acid vesicles was achieved by adding the fluorophore with the organic solvent for a final concentration of 20 μM at the very beginning of the vesicle-formation process. Several baseline experiments were performed. The linearity of dilution of oleic acid vesicles was examined and results show that the emission intensity of DPH (Figure 46) increases logarithmically while the anisotropy (Figure 47) shows no change with the increase of concentration of oleic acid vesicles with entrapped DPH.
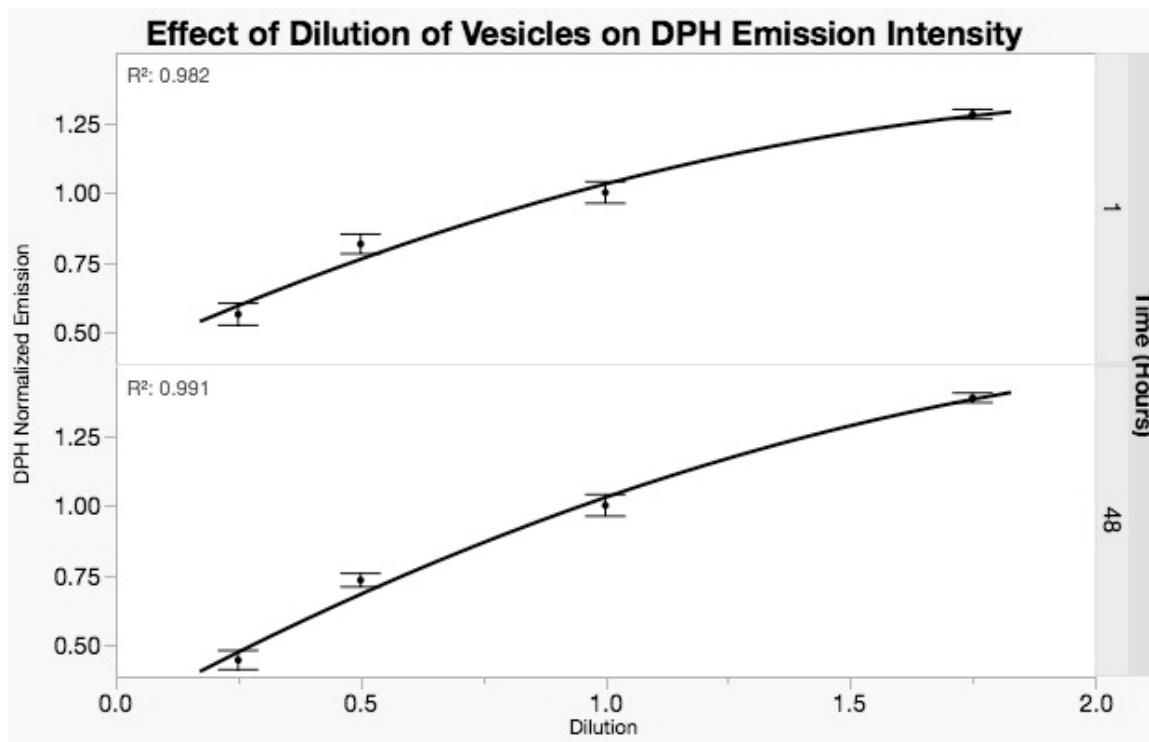
Figure 46 - Graph of DPH Emission Intensity upon Dilution of Oleic Acid Vesicle Solutions
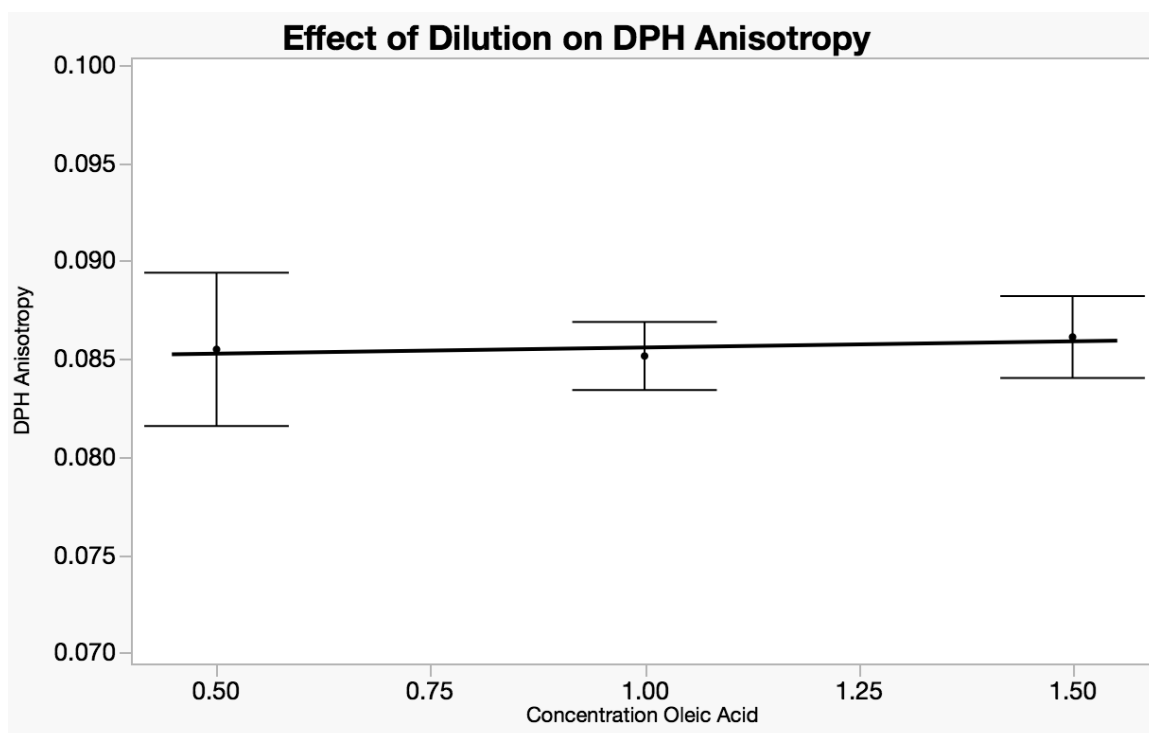
Figure 47 - Graph of DPH Anisotropy upon Dilution of Oleic Acid Vesicle Solutions

4.3.2.3 Effect of THF on DPH Anisotropy

The effect of THF (used to dissolve DPH) on DPH anisotropy in oleic acid vesicles was determined (Figure 48). THF does reduce the anisotropy of DPH at a linear rate up to 5% THF and exponentially at 10% THF and higher. This reduction corresponds to a rapid loss of visible opacity indicating a destruction of oleic acid vesicles and dispersion of free oleic acid molecules but should not affect further experiments since the DPH dissolved in THF is added before the organic solvent drying process in the formation of the vesicles. These results do emphasize the importance of the drying process. All the THF must be removed before vesicles can form.
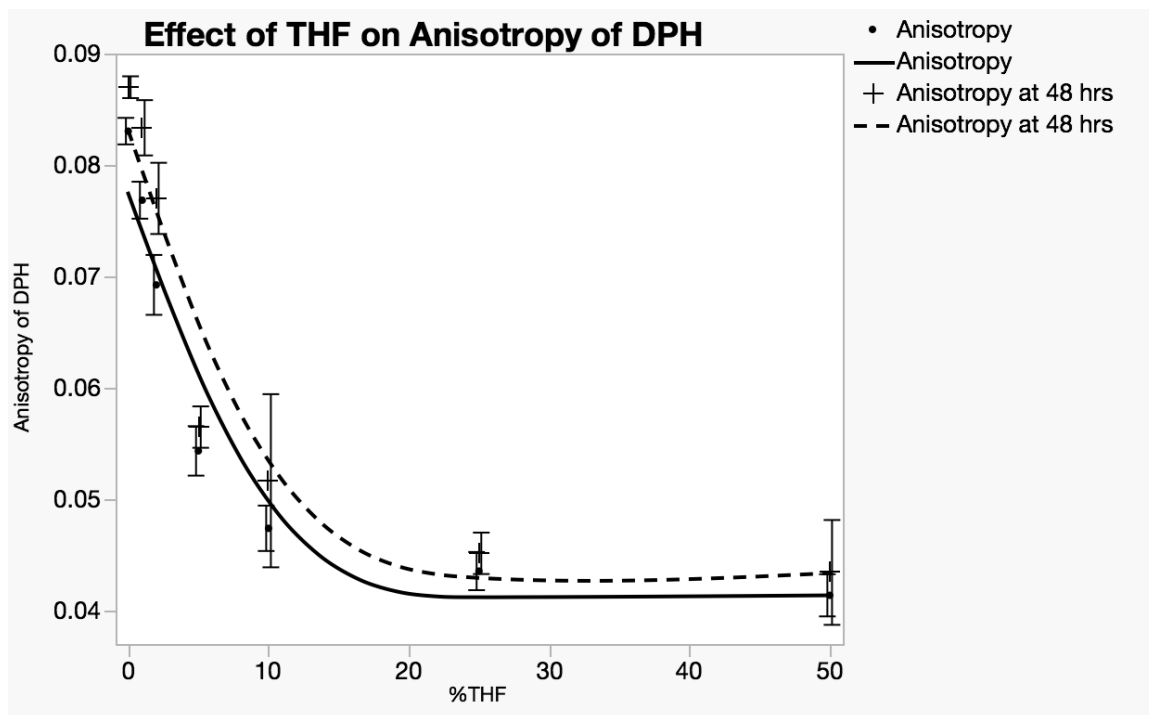
Figure 48 - Graph of the Effect of THF on DPH Anisotropy in Oleic Acid Vesicle Solutions

4.3.2.4 Effect of Methanol on DPH Emission Intensity and Anisotropy

Upon dilution with increasing concentrations of methanol, as was seen in the emission intensity of fluorescein, the emission intensity and anisotropy of DPH shows different results at low concentrations of methanol than in the higher ranges. Shown are only concentrations less than 35% methanol. Above this threshold value, the vesicles have all been destroyed and the oleic acid is dispersed.

The emission intensities of DPH (Figure 49), as read immediately after dilution and 48 hours later, are steady as the methanol concentration increase up to 5% methanol and then decrease to a low point at 15-30% methanol before increasing again when vesicles are destroyed by the higher concentrations.
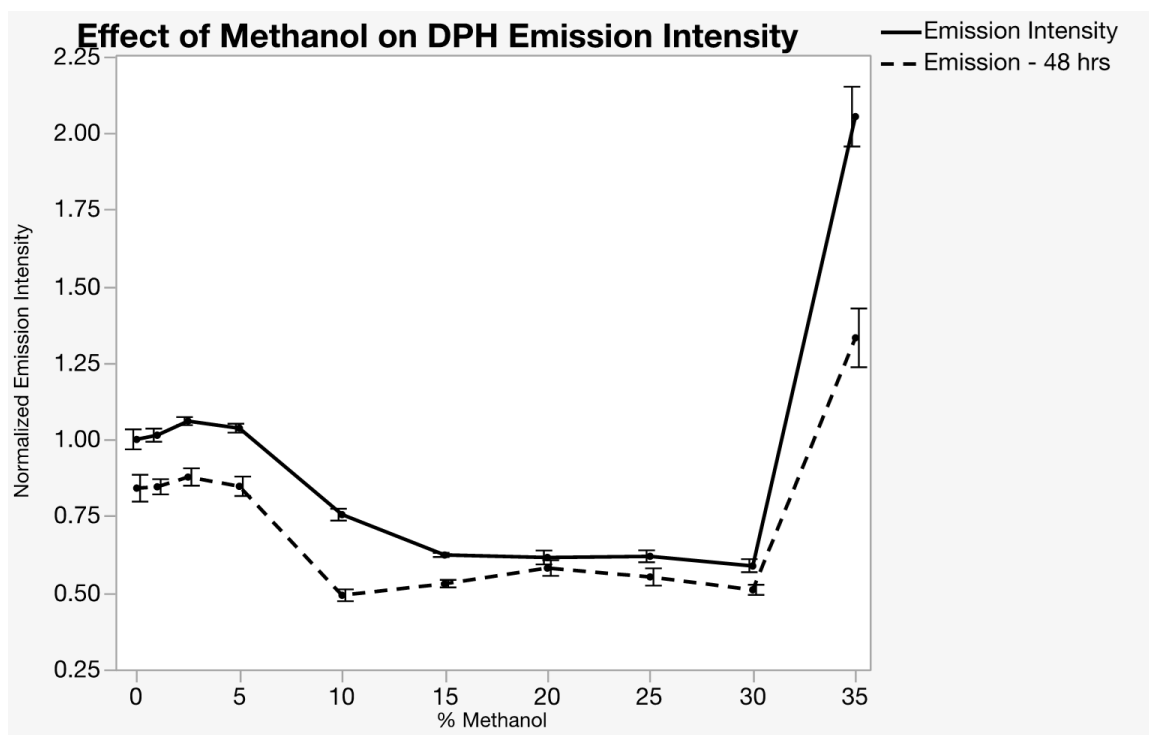
Figure 49 Graph of the Effect of Methanol on DPH Emission Intensity in Oleic Acid Vesicle Solutions

These shifts in DPH emission intensity correspond to those seen in fluorescein emission intensities as methanol concentration increases.

The DPH anisotropy (Figure 50) remains the same until the methanol concentration gets to 15% and then the anisotropy decreases as the methanol concentration continues to increase. These shifts in emission intensity and anisotropy can be attributed to an increase in fluidity of the vesicle membrane since a decrease in DPH anisotropy indicates an increase in the movement of the fluorophore inside the membrane of the vesicles. This decrease in DPH anisotropy confirms the hypothesis that methanol causes a change in fluidity of the oleic acid vesicles.
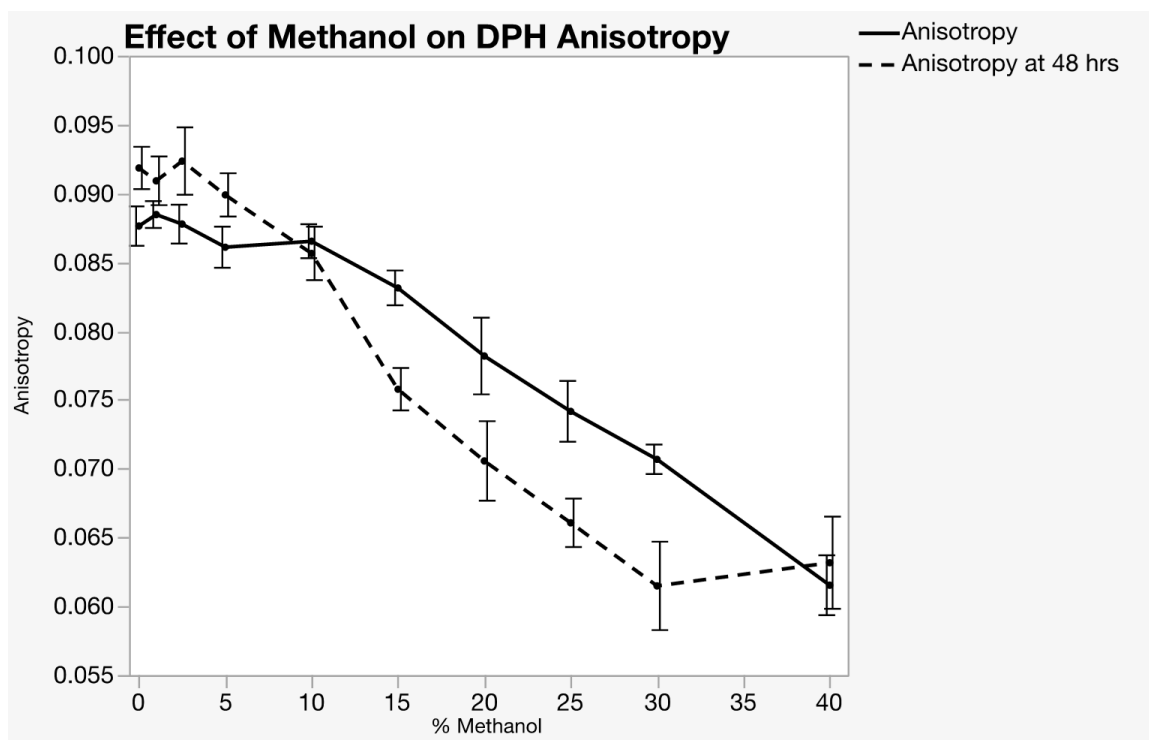
Figure 50 - Graph of the Effect of Methanol on DPH Anisotropy in Oleic Acid Vesicle Solutions

4.3.2.5 Fluorescein emission and DPH Anisotropy Simultaneously

It was theorized that fluorescein emission intensity and DPH anisotropy could be tested simultaneously since fluorescein is polar and is trapped in the interior solution of the vesicles while DPH is nonpolar and is embedded inside the vesicle membrane. More importantly, the excitation and emission wavelengths of the two fluorophores do not overlap. Fluorescein excitation is at 493 nm and emission is detected at 512 nm while DPH excitation is at 350 nm and emission detected at 452 nm. Any interference between the two fluorophores was tested by comparing data (normalized with and without methanol as the positive and negative blanks respectively) from triplicate sets of vesicles made with only fluorescein added or only DPH added to vesicles made with both fluorescein and DPH added. Results (Figure 51) show that both fluorescein emission intensities and DPH anisotropies are comparable with a 95% confidence level if taken alone or with the other fluorophore present.
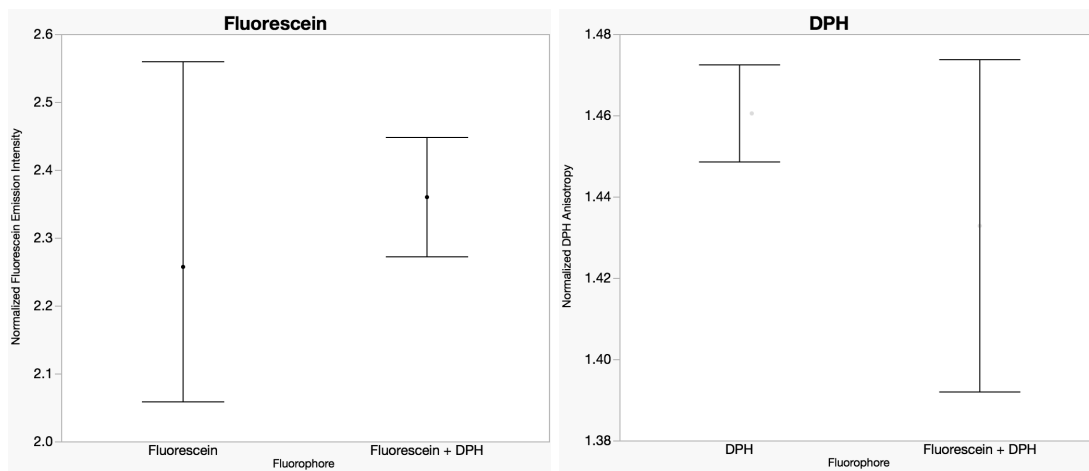
Figure 51 - Graph of Comparison of DPH and Fluorescein Emission Intensities when Read Together or Alone in Solution

4.3.2.6 Effect of Terpenes on DPH Anisotropy

Vesicle solutions were added to the 5 mM terpene/terpenoid solutions prepared as described in the methods section in a 1:10 (vesicle:terpene) ratio. DPH anisotropy was detected for these solutions and compared to a negative blank consisting of vesicles similarly diluted in bicine buffer with 1% methanol and allowed to equilibrate for 48 hours. Vesicles were also diluted in 40% methanol/bicine as a positive blank of fully dispersed oleic acid molecules with the resulting low point of DPH anisotropy.

Three dilutions in terpene/terpenoid solutions were performed for each of three solutions of vesicles. The entire procedure was repeated three times to ensure repeatable results. The statistical test ANOVA with post hoc Dunnett's multiple comparisons test was applied to the data to determine if there was a statistical difference in emission intensity between the solutions of vesicles diluted in the negative bicine blank and the solutions of vesicles diluted in the terpene. A few of the terpenes show a significant difference ($P < 0.05$)from the bicine blank as can be seen in Table 8. These include the acyclic alcohols, the aromatic aldehydes, eugenol, and octyl acetate.

Octyl acetate, which is heavily present in most incense samples, and the acyclic alcohols all show a significant decrease in anisotropy from the bicine blank similar to what was seen in the higher concentrations of methanol. 40% methanol, as a positive blank result, is also shown for comparison. The aromatic aldehyde terpenoids however show an increase in anisotropy from the bicine blank that is not seen in any of the methanol concentrations. Eugenol, an aromatic alcohol, also

shows a drastic increase in anisotropy. However, the other two aromatic alcohols do

not show any significant difference from the blank. Eugenol was seen to have a

visible color difference which could account for the much higher observation in

anisotropy.

Table 8 - Effect of Terpenes on DPH Anisotropy

Family of Terpenes	Compound	pKa	Anisotrop	CV	P value
Acyclic	Ocimene	N/A	0.0989	2.29	0.26
Monocyclic	Limonene	N/A	0.0928	2.14	0.99
Monoterpenes	a-Phellandrene	N/A	0.0944	4.14	0.99
	a-Terpinene	N/A	0.0937	2.20	0.99
Bicyclic	Camphene	N/A	0.0942	2.59	0.99
Monoterpenes	a-Pinene	N/A	0.0889	2.90	0.99
	3-Carene	N/A	0.0934	2.42	0.99
Bicyclic	t-Caryophyllene	N/A	0.0954	13.2	0.97
Acyclic Alcohols	Linalool	18.46	0.0822	2.50	<0.05
	Geraniol	16.33	0.0825	3.16	<0.05
	Citronellol	17.11	0.0857	3.10	0.45
Acyclic Aldehyde	Citronellal	18.32	0.0942	3.74	0.99
Aromatic Terpene	Cymene	N/A	0.0919	3.17	0.99
Aromatic Alcohols	Thymol	10.62	0.0914	3.21	0.99
	Carvacrol	10.42	0.0987	2.60	0.17
	Eugenol	10.19	0.108	2.89	<0.05
Aromatic Aldehydes	Cuminaldehyde	-7.1	0.109	3.73	<0.05
	Anisaldehyde	15.96	0.109	2.86	<0.05
	Cinnamaldehyde	-4.4	0.164	3.04	<0.05
Bicyclic Ketones	Camphor	-7.5	0.0879	2.62	0.99
	a-Thujone	-7.4	0.0852	2.24	0.51
Non-Terpenes	Methanol	15.5	0.0603	10.4	<0.05
(relevant to our	Octyl acetate	-7	0.0816	8.23	<0.05
	Bicine	N/A	0.0915	1.88	N/A

P-value <0.05 is considered significantly different from bicine blank.

The hypothesis that terpenes with structural similarities will react similarly

is supported. However, the hypothesis that the terpenes will react according to their

pKa's is only somewhat supported. Terpenes with no discernable pKa show no

effect on oleic acid vesicles which supports the hypothesis. Also, the acyclic alcohols

with pKa's similar to methanol do show a similar reduction in anisotropy. The same observation is confirmed in octyl acetate with a similar pKa and a similar reduction in anisotropy. All of these results point to an increase in the fluidity of the oleic acid vesicle.

The results which do not support the theory of a correlation between pKa and a reduction of DPH anisotropy are the aromatic alcohols, which show no significant effect on anisotropy, and the aromatic aldehydes which show an increase in anisotropy rather than a decrease. These two structurally similar groups of terpenoids do both show a significant decrease in DPH emission intensity which points to the hypothesis that beyond increasing fluidity of the membrane, some terpenes, like the higher concentrations of methanol, can cause aggregation and perhaps some form of fusion.

4.4 Permeability of vesicle membranes

Permeability of the vesicle membrane was tested in our study using fluorescein trapped inside the oleic acid vesicles. The fluorescein method was examined as a baseline for establishing the method of forming oleic acid vesicles in the previous chapter with unexpected results upon the addition of methanol as a dispersant used to destroy vesicles. No change in fluorescein emission intensity is seen at low concentrations of methanol (0-10%) but this lack of change can be explained by the previous fluidity experiment. An increase in fluorescein emission intensity is observed at 15% methanol, however. An increase in permeability in vesicle membranes could still be the explanation for these results and must be

explored as a possible reactivity of oleic acid vesicles in solution with terpenes/terpenoids.

4.4.1 Permeability Method

The method for testing permeability was detailed in the previous chapter in the formation method of oleic acid vesicles. A summary is given here as well.

Fluorescein, sodium salt was dissolved in 0.2 M bicine buffer, pH 9.8 to a concentration of 1.0 µM. This fluorescein-bicine solution was used to disperse the oleic acid, forming vesicles while trapping fluorescein inside the vesicles.

Dialysis was performed to remove fluorescein molecules not trapped inside the vesicles by placing the vesicle solution in dialysis tubing and soaking in a 10-15 mM oleic acid in bicine buffer solution. Four steps of dialysis (4 hours twice, overnight, and finally 24 hours) were performed allowing time for equilibrium to be established each time before replacing the oleic acid:bicine buffer with fresh dialysis buffer.

Vesicles formed in our method are heterogeneous in size as Zhu [39] determined. Extrusion was performed in a modified manner from Zhu's work using Whatman polycarbonate track-etched membrane, 5-micron pore size. Our study manually pressed the vesicle solution through the membrane using a syringe and a Whatman Reusable Stainless-Steel Syringe-type Membrane Filter Holder.

Fluorescence emission intensity was determined at excitation wavelength 493 nm and emission wavelength 512 nm. Vesicle solutions had to be diluted by a factor of 10 with bicine buffer before determining emission intensity due to opacity of the vesicle solution.

4.4.2 Results of Permeability Study

Linearity of fluorescein in bicine buffer, in 10 mM oleic acid in bicine buffer and in oleic acid vesicles was established in the previous chapter. Likewise, the effect of methanol on fluorescein in these solutions was determined and is detailed in the previous chapter.

4.4.2.1 Effect of Terpenes on Fluorescein Emission Intensity

Vesicle solutions were added to 5 mM terpene/terpenoid solutions in a 1:10 (vesicle:terpene) ratio. After 48 hours, fluorescein emission intensity was detected and compared to a negative blank consisting of vesicles similarly diluted in bicine buffer with 1% methanol but no added terpene and a positive blank of 40% methanol in bicine buffer.

Three dilutions in terpene/terpenoid solutions were done for each of three solutions of vesicles. The entire procedure was repeated several times to ensure repeatable results. ANOVA with a post hoc Dunnett's multiple comparisons test was applied to the normalized data with P-value <0.05 considered significantly different from bicine blank.

There are only a few terpenoids with a significant difference from the negative bicine blank as in shown in Table 9. One interesting factor to note is that the mean emission intensity is lower than that of the negative blank for all these terpenoid solutions. This reduction in emission intensity is contrary to the expected increase in fluorescein emission intensity and so disproves the theory that terpenoids cause an increase in permeability. This decrease in fluorescein emission intensity is similar to that seen at 20-35% methanol. The corresponding visible

increase in opacity was also seen in these solutions. These results were theorized to

be a possible aggregation of oleic acid vesicles.

Table 9 - Effect of Terpenes on Fluorescein Emission Intensity

Family of Terpenes	Compound	pKa	Fluorescein	CV	P value
Acyclic	Ocimene	N/A	1.02	2.55	0.82
Monocyclic	Limonene	N/A	0.973	2.36	0.23
Monoterpenes	a-Phellandrene	N/A	0.986	2.52	0.95
	a-Terpinene	N/A	0.989	3.35	0.99
Bicyclic	Camphene	N/A	0.978	2.37	0.49
Monoterpenes	a-Pinene	N/A	0.988	2.70	0.99
	3-Carene	N/A	0.979	2.34	0.57
Bicyclic	t-Caryophyllene	N/A	0.974	2.87	0.28
Acyclic Alcohols	Linalool	18.46	1.01	2.70	0.96
	Geraniol	16.33	1.02	3.10	0.84
	Citronellol	17.11	1.01	3.02	0.99
Acyclic Aldehyde	Citronellal	18.32	0.961	3.08	<0.05
Aromatic Terpene	Cymene	N/A	0.976	2.39	0.37
Aromatic Alcohols	Thymol	10.62	0.991	2.70	0.25
	Carvacrol	10.42	1.03	3.09	0.99
	Eugenol	10.19	0.863	2.61	<0.05
Aromatic Aldehydes	Cuminaldehyde	-7.1	0.953	2.52	<0.05
	Anisaldehyde	15.96	0.936	2.54	<0.05
	Cinnamaldehyde	-4.4	0.900	2.92	<0.05
Bicyclic Ketones	Camphor	-7.5	1.01	3.34	0.99
	a-Thujone	-7.4	1.00	3.05	0.65
Non-Terpenes	Methanol	15.5	2.33	6.18	<0.05
(relevant to our	Octyl acetate	-7	0.975	2.55	0.30
	Bicine	N/A	1.00	2.19	N/A

P-value <0.05 is considered significantly different from bicine blank.

4.5 Aggregation of vesicles

Results from the previous experiment examining the release of fluorescein

trapped inside an oleic acid vesicle upon the addition of terpene/terpenoids

suggested that the permeability or leakage of oleic acid vesicles is not the

mechanism by which these vesicles degrade. The decrease in fluorescein emission

intensity with the corresponding increase in visible opacity suggests that aggregation of vesicles is occurring.

Aggregation of fatty acid bilayer vesicles can be detected by monitoring Spectro turbidity measurements [75, 77]. An increase in optical density upon the addition of a reactive material has been shown to correlate to an increase in aggregation of vesicles.

4.5.1 Aggregation Method

Vesicles were formed as in previous experiments without adding any fluorophore. After dissolving oleic acid in organic solvent and drying, bicine buffer was added to make 80-100 mM solutions. These were vortexed, shaken overnight and extruded as previous described.

Vesicle solutions were diluted 1:10, as previously described and absorption read at 400 and 600 nm on an Agilent UV/Vis Spectrophotometer.

4.5.2 Results of Aggregation Study

Several background tests were performed to determine linearity of dilution and the effect of methanol on turbidity.

4.5.2.1 Linearity of Turbidity upon Dilution of Oleic Acid Vesicles

Oleic acid vesicles, formed at ~100mM, were diluted with bicine buffer in a range from 2-80 mM oleic acid. Absorbance was read at 400 and 600 nm immediately after vesicle solutions were diluted and again 48 hours later. Absorbance at both 400 and 600 nm were exponential over this range of concentrations as seen in Figure 52.
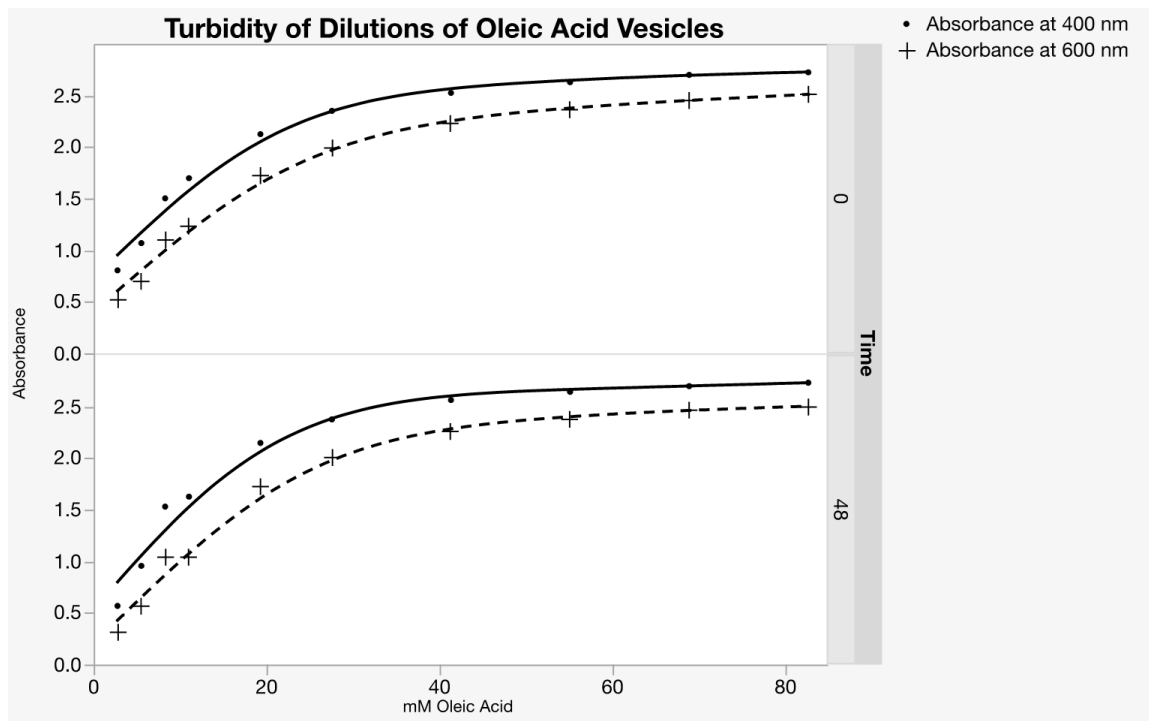
Figure 52 - Graph of the Effect of Dilution on Turbidity of Oleic Acid Vesicle Solutions

However, at dilution concentrations of up to 1:10, absorbance is linear, with the best linearity seen at 400 nm. (Figure 53) The linearity of dilution confirms the practice of diluting vesicle solutions 1:10 with bicine buffer before reading absorbance as was standard practice for all experiments.
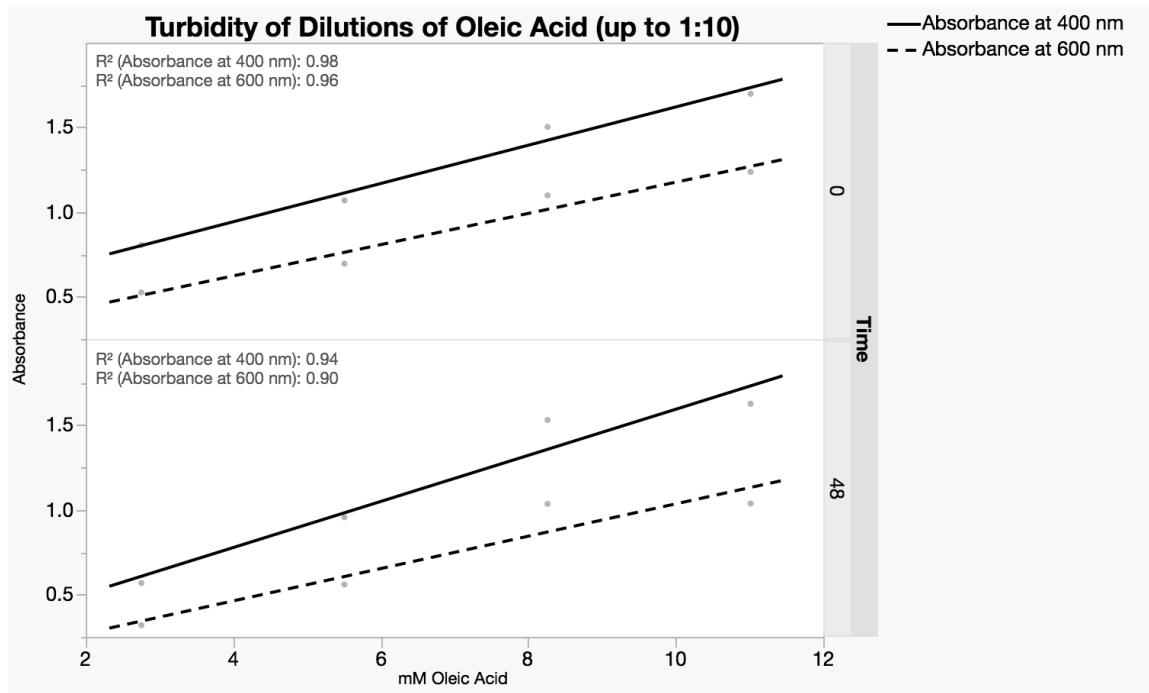
Figure 53 - Graph of the Effect of Dilution (up to 1:10) on Turbidity of Oleic Acid Vesicle Solutions

4.5.2.2 Effect of Methanol on Turbidity of Oleic Acid Vesicles

Oleic acid vesicle solutions were diluted 1:10 with mixtures of methanol and bicine buffer. Absorbance was read at 400 and 600 nm immediately upon addition of vesicles and again 48 hours later. The results, shown in Figure 54, confirm the findings of the previous two experiments – as methanol concentration increases, turbidity initially decreases but at 10-15% methanol the visible turbidity and the absorbance at both 400 and 600 nm increases until 35-40% methanol when the solution appears entirely clear and the absorbance drops to near zero.
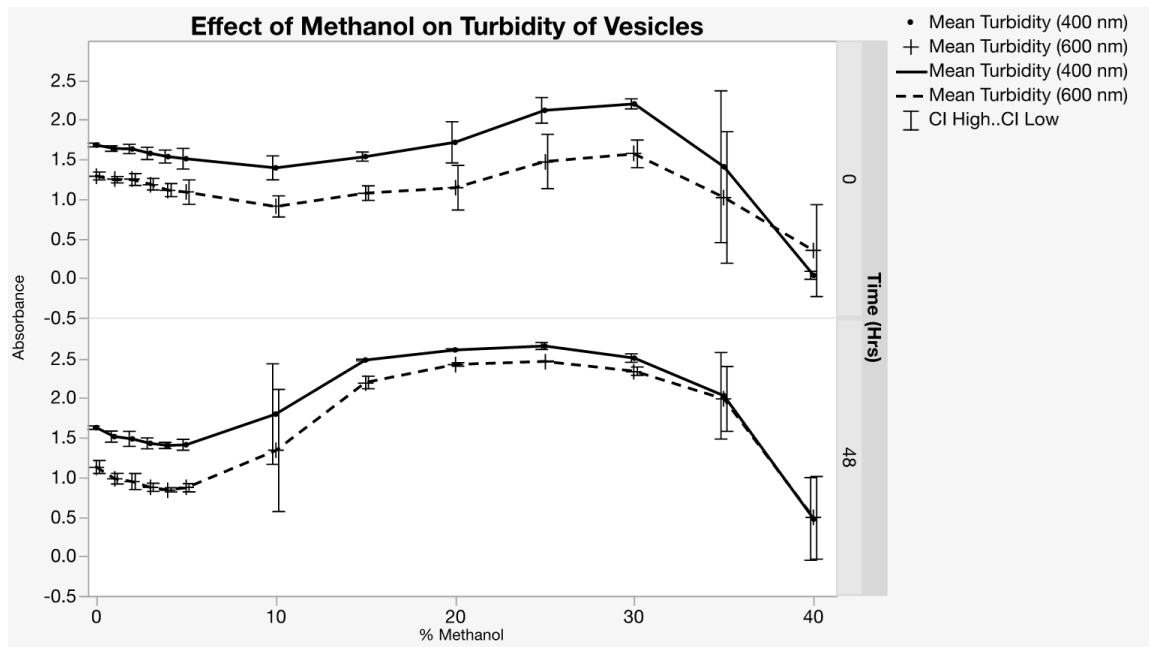
Figure 54 - Graph of the Effect of Methanol on Turbidity of Oleic Acid Vesicle Solutions

There are several aspects of the graph of turbidity as methanol concentration increases that are of particular interest. First is the methanol concentrations which show a high degree of absorbance variability (seen in the graph as large error bars). These are the concentrations at which turbidity is either increasing or decreasing. Our hypothesis is that this change in turbidity is related to a change in aggregation of vesicles. At these concentrations of methanol, equilibrium is likely not achieved before the absorbance is read. Rather the aggregation and separation of oleic acid vesicles is likely to be in constant flux.

The second point of interest is the difference between the immediate readings and the readings taken 48 hours later. The increase in absorbance is much more drastic in the 15-35% methanol range after allowing the solutions to sit for 48 hours. Also, the variance as the turbidity increases or decreases is larger. Visibly these solutions appear to separate and the dispersion collects at the top of the vial.

These vials were shaken gently before pouring into the cuvette for absorbance reading. The high degree of variance supports the theory that equilibrium has not been achieved (or rather has been disturbed and not re-achieved) since readings were taken immediately after mixing rather than reading the separated solutions or allowing the newly mixed solutions a chance to re-equilibrate.

4.5.2.3 Effect of Terpenes on Turbidity of Oleic Acid Vesicles

Oleic acid vesicles were prepared as described previously and diluted 1:10 with terpene solutions as in previous experiments. Turbidity was detected for these solutions and compared to a negative blank consisting of vesicles similarly diluted in bicine buffer with 1% methanol. Vesicles were also diluted in 40% methanol/bicine as a positive blank of fully dispersed oleic acid molecules with the resulting low point of turbidity. The resulting absorbances were normalized to the bicine blank and ANOVA with post hoc Dunnett's multiple comparisons test was performed to show that the terpenoids with significant differences in the two previous experiments also have a statistically significant difference from the bicine blank in the turbidity experiment as shown in Table 10.

All the compounds that also show both a decrease in emission intensity of fluorescein and an increase in anisotropy of DPH show an increase in absorbance (due to an increase in turbidity) This increase in turbidity confirms the theory that the previous results are most likely due to aggregation of vesicles caused by the terpenoid added.

Table 10 - Effect of Terpenes on Turbidity

Family of Terpenes	Compound	pKa	Turbidit	CV	P value
Acyclic	Ocimene	N/A	0.887	3.54	0.07
Monocyclic	Limonene	N/A	0.983	4.07	0.99
Monoterpenes	a-Phellandrene	N/A	0.858	4.03	<0.05
	a-Terpinene	N/A	0.962	4.99	0.99
Bicyclic	Camphene	N/A	1.00	3.51	0.99
Monoterpenes	a-Pinene	N/A	1.00	4.20	0.99
	3-Carene	N/A	0.984	4.13	0.99
Bicyclic	t-Caryophyllene	N/A	1.03	6.07	<0.05
Acyclic Alcohols	Linalool	18.46	1.10	2.72	<0.05
	Geraniol	16.33	1.11	2.28	<0.05
	Citronellol	17.11	1.06	2.61	<0.05
Acyclic Aldehyde	Citronellal	18.32	0.965	3.60	0.23
Aromatic Terpene	Cymene	N/A	1.02	3.31	0.60
Aromatic Alcohols	Thymol	10.62	1.14	1.73	<0.05
	Carvacrol	10.42	1.14	3.29	<0.05
	Eugenol	10.19	1.15	1.93	<0.05
Aromatic Aldehydes	Cuminaldehyde	-7.1	1.11	4.92	<0.05
	Anisaldehyde	15.96	1.04	6.83	<0.05
	Cinnamaldehyde	-4.4	1.10	2.55	<0.05
Bicyclic Ketones	Camphor	-7.5	1.04	3.53	<0.05
	a-Thujone	-7.4	1.04	4.38	<0.05
Non-Terpenes	Methanol	15.5	0.0126	51.3	<0.05
(relevant to our	Octyl acetate	-7	1.04	2.98	<0.05
	Bicine	N/A	1.00	2.19	N/A

P-value <0.05 is considered significantly different from bicine blank.

All the alcohols tested, both aromatic and non-aromatic, also show a positive difference in turbidity from the bicine blank. This increase in turbidity corresponds to an aggregation of vesicles according to the working theory. The results from all three experiments performed on the three reactivities of oleic acid vesicle support the hypothesis that terpenes, particularly those with a pKa and therefore the ability to act as a proton donor/acceptor, will interfere with the protective hydration shell surrounding oleic acid vesicles.

4.6 Fusion of vesicles

Fusion of fatty acid vesicles in general, and oleic acid vesicles specifically, is not very likely due to the extensive hydration of the exterior of the vesicle membrane as was discussed in the introduction [83]. There are instances however where fusion of oleic acid vesicles has been seen [74, 101]. These studies used an addition to the system such as a long chain alcohol or a salt to dehydrate the outer membrane to a point that the adhesion energy is overcome [102] and vesicles can approach one another for a sufficient duration and one of three things can happen: simple adhesion with no change in either vesicle; leakage from one vesicle to another without full fusion; and full fusion of vesicles. The hypothesis for our fusion experiment is that the aromatic alcohol and aldehyde terpenoids tested provide the dehydration necessary and fusion occurs as a result.

4.6.1 Fusion Methods

Detecting fusion in oleic acid vesicles is a difficult endeavor. Several heavy metal complex ion methods were attempted for our study as outlined below with no success. The most reliable method for detecting fusion in phospholipid vesicles is to entrap terbium (III) chloride and DPA (Dipicolinic acid) separately inside the vesicles. No fluorescence emission is seen in each of these vesicle solutions when examined separately. However, fluorescence of the $Tb(DPA)^{3+}$ complex ion, excited at 276 nm and emitting at 545 nm, is detected if fusion occurs when these vesicles solutions are combined. This complex ion method has not previously been attempted to study the fusion of oleic acid vesicles.

The lanthanide complex method was attempted with oleic acid adding the terbium ion and the DPA with the bicine buffer. All solutions containing terbium, however, simply precipitate terbium oleate upon the combining of the prepared oleic acid film and the terbium-doped bicine buffer. Citrate was added to the Tb^{3+}/bicine buffer solution previous to adding the oleic acid to attempt to bind the terbium temporarily and prevent precipitation but to no avail.

An alternate metal-complex ion combination was researched working with Cu-EDTA and Cu-Ethylenediamine which form complexes that emit light in the visible range with peaks at 550 nm for ethylenediamine and in the 745 nm for EDTA. Oleic acid vesicles were formed around these copper complexes at very low concentrations (10 mM) but the emission at the low concentration is too small to detect. At higher concentrations where emission is detectable, the copper precipitates with the oleate present in solution just as with the terbium experiments.

4.6.1.1 FRET Method

An alternative method to complexing agents in determining fusion in vesicles is FRET (Fluorescence Resonance Energy Transfer) which utilizes the energy transfer that occurs between a pair of fluorophores where the donor emission wavelength overlaps with the acceptor excitation wavelength. The resulting energy transfer from one fluorophore to the other occurs only if the fluorophore molecules are physically in close proximity to one another. This energy transfer is detectable as either a decrease in the emission intensity of the donor

fluorophore or as an increase in the emission intensity of the acceptor fluorophore.

FRET can be measured as an efficiency of this energy transfer by Equation 4:

$$E = 1 - F_{da}/F_d \qquad (4)$$

where F_{da} and F_d are the donor emission intensity in the presence and absence of

the acceptor, respectively.

Several donor-acceptor pairs have been studied in the determination of

fusion in phospholipid vesicles. However, the pair chosen for our study were DPH

and Nile Red [103] in order to build off the previous work done with DPH in the

study of the fluidity of oleic vesicles. DPH is excited at a wavelength of 375 nm and

emits at 450 nm while Nile Red is excited at 550 nm and emits at 625 nm as can be

seen in Figure 55, where the middle overlapping peaks are the emission scan of DPH

and the excitation scan of Nile Red.
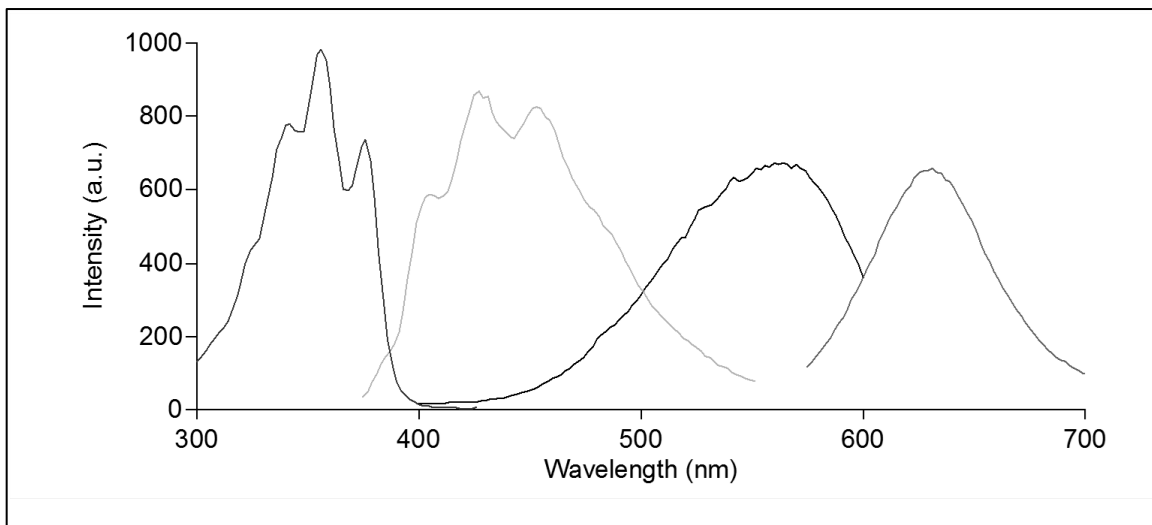
Figure 55 - Fluorescence Scans of Excitation and Emission for DPH and Nile Red

4.6.2 Results of Fusion Study

Linearity of DPH and Nile Red in 10 mM oleic acid in bicine buffer and in oleic

acid vesicles was established in the previous chapter. Likewise, the effect of

methanol on DPH emission intensity in oleic acid vesicles is given earlier in the current chapter under the discussion of the fluidity of vesicle membranes.

4.6.2.1 Effect of Methanol on Nile Red Emission Intensity

Experimentation was done similar to the background work performed on the effect of methanol on DPH emission intensity. Oleic acid vesicles with Nile Red embedded in the vesicle membrane were diluted in increasing concentrations of methanol and fluorescence emission intensity of Nile Red was read. The emission intensities detected in the methanol range where fusion is hypothesized (20-35% methanol) show the same decrease as seen in previous experiments indicating that opacity has increased. (Figure 56)
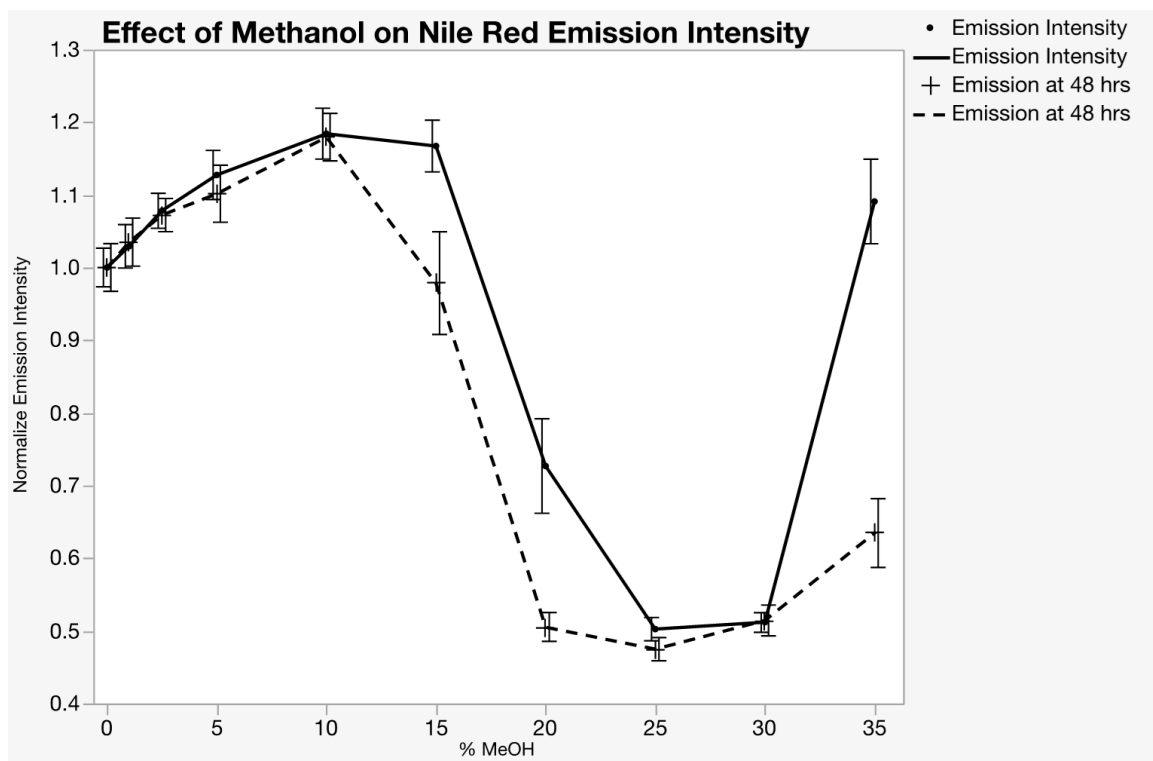
Figure 56 - Graph of the Effect of Methanol on Nile Red Emission Intensity in Oleic Acid Vesicle Solutions

4.6.2.2 DPH/Nile Red FRET Efficiency

FRET efficiency for the donor/acceptor pair DPH/Nile Red was optimized by creating a calibration curve for a range of ratios of DPH to Nile Red. Oleic acid vesicles with 20 μM DPH were prepared as detailed previously. Nile Red (1 mM in methanol) was added at various final ratios of DPH:Nile Red (2:1 to 1:2.5) both before and after the vesicle solution was diluted for emission reading. Emission intensity for the donor DPH was read at 4, 8, 24, and 48 hours. FRET efficiency was calculated by the equation given above.

In Figure 57, results from the Nile Red being added before and after dilution are compared. This experiment is important because the methanol concentration before dilution increases up to almost 5% as the Nile Red ratio increases because the Nile Red is dissolved in methanol. The emission intensity of both fluorophores is correspondingly higher and increases as Nile Red concentration increases simply because of the effect methanol has on the vesicles. The Nile Red must therefore be added after dilution for accurate FRET efficiency.
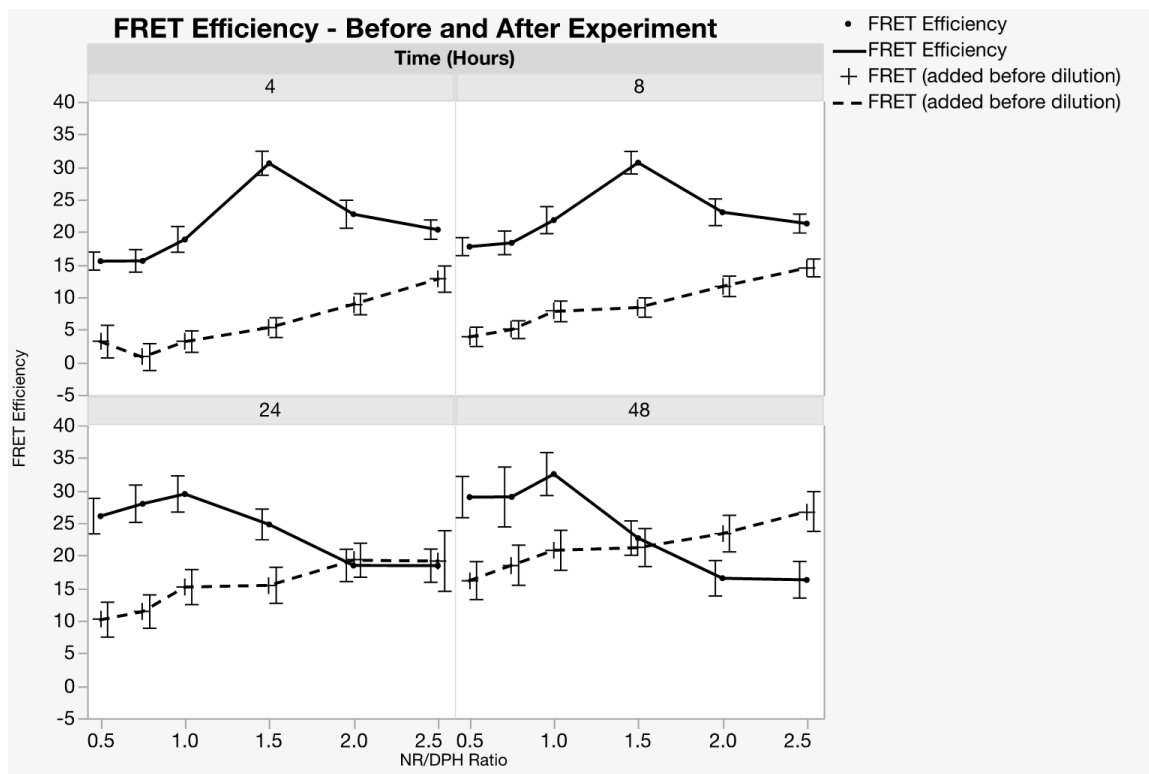
Figure 57 - Graph of the Effect of Methanol on Nile Red Emission Intensity added Before and After Dilution of Oleic Acid Vesicle Solutions

FRET efficiencies over time at the increasing ratios of Nile Red to DPH were compared with varying results as seen in Figure 58. In the first 8 hours, the ratio DPH:Nile Red of 1:1.5 gave the highest FRET efficiency. However, by 24 hours, the highest FRET efficiency was at the DPH:Nile Red ratio of 1:1 and even more so, at 48 hours (Figure 59).
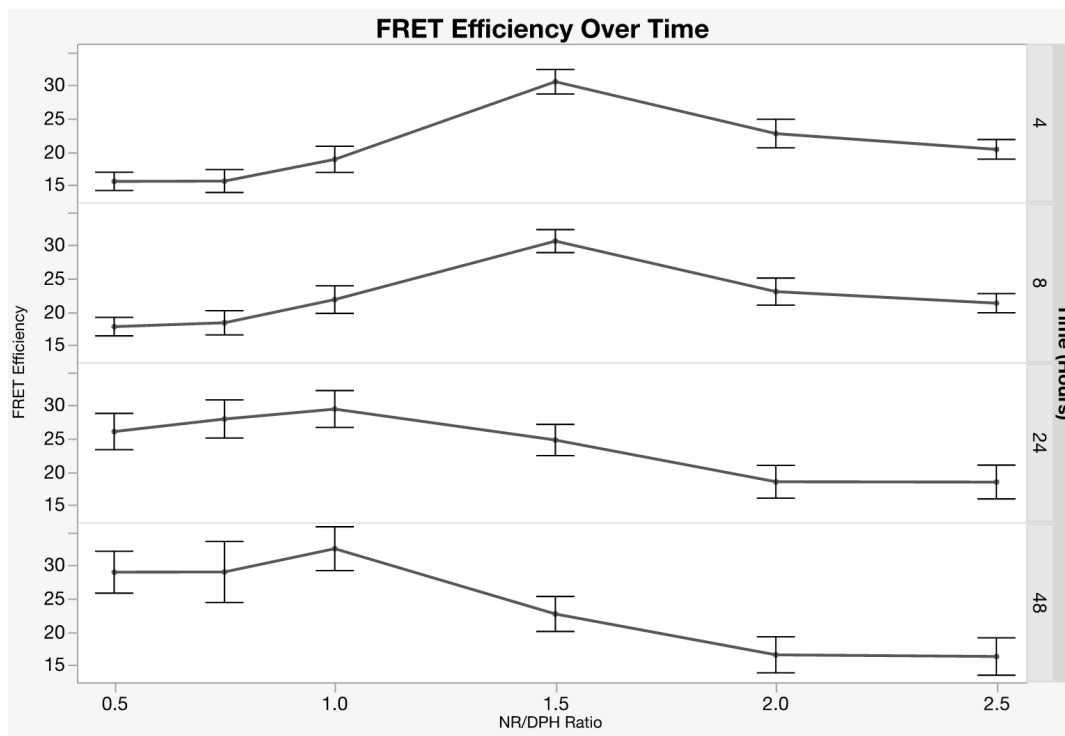
Figure 58 - Graph of the Effect of Various Ratios of DPH:Nile Red on FRET Efficiency of Oleic Acid Vesicle Solutions
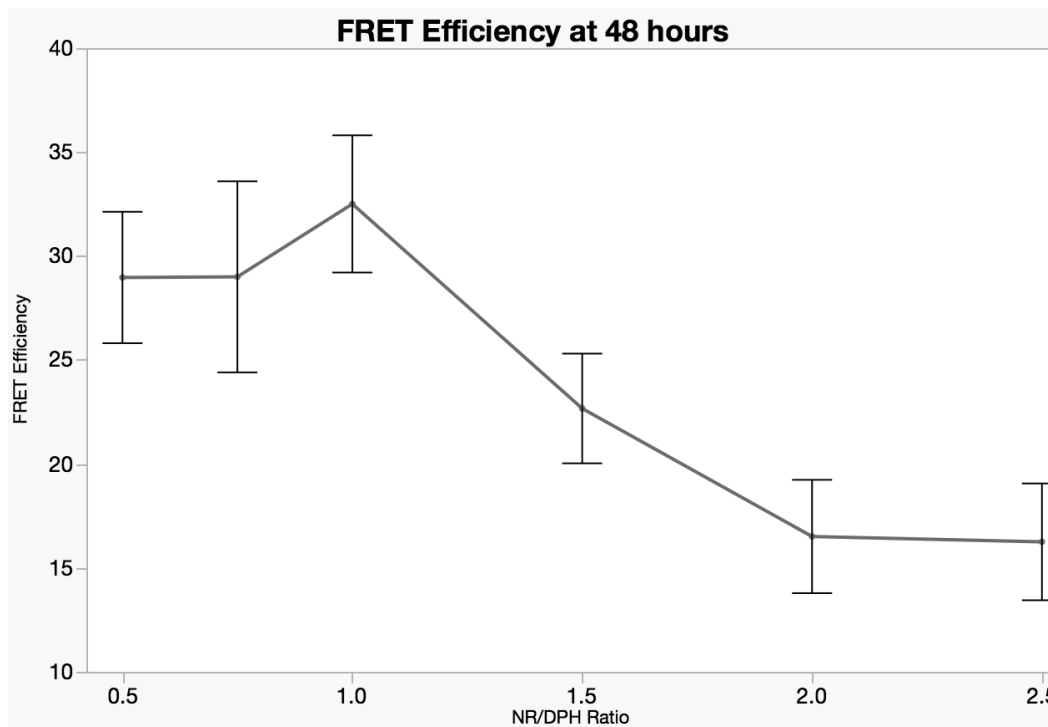
Figure 59 - Graph of the Effect of Various Ratios of DPH:Nile Red on FRET Efficiency of Oleic Acid Vesicle Solutions at 48 Hours

Therefore, the optimal ratio of DPH to Nile Red for FRET experiments in oleic acid vesicles is considered to be 1:1 with a FRET efficiency which increases in a non-linear fashion over 48 hours.

4.6.2.3 Effect of Methanol on DPH/Nile Red FRET Efficiency

The FRET method using DPH as the donor fluorophore and Nile Red as the acceptor fluorophore was applied to the working hypothesis that 20-35% methanol and certain terpenoids cause fusion in oleic acid vesicles. Vesicles were made as previously described entrapping DPH in one triplicate batch of vesicles and Nile Red in a separate triplicate batch of vesicles. The fluorophores were added at twice the concentration, 40 μM instead of 20 μM. The dilution process for emission reading was adjusted accordingly, adding each of the fluorophore-embedded vesicle solutions at a ratio of 1:5 instead of 1:10 to achieve similar final concentrations of both fluorophore and oleic acid as in previous experiments. Dilutions were made in increasing concentrations of methanol as described previously and DPH emission intensity was read at 48 hours. The FRET efficiency was calculated as before.

The results shown in Figure 60 reveal that a small amount of FRET is occurring at all concentrations of methanol above 5%. This is an indication that fusion is also occurring upon the addition of methanol which confirms the theory that aggregation is leading to fusion in these oleic acid vesicles upon the addition of methanol.
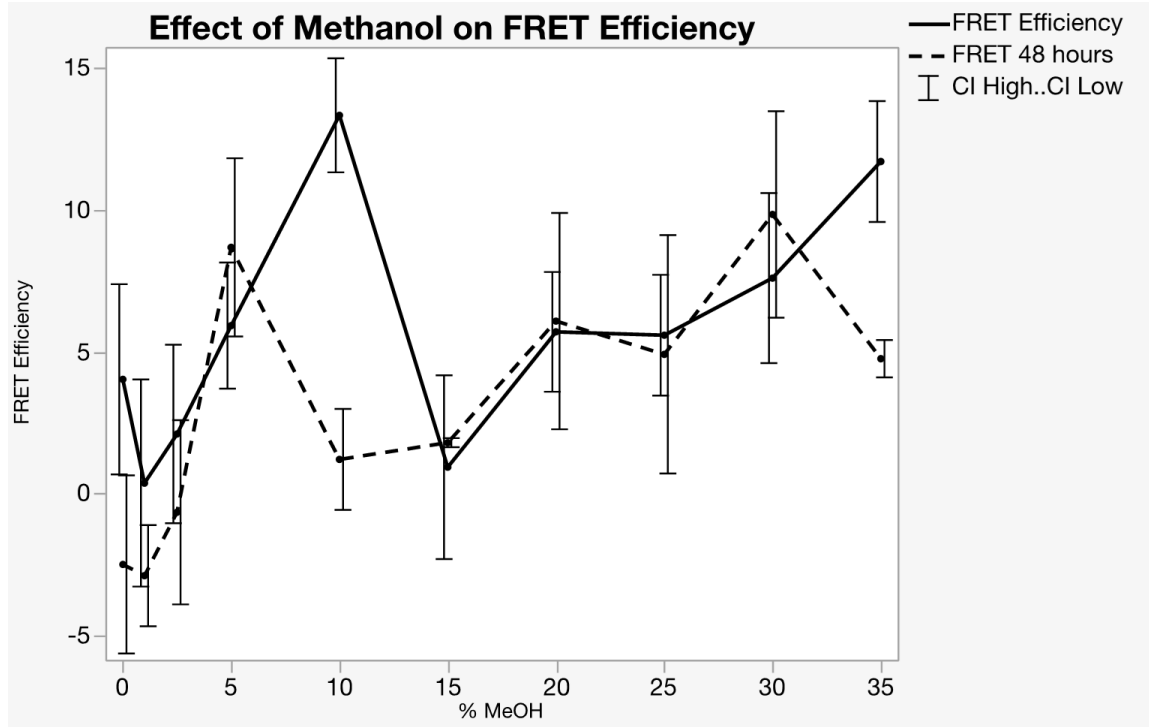
Figure 60 - Graph of the Effect of Methanol on FRET Efficiency of DPH:Nile Red in Oleic Acid Vesicle Solutions

4.6.2.4 Effect of Terpenes on DPH/Nile Red FRET Efficiency

The same experiment as performed previously was done with the terpenoids that showed a reaction in the turbidity study – the alcohols and aldehydes, as well as octyl acetate. These terpenes do show some FRET efficiency of this pair of fluorophores after 48 hours as can be seen in Table 11, however the variance of this experiment is so high as to negate the significance of the small amount of FRET seen. ANOVA with post hoc Dunnett's multiple comparisons test was performed and p-values show no significant difference from the bicine blank for any of the terpenes tested because of these high variances. This experiment must be re-examined.

Table 11 – Effect of Terpenes on FRET Efficiency

Family of Terpenes	Compound	pKa	FRET	CV	P value
Acyclic Alcohols	Linalool	18.46	-6.22	32.3	0.80
	Geraniol	16.33	0.244	2940	0.96
	Citronellol	17.11	1.95	119	0.65
Aromatic Alcohols	Thymol	10.62	1.23	603	0.81
	Carvacrol	10.42	5.33	20.2	0.11
	Eugenol	10.19	3.46	15.8	0.33
Aromatic Aldehydes	Cuminaldehyde	-7.1	0.608	727	0.92
	Anisaldehyde	15.96	3.01	63.4	0.41
	Cinnamaldehyde	-4.4	2.60	115	0.50
Non-Terpenes	Methanol	15.5	4.76	13.8	0.15
(relevant to our	Octyl acetate	-7	0.533	167	0.93
	Bicine	N/A	-2.46	130	N/A

P-value <0.05 is considered significantly different from bicine blank.

The hypothesis was that the loss of emission intensity in the 20-35% range of
methanol solutions is due to aggregation and possible fusion of the oleic acid
vesicles and that fusion could be detected by an increase in FRET efficiency. Fusion
places the FRET pair in close enough proximity for energy transfer to occur. These
results do not support the hypothesis. However, this is more likely a problem with
the experiment than with the theory being tested. The methanol results for FRET
are not consistent with the results from the previous experiment on aggregation
which would suggest that the method of determining FRET efficiency does not
correlate entirely to detecting when fusion is occurring.

One possible explanation for the lack of support for the hypothesis is that
fusion is not occurring. There are three possible outcomes of aggregation: simple
adhesion with no change in either vesicle; leakage from one vesicle to another
without full fusion; and full fusion of vesicles. The loss of emission intensity seen in

vesicles containing only the DPH or the Nile Red upon the addition of 20-35%

methanol and certain terpenoids (the aromatic aldehydes) could be due to

aggregation with no corresponding fusion based on the corresponding increase in

turbidity. However, the high FRET efficiency at 10% methanol would suggest that at

least some semi and/or full fusion is occurring.

Chapter 5 - Conclusions

Our study began with an interest in the components that make up ecclesiastical incense. A method for analyzing incense was optimized using SPME-GC-MS and a library of compounds was formulated. A list of all compounds found in incense was determined to be impossible to complete and quantify. The developed library did show a large number of a family of compounds known as terpenes. These terpenes have been shown to have health benefits and so attention was turned to finding an *in vitro* model by which these benefits can be studied chemically. The project led to a development of forming oleic acid vesicles and of studying their reactivity in the presence of terpenes through the use of fluorescence trapped inside the vesicles.

5.1 Incense and terpenes

Incense has been used in Catholic and Orthodox churches since the 4th century [1]. A haze often hangs in these churches from the combustion of incense. The smoke settles on any objects positioned in these spaces and is inhaled by the people present during its usage. This observation lead to the first project for our study of determining the chemical compounds present in the smoke. The majority of the compounds released in the combustion of incense are volatile so gas chromatography is the standard method for analyzing these chemicals. Mass spectrometry gives the power to identity the components and solid phase microextraction is an ideal method for collecting samples and injecting them into the GC-MS. A SPME-GC-MS method was optimized for this process of analysis as seen in chapter 2.

Temperature and equilibrium time were addressed. The temperatures of the

standard charcoal method of burning incense in a censor were compared with

burning on a hotplate. It was found that different compounds are released from

burning incense based on the temperature, the duration of the burn, and the time

allowed for equilibrium with the SPME fiber. The smaller, lighter compounds were

found to be more prevalent in the earlier burns while allowing the incense to burn

for longer led to a greater presence of the larger, heavier compounds.

Incense as used in the Orthodox church is prepared by adding scents from

essential oils to a frankincense resin base. An experiment was performed to

compare the compounds found in the added scent with the compounds found in the

frankincense base and finally with compounds found in the completed incense. The

completed incense, a honeysuckle variation, was found to be comprised of the

combination of the compounds found in each of the ingredients that made up the

whole. This experiment confirmed the methodology of analyzing incense using

SPME-GC-MS.

One of the groups of chemicals found in incense was a family of compounds

known as terpenes. Terpenes are commonly found in essential oils and have been

shown to have numerous health benefits including anti-oxidant and pro-oxidant

[19-21], anti-fungal [22], anti-microbial [23-24] and anti-bacterial [25-27] activities.

5.2 Oleic Acid Vesicles and terpenes

A model system for analyzing these health benefits was the driving factor for

the second part of our study. The idea for our project came from the work of a group

in the Department of Molecular Biology at the Howard Hughes Medical Institute

who have done extensive research into fatty acid vesicles as protocells [37-54]. Fatty acid vesicles are simpler and more reactive than a complex biological organism. They have a bilayer membrane with biomimicry properties which makes them a good *in vitro* model to study possible reactivities of terpenes.

Oleic acid was chosen as the fatty acid used to make vesicles because of the amount of work done previously on the formation of oleic acid vesicles. Also, these vesicles are intended to be simple models and oleic acid is one of the simplest of the unsaturated fatty acids with only one double-bond bend in the long nonpolar tail. Linoleic acid has also been studied in literature but the double bend in the nonpolar region of the molecule would lead to more diversity in the interior of the bilayer membrane and thus complicate the understanding of the reactivity of these vesicles.

The first experiment in our project involved the optimization of the formation of oleic acid vesicles as detailed in chapter 3. There were several variables that needed to be addressed to reproducibly form bilayer, unilamellar vesicles that could be analyzed for reactivity to terpenes. The film rehydration method was utilized to create vesicles by adhering oleic acid molecules in layers onto a round-bottom glass flask and then peeling them off into spherical vesicles through the addition of an aqueous buffer held at the pKa of the oleic acid, pH 9.8. The resulting heterogeneous mixture of unilamellar and multilamellar vesicles of many sizes was extruded through a poly-carbonate membrane to make the solution a more uniform sample of unilamellar vesicles of similar sizes.

Fluorescence was chosen as the method for analyzing the reactivity of these vesicles. Several fluorophores were explored including the polar Fluorescein and the

nonpolar DPH and Nile Red. Fluorescein was trapped in the interior contents of the vesicle while the nonpolar fluorophores were embedded inside the bilayer membrane.

An unexpected result upon the addition of methanol was found in the process of performing background tests on these solutions of vesicles. Methanol was added to completely disperse the oleic acid from the membranes and release the trapped fluorescein allowing for measurement of a positive blank with the maximum amount of fluorescence possible. Much more methanol was required for the dispersion process than was expected leading to a hypothesis that the protective hydration shell around oleic acid vesicles causes them to degrade gradually rather than the oleic acid molecules dispersing completely and suddenly.

The mechanism by which oleic acid vesicles degrade became the new focus for the study as detailed in chapter 4. The first proposed hypothesis for the degradation of oleic acid vesicles was an increase in permeability of the vesicle membrane. A leakage from the vesicles could be demonstrated by a steady increase in fluorescein emission intensity as the fluorophore leaks from the vesicles as methanol is added to degrade the vesicles. The hypothesis was disproved because the emission intensity did not change as methanol was increased and in fact decreased in samples containing 20-35% methanol.

The hypothesis of how oleic acid vesicles degrade was modified to reflect these results. It was proposed that degradation begins with an increase in the fluidity of the vesicle membrane rather than leakage. Fluorescein may not be escaping the vesicles however the stability of the membrane is still reduced by a

decrease in the bilayer viscosity due to a dehydration of the protective, hydrogen-bonded water shell around the vesicles. Fluidity was measured using the fluorophore DPH which was embedded in the nonpolar region of the vesicle membrane. Fluorescence anisotropy can be examined because the fluorophore is trapped reducing its ability to move freely. The results of the anisotropy experiment showed that anisotropy, and thus fluidity of the vesicle membranes, is not affected at very low concentrations of methanol. As the concentration of methanol increases and degradation of the vesicle membrane continues, the anisotropy dropped indicating an increase in fluidity of the membrane.

The results of anisotropy do not explain the loss of fluorescein emission intensity in solutions with 20-35% methanol however. An additional hypothesis was formed for this region of the degradation of oleic acid vesicle membranes. It was proposed that vesicles were aggregating and possibly even fusing based on the observation that the solutions of vesicles containing 20-35% methanol were visibly more opaque. The visible opacity or turbidity has been correlated to aggregation [75, 77]. Visible turbidity was measured and verified the hypothesis that aggregation is occurring.

Fusion proved to be a bit harder to examine. Several methods of testing for fusion were attempted and FRET, with the donor/acceptor pair of DPH/Nile Red, was determined to work with the oleic acid vesicles. The FRET method also utilizes the tight spaces of the inside of the bilayer membrane by trapping a fluorophore pair inside the membrane. The donor fluorophore is excited and loses energy to the acceptor fluorophore rather than as emitted light. DPH and Nile Red were shown to

have the overlapping donor emission-acceptor excitation energies needed for the energy transfer process. Energy transfer was shown to occur in solutions made with DPH embedded in the vesicle to which Nile Red was added. Vesicles were then formed with DPH embedded in one solution of vesicles and Nile Red in a separate solution of vesicles. An increase in FRET efficiency was seen in solutions containing more than 5% methanol indicating that fusion does indeed follow aggregation in oleic acid vesicles upon the addition of methanol.

5.2.1 The Terpenes Family of Compounds

Each of these reactivities of oleic acid vesicles was also examined with a range of terpenes. The terpenes used were chosen for their structural variations, from acyclic to bicyclic, mostly monoterpenes, and various terpenoids – alcohols, aldehydes and ketones, along with numerous aromatic compounds. Results similar to those seen the 20-35% methanol solution were seen in the aromatic alcohols and aldehydes.

These results allow for a possible mechanism to be proposed. A study by Kurita [22] showed that certain terpenoid aldehydes were anti-fungal because of their ability to form charge transfer complexes with electron donors. Another study has shown that oleic acid vesicles have a protective hydration shell which must be removed to allow for aggregation and fusion [74]. The proposed explanation for the results seen in our study is that the aromatic terpenoid alcohols and aldehydes dehydrate the vesicle by acting as electron acceptors disrupting the hydrogen-bond lattice of the water in the aqueous buffer. The disruption in the equilibrium of the

protective hydration shell then allows for aggregation, fusion and a disruption in the membrane itself.

5.3 Future work

The two branches of our study, incense and oleic acid vesicles, lead to a two-branched approach to future work.

With respect to the analysis of incense, there is much more work than can be done to document the many forms of incense as they are used in the Orthodox church. There are questions that were not addressed in the area of concentration of smoke, and relative concentrations of terpenes; in the area of duration of burn and how that affects the types and concentrations of terpenes released; and in the area of exposure to people and to objects such as the art located in the space.

Future work on the usage of oleic acid vesicles to analyze for reactivities caused by the terpene family of compounds should include several experiments: An experiment with ethanol (chemically similar to methanol, but very different in aqueous mixture) and possible effects it may have on oleic acid vesicles would give some insight into the hydration shielding of our vesicles.

Experimentation with the effect the buffer may have on the stability of oleic acid vesicles is an interesting question. Both the concentration of bicine buffer and the chemical composition should be examined. A chemically-similar choice would be Tricine at the same concentration and pH. Tricine is structurally different enough, and with one more hydroxyl group might also provide additional insight in the hydration shielding of oleic acid vesicles.

Further experimentation with families of terpenes, particularly the aromatic and non-aromatic alcohols, would help to determine the relative effect of the aromatic and the hydroxyl functional groups. Also, other compounds found in natural products such as vanillin, a phenolic aldehyde, and the lignin family of alcohols, which are also hydrophobic, would be very interesting to examine. An extension to studying natural products or essential oils, all mixtures of the terpene family of compounds, would be another branch of experimentation in using the reactivities we have discovered with these oleic acid vesicles.

Finally, the one definite experiment that needs to be done is to revise the FRET method to enable detecting fusion and to distinguish between full fusion, hemi-fusion, and adhesion when aggregation is known to occur. Discovering the difference between these occurrences would allow for a better understanding into the mechanisms by which oleic acid vesicles are simultaneously very reactive and very stable. This apparent paradox is assuredly governed by the equilibrium of these vesicles and by the hydration shielding surrounding them in aqueous solutions.

References

1.   Kenna, M. E., Why Does Incense Smell Religious?: Greek Orthodoxy and the Anthropology of Smell. *J. Mediterranean Studies* 2005, *15* (1).

2.   Basar, S.; Koch, A.; König, W. A., A verticillane-type diterpene from Boswellia carterii essential oil. *Flavour and Fragrance Journal* 2001, *16* (5), 315-318.

3.   Kasali, A. A.; Adio, A. M.; Oyedeji, A. O.; Eshilokun, A. O.; Adefenwa, M., Volatile constituents of Boswellia serrata Roxb. (Burseraceae) bark. *Flavour and Fragrance Journal* 2002, *17* (6), 462-464.

4.   Başer, K. H. C.; Demirci, B.; Dekebo, A.; Dagne, E., Essential oils of some Boswellia spp., Myrrh and Opopanax. *Flavour and Fragrance Journal* 2003, *18* (2), 153-156.

5.   Hamm, S.; Bleton, J.; Connan, J.; Tchapla, A., A chemical investigation by headspace SPME and GC–MS of volatile and semi-volatile terpenes in various olibanum samples. *Phytochemistry* 2005, *66* (12), 1499-1514.

6.   Tran, T. C.; Marriott, P. J., Characterization of incense smoke by solid phase microextraction—Comprehensive two-dimensional gas chromatography (GC×GC). *Atmospheric Environment* 2007, *41* (27), 5756-5768.

7.   Mannino, M. R.; Orecchio, S., Polycyclic aromatic hydrocarbons (PAHs) in indoor dust matter of Palermo (Italy) area: Extraction, GC–MS analysis, distribution and sources. *Atmospheric Environment* 2008, *42* (8), 1801-1817.

8.   Chiu, H.-H.; Chiang, H.-M.; Lo, C.-C.; Chen, C.-Y.; Chiang, H.-L., Constituents of volatile organic compounds of evaporating essential oil. *Atmos. Environ.* 2009, *43* (36), 5743-5749.

9.   Manoukian, A.; Quivet, E.; Temime-Roussel, B.; Nicolas, M.; Maupetit, F.; Wortham, H., Emission characteristics of air pollutants from incense and candle burning in indoor atmospheres. *Environ. Sci. Pollut. Res.* 2013, *20* (7), 4659-4670.

10.   Mathe, C.; Connan, J.; Archier, P.; Mouton, M.; Vieillescazes, C., Analysis of frankincense in archaeological samples by gas chromatography-mass spectrometry. *Ann. Chim. (Rome, Italy)* 2007, *97* (7), 433-445.

11.   Mertens, M.; Buettner, A.; Kirchhoff, E., The volatile constituents of frankincense – a review. *Flavour and Fragrance Journal* 2009, *24* (6), 279-300.

12.   Lombardozzi, A.; Strano, M.; Cortese, M.; Ricciutelli, M.; Vittori, S.; Maggi, F., Qualitative analysis of the smoke-stream of different kinds of incense by SPME/GC-MS. *Nat. Prod. Commun.* 2010, *5* (8), 1317-1320.

13.   Assefa, M.; Dekebo, A.; Kassa, H.; Habtu, A.; Fitwi, G.; Redi-Abshiro, M., Biophysical and chemical investigations of frankincense of Boswellia papyrifera from north and northwestern Ethiopia. *J. Chem. Pharm. Res.* 2012, *4* (2), 1074-1089.

14.   Woolley, C. L.; Suhail, M. M.; Smith, B. L.; Boren, K. E.; Taylor, L. C.; Schreuder, M. F.; Chai, J. K.; Casabianca, H.; Haq, S.; Lin, H.-K.; Al-Shahri, A. A.; Al-Hatmi, S.; Young, D. G., Chemical differentiation of Boswellia sacra and Boswellia carterii essential oils by gas chromatography and chiral gas chromatography-mass spectrometry. *J. Chromatogr. A* 2012, *1261*, 158-163.

15.   Bekana, D.; Kebede, T.; Assefa, M.; Kassa, H., Comparative Phytochemical Analyses of Resins of Boswellia Species (B. papyrifera (Del.) Hochst., B. neglecta S.

Moore, and B. rivae Engl.) from Northwestern, Southern, and Southeastern Ethiopia. *ISRN Analytical Chemistry* 2014, *2014*, 9.

16. Arakaki, R. Defending Incense. http://orthodoxbridge.com/defending-incense/ (accessed August 3, 2015).

17. Seraphim, F. D. Athonite Style Incense. http://orthodoxincense.com/domesticincense.html (accessed July 31, 2015).

18. Sell, C., *A Fragrant Introduction to Terpenoid Chemistry*. Royal Society of Chemistry: Cambridge, Great Britain, 2003; p 410.

19. Ruberto, G.; Baratta, M. T., Antioxidant activity of selected essential oil components in two lipid model systems. *Food Chemistry* 2000, *69* (2), 167-174.

20. Gonzalez-Burgos, E., & Gomez-Serranillos, M., Terpene Compounds in Nature: A Review of Their Potential Antioxidant Activity. *Current Medicinal Chemistry* 2012, *19* (31), 5319-5341.

21. Chauhan, A. K.; Kang, S. C., Thymol disrupts the membrane integrity of Salmonella ser. typhimurium *in vitro* and recovers infected macrophages from oxidative stress in an ex vivo model. *Research in Microbiology* 2014, *165* (7), 559-565.

22. Kurita, N., Miyaji, M., Kurane, R., Takahara, Y., Ichimura, K., Antifungal Activity and Molecular Orbital Energies of Aldehyde Compounds from Oils of Higher Plants. *Agricultural and Biological Chemistry* 1979, *43* (11), 2365-2371.

23. Dorman, H. J. D.; Deans, S. G., Antimicrobial agents from plants: antibacterial activity of plant volatile oils. *Journal of applied microbiology* 2000, *88* (2), 308-316.

24. Paduch, R.; Kandefer-Szerszeń, M.; Trytek, M.; Fiedurek, J., Terpenes: substances useful in human healthcare. *Archivum Immunologiae et Therapiae Experimentalis* 2007, *55* (5), 315.

25. Trombetta, D.; Castelli, F.; Sarpietro, M. G.; Venuti, V.; Cristani, M.; Daniele, C.; Saija, A.; Mazzanti, G.; Bisignano, G., Mechanisms of antibacterial action of three monoterpenes. *Antimicrob. Agents Chemother.* 2005, *49* (6), 2474-2478.

26. Cristani, M.; D'Arrigo, M.; Mandalari, G.; Castelli, F.; Sarpietro, M. G.; Micieli, D.; Venuti, V.; Bisignano, G.; Saija, A.; Trombetta, D., Interaction of Four Monoterpenes Contained in Essential Oils with Model Membranes: Implications for Their Antibacterial Activity. *Journal of Agricultural and Food Chemistry* 2007, *55* (15), 6300-6308.

27. Xu, J.; Zhou, F.; Ji, B. P.; Pei, R. S.; Xu, N., The antibacterial mechanism of carvacrol and thymol against Escherichia coli. *Lett. Appl. Microbiol.* 2008, *47* (3), 174-179.

28. Maleknia, S. D., Adams, M.A., Reactions of Oxygen-containing Terpenes with peptides and proteins. *Proc 4th Intl. Peptide Symp.* 2007, 334-335.

29. Williams, T. L.; Vareiro, M. M. L. M.; Jenkins, A. T. A., Fluorophore-Encapsulated Solid-Supported Bilayer Vesicles: A Method for Studying Membrane Permeation Processes. *Langmuir* 2006, *22* (15), 6473-6476.

30. Gebicki, J. M.; Hicks, M., Ufasomes are stable particles surrounded by unsaturated fatty acid membranes. *Nature* 1973, *243*.

31. Huang, C.-H., Phosphatidylcholine vesicles. Formation and physical characteristics. *Biochemistry* 1969, *8* (1), 344-352.

32.   Enoch, H. G.; Strittmatter, P., Formation and Properties of 1000- angstrom - Diameter, Single-Bilayer Phospholipid Vesicles. *Proceedings of the National Academy of Sciences of the United States of America* 1979, *76* (1), 145-149.

33.   Kantor, H. L.; Prestegard, J. H., Fusion of phosphatidylcholine bilayer vesicles: role of free fatty acid. *Biochemistry* 1978, *17* (17), 3592-3597.

34.   Marshall, S. E.; Hong, S.-H.; Thet, N. T.; Jenkins, A. T. A., Effect of Lipid and Fatty Acid Composition of Phospholipid Vesicles on Long-Term Stability and Their Response to Staphylococcus aureus and Pseudomonas aeruginosa Supernatants. *Langmuir* 2013, *29* (23), 6989-6995.

35.   Gebicki, J. M.; Hicks, M., Preparation and properties of vesicles enclosed by fatty acid membranes. *Chem. Phys. Lipids* 1976, *16* (2), 142-60.

36.   Hicks, M.; Gebicki, J. M., Microscopic studies of fatty acid vesicles. *Chemistry and Physics of Lipids* 1977, *20* (3), 243-252.

37.   Szostak, J. W.; Bartel, D. P.; Luisi, P. L., Synthesizing life. *Nature* 2001, *409*.

38.   Budin, I.; Bruckner, R. J.; Szostak, J. W., Formation of Protocell-like Vesicles in a Thermal Diffusion Column. *Journal of the American Chemical Society* 2009, *131* (28), 9628-9629.

39.   Zhu, T. F.; Szostak, J. W., Preparation of large monodisperse vesicles. *PLoS One* 2009, *4* (4), No pp. given.

40.   Zhu, T. F.; Budin, I.; Szostak, J. W., Chapter Twenty - Preparation of Fatty Acid or Phospholipid Vesicles by Thin-film Rehydration. In *Methods in Enzymology*, Jon, L., Ed. Academic Press: 2013; Vol. Volume 533, pp 267-274.

41.   Zhu, T. F.; Budin, I.; Szostak, J. W., Chapter Twenty-one - Vesicle Extrusion Through Polycarbonate Track-etched Membranes using a Hand-held Mini-extruder. In *Methods in Enzymology*, Jon, L., Ed. Academic Press: 2013; Vol. Volume 533, pp 275-282.

42.   Zhu, T. F.; Budin, I.; Szostak, J. W., Chapter Twenty-two - Preparation of Fatty Acid Micelles. In *Methods in Enzymology*, Jon, L., Ed. Academic Press: 2013; Vol. Volume 533, pp 283-288.

43.   Budin, I.; Prwyes, N.; Zhang, N.; Szostak, Jack W., Chain-Length Heterogeneity Allows for the Assembly of Fatty Acid Vesicles in Dilute Solutions. *Biophysical Journal* 2014, *107* (7), 1582-1590.

44.   Hanczyc, M. M.; Fujikawa, S. M.; Szostak, J. W., Experimental Models of Primitive Cellular Compartments: Encapsulation, Growth, and Division. *Science* 2003, *302* (5645), 618-622.

45.   Chen, I. A.; Szostak, J. W., A Kinetic Study of the Growth of Fatty Acid Vesicles. *Biophysical Journal* 2004, *87* (2), 988-998.

46.   Zhu, T. F.; Szostak, J. W., Coupled Growth and Division of Model Protocell Membranes. *Journal of the American Chemical Society* 2009, *131* (15), 5705-5713.

47.   Budin, I.; Debnath, A.; Szostak, J. W., Concentration-Driven Growth of Model Protocell Membranes. *Journal of the American Chemical Society* 2012, *134* (51), 20812-20819.

48.   Adamala, K.; Szostak, J. W., Competition between model protocells driven by an encapsulated catalyst. *Nat Chem* 2013, *5* (6), 495-501.

49.   Chen, I. A.; Roberts, R. W.; Szostak, J. W., The emergence of competition between model protocells. *Science* 2004, *305*.

50.   Bruckner, R. J.; Mansy, S. S.; Ricardo, A.; Mahadevan, L.; Szostak, J. W., Flip-flop-induced relaxation of bending energy: implications for membrane remodeling. *Biophys J* 2009, *97*.

51.   Adamala, K.; Szostak, J. W., Nonenzymatic Template-Directed RNA Synthesis Inside Model Protocells. *Science* 2013, *342* (6162), 1098.

52.   Chen, I. A.; Szostak, J. W.; Orgel, L., Membrane Growth Can Generate a Transmembrane pH Gradient in Fatty Acid Vesicles. *Proceedings of the National Academy of Sciences of the United States of America* 2004, *101* (21), 7965-7970.

53.   Fujikawa, S. M.; Chen, I. A.; Szostak, J. W., Shrink-Wrap Vesicles. *Langmuir* 2005, *21* (26), 12124-12129.

54.   Zhu, T. F.; Szostak, J. W., Exploding vesicles. *Journal of Systems Chemistry* 2011, *2* (1), 4.

55.   Hargreaves, W. R.; Deamer, D. W., Liposomes from ionic, single-chain amphiphiles. *Biochemistry* 1978, *17* (18), 3759-3768.

56.   Haines, T. H., Anionic lipid headgroups as a proton-conducting pathway along the surface of membranes: a hypothesis. *Proceedings of the National Academy of Sciences of the United States of America* 1983, *80* (1), 160-164.

57.   Cistola, D. P.; Hamilton, J. A.; Jackson, D.; Small, D. M., Ionization and phase behavior of fatty acids in water: application of the Gibbs phase rule. *Biochemistry* 1988, *27* (6), 1881-1888.

58.   Olson, F.; Hunt, C. A.; Szoka, F. C.; Vail, W. J.; Papahadjopoulos, D., Preparation of liposomes of defined size distribution by extrusion through polycarbonate membranes. *Biochim. Biophys. Acta, Biomembr.* 1979, *557* (1), 9-23.

59.   Hope, M. J.; Bally, M. B.; Webb, G.; Cullis, P. R., Production of large unilamellar vesicles by a rapid extrusion procedure. Characterization of size distribution, trapped volume and ability to maintain a membrane potential. *Biochim. Biophys. Acta, Biomembr.* 1985, *812* (1), 55-65.

60.   Blöchliger, E.; Blocher, M.; Walde, P.; Luisi, P. L., Matrix Effect in the Size Distribution of Fatty Acid Vesicles. *The Journal of Physical Chemistry B* 1998, *102* (50), 10383-10390.

61.   Rasi, S.; Mavelli, F.; Luisi, P. L., Cooperative Micelle Binding and Matrix Effect in Oleate Vesicle Formation. *The Journal of Physical Chemistry B* 2003, *107* (50), 14068-14076.

62.   Rasi, S.; Mavelli, F.; Luisi, P. L., Matrix Effect in Oleate Micelles-Vesicles Transformation. *Origins of life and evolution of the biosphere* 2004, *34* (1), 215-224.

63.   Markvoort, A. J.; Pfleger, N.; Staffhorst, R.; Hilbers, P. A. J.; van Santen, R. A.; Killian, J. A.; de Kruijff, B., Self-Reproduction of Fatty Acid Vesicles: A Combined Experimental and Simulation Study. *Biophysical Journal* 2010, *99* (5), 1520-1528.

64.   Mui, B. L.; Cullis, P. R.; Evans, E. A.; Madden, T. D., Osmotic properties of large unilamellar vesicles prepared by extrusion. *Biophys J* 1993, *64*.

65.   Mally, M.; Peterlin, P.; Svetina, S., Partitioning of Oleic Acid into Phosphatidylcholine Membranes Is Amplified by Strain. *The Journal of Physical Chemistry B* 2013, *117* (40), 12086-12094.

66.   Kampf, J. P.; Cupp, D.; Kleinfeld, A. M., Different Mechanisms of Free Fatty Acid Flip-Flop and Dissociation Revealed by Temperature and Molecular Species

Dependence of Transport across Lipid Vesicles. *Journal of Biological Chemistry* 2006, *281* (30), 21566-21574.

67.   Shinitzky, M.; Barenholz, Y., Dynamics of the Hydrocarbon Layer in Liposomes of Lecithin and Sphingomyelin Containing Dicetylphosphate. *Journal of Biological Chemistry* 1974, *249* (8), 2652-2657.

68.   Shinitzky, M.; Barenholz, Y., Fluidity parameters of lipid regions determined by fluorescence polarization. *Biochimica et Biophysica Acta (BBA) - Reviews on Biomembranes* 1978, *515* (4), 367-394.

69.   Sikkema, J., de Bont, J.A., Poolman, B, Interactions of cyclic hydrocarbons with biological membranes. *Journal of Biological Chemistry* 1994, *269* (11), 8022-8028.

70.   Kaiser, R. D.; London, E., Location of Diphenylhexatriene (DPH) and Its Derivatives within Membranes: Comparison of Different Fluorescence Quenching Analyses of Membrane Depth. *Biochemistry* 1998, *37* (22), 8180-8190.

71.   Bothun, G. D.; Knutson, B. L.; Strobel, H. J.; Nokes, S. E., Liposome Fluidization and Melting Point Depression by Pressurized CO2 Determined by Fluorescence Anisotropy. *Langmuir* 2005, *21* (2), 530-536.

72.   Suga, K.; Yokoi, T.; Kondo, D.; Hayashi, K.; Morita, S.; Okamoto, Y.; Shimanouchi, T.; Umakoshi, H., Systematical Characterization of Phase Behaviors and Membrane Properties of Fatty Acid/Didecyldimethylammonium Bromide Vesicles. *Langmuir* 2014, *30* (43), 12721-12728.

73.   Meers, P.; Hong, K.; Papahadjopoulos, D., Free fatty acid enhancement of cation-induced fusion of liposomes: synergism with synexin and other promoters of vesicle aggregation. *Biochemistry* 1988, *27* (18), 6784-6794.

74.   Kundu, N.; Banerjee, P.; Kundu, S.; Dutta, R.; Sarkar, N., Sodium Chloride Triggered the Fusion of Vesicle Composed of Fatty Acid Modified Protic Ionic Liquid: A New Insight into the Membrane Fusion Monitored through Fluorescence Lifetime Imaging Microscopy. *The Journal of Physical Chemistry B* 2017, *121* (1), 24-34.

75.   Ruiz-Mirazo, K.; Stano, P.; Luisi, P. L., Lysozyme Effect on Oleic Acid/Oleate Vesicles. *Journal of Liposome Research* 2006, *16* (2), 143-154.

76.   Douliez, J.-P.; Zhendre, V.; Grélard, A.; Dufourc, E. J., Aminosilane/Oleic Acid Vesicles as Model Membranes of Protocells. *Langmuir* 2014, *30* (49), 14717-14724.

77.   Caschera, F.; Stano, P.; Luisi, P. L., Reactivity and fusion between cationic vesicles and fatty acid anionic vesicles. *Journal of Colloid and Interface Science* 2010, *345* (2), 561-565.

78.   Wilschut, J.; Duzgunes, N.; Fraley, R.; Papahadjopoulos, D., Studies on the mechanism of membrane fusion: kinetics of calcium ion induced fusion of phosphatidylserine vesicles followed by a new assay for mixing of aqueous vesicle contents. *Biochemistry* 1980, *19* (26), 6011-6021.

79.   Struck, D. K.; Hoekstra, D.; Pagano, R. E., Use of resonance energy transfer to monitor membrane fusion. *Biochemistry* 1981, *20* (14), 4093-4099.

80.   Duzgunes, N.; Allen, T. M.; Fedor, J.; Papahadjopoulos, D., Lipid mixing during membrane aggregation and fusion: why fusion assays disagree. *Biochemistry* 1987, *26* (25), 8435-8442.

81.   Holopainen, J. M. L., Jukka Y A; Kinnunen, Paavo K J, Evidence for the extended phospholipid conformation in membrane fusion and hemifusion. *Biophys J* 1999, *76* (4), 2111-20.

82.   Malinin, V. S.; Haque, M. E.; Lentz, B. R., The Rate of Lipid Transfer during Fusion Depends on the Structure of Fluorescent Lipid Probes: A New Chain-Labeled Lipid Transfer Probe Pair. *Biochemistry* 2001, *40* (28), 8292-8299.

83.   Luisi, P. L.; Souza, T. P. d.; Stano, P., Vesicle Behavior: In Search of Explanations. *The Journal of Physical Chemistry B* 2008, *112* (46), 14655-14664.

84.   Ohki, S.; Arnold, K., Experimental evidence to support a theory of lipid membrane fusion. *Colloids and Surfaces B: Biointerfaces* 2008, *63* (2), 276-281.

85.   Sunami, T.; Caschera, F.; Morita, Y.; Toyota, T.; Nishimura, K.; Matsuura, T.; Suzuki, H.; Hanczyc, M. M.; Yomo, T., Detection of Association and Fusion of Giant Vesicles Using a Fluorescence-Activated Cell Sorter. *Langmuir* 2010, *26* (19), 15098-15103.

86.   Grob, R. L., *Modern Practice of Gas Chromatograph*. 3rd ed.; Wiley: New York, 1995; p 888.

87.   Khandpur, R. S., *Handbook of Analytical Instruments*. McGraw-Hill: New York, 2007; p 770.

88.   Wallenstein, D.; Fougret, C.; Brandt, S.; Hartmann, U., Application of Inverse Gas Chromatography for Diffusion Measurements and Evaluation of Fluid Catalytic Cracking Catalysts. *Industrial & Engineering Chemistry Research* 2016, *55* (19), 5526-5535.

89.   Restek Rxi-5ms Columns. https://www.restek.com/catalog/view/6729 (accessed 12/13/18).

90.   Gross, J. H., *Mass Spectrometry: a textbook*. 2nd ed.; Springer: Heidelburg, 2011; p 753.

91.   Miller, P. E.; Denton, M. B., The quadrupole mass filter: Basic operating concepts. *Journal of Chemical Education* 1986, *63* (7), 617.

92.   Lakowicz, J. R., *Principles of fluorescence spectroscopy*. 2006; p 1-954.

93.   Sharma, A., *Introduction to fluorescence spectroscopy*. New York : J. Wiley: New York, 1999.

94.   Farr, E. P.; Quintana, J. C.; Reynoso, V.; Ruberry, J. D.; Shin, W. R.; Swartz, K. R., Introduction to Time-Resolved Spectroscopy: Nanosecond Transient Absorption and Time-Resolved Fluorescence of Eosin B. *Journal of Chemical Education* 2018, *95* (5), 864-871.

95.   Bigger, S. W.; Bigger, A. S., FluAnisot: A Simulated Experiment in Fluorescence Anisotropy Measurement. *Journal of Chemical Education* 2013, *90* (3), 386-387.

96.   Coleman, W. M.; Perfetti, T. A.; Lawrence, B. M., Automatic Injection Solid-Phase Microextraction—Chiral-Gas Chromatography—Mass Selective Detection Analyses of Essential Oils. *Journal of Chromatographic Science* 1998, *36* (12), 575-578.

97.   Wang, D.-J. S., Xi-Kai; Zhao, Xian-En; Wang, Xiao; Li, Sheng-Bo; Du, Jin-Hua, Comparative Analysis of Volatile Oils from Lonicera japonica Thunb. var. chinensis wakey by HS-SPME and GC-MS. *Asian Journal of Chemistry* 2013, *25* (2), 803-806.

98.   Hamm, S.; Lesellier, E.; Bleton, J.; Tchapla, A., Optimization of headspace solid phase microextraction for gas chromatography/mass spectrometry analysis of widely different volatility and polarity terpenoids in olibanum. *Journal of Chromatography A* 2003, *1018* (1), 73-83.

99.   Ai, J., Headspace Solid Phase Microextraction. Dynamics and Quantitative Analysis before Reaching a Partition Equilibrium. *Anal. Chem.* 1997, *69* (16), 3260-3266.

100.   Hung, C.-H.; Lee, C.-Y.; Yang, C.-L.; Lee, M.-R., Classification and differentiation of agarwoods by using non-targeted HS-SPME-GC/MS and multivariate analysis. *Analytical Methods* 2014, *6* (18), 7449 - 7456.

101.   Rendón, A.; Carton, David G.; Sot, J.; García-Pacios, M.; Montes, L. R.; Valle, M.; Arrondo, J.-Luis R.; Goñi, Felix M.; Ruiz-Mirazo, K., Model Systems of Precursor Cellular Membranes: Long-Chain Alcohols Stabilize Spontaneously Formed Oleic Acid Vesicles. *Biophysical Journal* 2012, *102* (2), 278-286.

102.   Rand, R. P. a. P., V.A, The Influence of Polar Group Identity on the Interactions Between Phospholipid Bilayers. In *Molecular Mechanisms of Membrane Fusion*, Ohki, S., Ed. Springer US: 1988; pp 73-81.

103.   Jain, B.; Das, K., Fluorescence resonance energy transfer between DPH and Nile Red in a lipid bilayer. *Chemical Physics Letters* 2006, *433* (1), 170-174.

Vita

Laura A. Walther

<u>EDUCATION</u>
2001   Eastern Kentucky University - M.S. degree
       Chemistry
                <u>Research</u>
Pyrethrins Concentrations in Commercially-Available Pet Products: A Method Development for the Analytical Quantification of Pyrethrins by SPE and GC-MS

1991   Asbury College - B.A. degree
       Chemistry
                <u>Research</u>
Hazardous Metal Concentrations in Local Water Sources Analyzed by AA/AE

<u>EMPLOYMENT HISTORY</u>

Asbury University	Wilmore, KY	
Instructor of Chemistry & Chemical Stockroom Supervisor		2002-Current
Chemistry Instructor		1991-1992
Chemical Stockroom Supervisor & Safety Officer		1993-1994

IBM	Lexington, KY	
PC Troubleshooting – Break/Fix Lab		1999

Nalco Chemical Company	Knoxville, TN	
Sales and Service Representative		1996-1998

Eastern Kentucky University	Richmond, KY	
Teaching Graduate Assistantship		1994-1996

World Gospel Mission	Hungary, East Europe	
ESL Teacher/Missionary		1992-1993